VILNIUS UNIVERSITY

EGIDIJUS KAZLAUSKAS

THERMODYNAMICS OF ARYL-DIHYDROXYPHENYL-THIADIAZOLE BINDING TO RECOMBINANT HUMAN HSP90

Doctoral dissertation

Physical sciences, biochemistry (04 P)

Vilnius, 2016

The work presented in this doctoral dissertation has been carried out at the Institute of Biotechnology, Vilnius University during 2007-2016.

Scientific supervisor - Prof. Dr. Daumantas Matulis (Vilnius University, physical sciences, biochemistry - 04 P)

VILNIAUS UNIVERSITETAS

EGIDIJUS KAZLAUSKAS

ARIL-DIHIDROKSIFENIL-TIADIAZOLŲ JUNGIMOSI SU REKOMBINANTINIU ŽMOGAUS HSP90 BALTYMU TERMODINAMIKA

Daktaro disertacija

Fiziniai mokslai, biochemija (04 P)

Vilnius, 2016

Disertacija rengta 2007-2016 m. Vilniaus universiteto Biotechnologijos institute. Disertacija ginama eksternu.

Mokslinis konsultantas: prof. dr. Daumantas Matulis (Vilniaus universitetas, fiziniai mokslai, biochemija - 04 P)

CONTENTS

LIST OF ABBREVIATIONS

17-AAG – 17-N-allylamino-17-demethoxygeldanamycin

17-DMAG – 17-dimethylaminoethylamino-17-demethoxygeldanamycin

ADP – adenosine diphosphate

ANS – 1-anilinonaphthalene-8-sulfonic acid

ATP – adenosine triphosphate

CypD – cyclophilin D

DMSO – dimethyl sulfoxide

DSC – differential scanning calorimetry

EC_{50} – half maximal effective concentration

eNOS – endothelial nitric oxide synthase

FTSA – fluorescence thermal shift assay

GA – geldanamycin

GI_{50} – half maximal growth inhibition

HEPES – 4-(2-hydroxyethyl)-1-piperazineethanesulfonic acid

HSE – heat shock element

HSP – heat shock protein

Hsp90N – N-terminal domain of Hsp90 (and accordingly Hsp90αN, Hsp90βN)

IC_{50} –half maximal inhibitory concentration

intr – intrinsic

IR – infrared

ITC – isothermal titration calorimetry

MS – mass spectrometry

n.d. – no data

NMR – nuclear magnetic resonance

obs – observed

PDB – Protein Data Bank

r.m.s.d. – root-mean-square deviation

RD – radicicol

Tris – tris(hydroxymethyl)aminomethane

INTRODUCTION

Despite many advances in modern medicine, severe diseases are still pretty common. For instance, statistically every second person will suffer from some type of cancer during his life [1], and quite a lot of these cases will be incurable. Due to its adaptability and persistence, traditional approaches to anticancer drug design often prove unsatisfactory: while the drug molecule inhibits one seemingly vital protein, the cancer cell finds different paths to circumvent this and proliferate. Consequently often combination therapies are being suggested with drugs inhibiting different oncogenic targets.

The heat shock protein 90 (Hsp90) is a chaperone that, while catering only for a limited clientele, manages to impact a significant fraction of proteome. This is achieved through chaperoning proteins that are hubs of many biological networks such as transcriptional factors and kinases [2]. Molecular mechanisms of the 6 hallmarks of cancer cells all involve Hsp90 clients [3]. Moreover, cancer cells tend to depend heavily on chaperones to maintain their mutated proteins and preserve proteostasis. Therefore successfully drugging Hsp90 might be the strike at the heart of oncogenic processes that is needed for the development of effective anticancer therapy. Furthermore, accumulated data suggests that inhibiting Hsp90 might be employed in fighting various other illnesses, including protozoan and neurodegenerative diseases.

While there are several synthetic Hsp90 inhibitors in development and in clinical trials, no Hsp90 targeting agent is currently available on the market. Most of the investigated Hsp90 inhibitors exhibited various side-effects that restrict their usage. As most of these traits do not seem to be caused by the Hsp90 inhibition itself, there is a high demand of new, efficacious Hsp90 inhibitors.

A series of potential Hsp90 inhibitors, aryl-dihydroxyphenyl-thiadiazoles (hereafter referred to as ICPD), has been synthesised at Vilnius University. They offer us a chance not only to develop a potential new chemical entity but

also to expand on the thermodynamic drug design. Historically, drug development has been structure-based optimisation of binding contacts; however, such approaches do not offer deeper understanding of the driving forces underlying the molecular interactions [4]. Thermodynamic analysis contributes significantly to revealing the bigger picture of the binding process.

Thermodynamic studies are capable of not only quantifying the tightness of binding but also dissecting it into enthalpic and entropic contributions, which essentially tells us about the nature of the driving forces of the binding process. Generally enthalpic contribution to the ligand affinity is more difficult to improve than the entropic contribution, as artificial engineering of non-covalent polar contacts is significantly less straightforward than addition of hydrophobic groups [5; 6].

Currently one of the biggest challenges in molecular biophysics is understanding the emerging correlation of thermodynamic and structural data [7]. It has to be noted that the thermodynamic data observed directly during experiments does not always correlate well with the structural data. Therefore intrinsic parameters have to be calculated by eliminating contribution of various events that accompany binding. These intrinsic parameters serve as a conceptual tool for analysis of the binding energetics from structural and chemical contexts [8]. However, at this stage such studies still have to be conducted in a case-by-case scenario, in order to map the differences in intrinsic binding energetics that accompany minor changes in chemical structure.

The goal of this study:

To explore the structure-thermodynamics relationship for ICPD compounds binding to human Hsp90.

Objectives:

1. To evaluate the affinity of ICPD compounds to recombinant human Hsp90.

2. To investigate events that might be coupled with the binding of ICPD compounds to Hsp90.

3. To analyse the thermodynamic mechanism of ICPD compounds binding to recombinant human Hsp90 by determining the intrinsic thermodynamic parameters.

4. To establish the links between each ICPD compound structure and its thermodynamic characteristics of binding to Hsp90.

Scientific novelty and practical value of the study:

In the present study we demonstrate a series of novel Hsp90 inhibitors that can potentially be developed into drugs against certain types of cancer (as suggested by cell growth inhibition assays) and certain other diseases. These compounds contain a unique thiadiazole ring in addition to a moiety, derived from natural Hsp90 inhibitor radicicol. We provide a detailed thermodynamic characterisation of these inhibitors binding to recombinant human Hsp90. In this study isothermal titration calorimetry is employed in conjunction with protein denaturation profile analysis techniques in order to dissect the thermodynamic mechanism of the protein–ligand binding event. We show for the first time that protonation of hydroxyl residue in resorcinol-based Hsp90 inhibitors is essential for binding. The mostly enthalpy-driven binding of three of our compounds makes them excellent candidates for further lead development. Based on our studies, these compounds have been patented both in Europe and the USA.

The major findings presented for defence in this thesis:

1. ICPD compounds are tight nanomolar binders of both human Hsp90α and Hsp90β isoforms. Affinity of ICPD compounds to Hsp90α is 4 to 6 times higher than to Hsp90β.

2. Protonation of hydroxyl group in ICPD compounds is essential for binding to Hsp90.

3. Intrinsically, binding of ICPD26, ICPD34, and ICPD47 to Hsp90 is driven mostly (~84 %) by enthalpy which makes them suitable candidates for further drug development.

4. Chlorine in the ICPD compounds increases enthalpic contribution to the intrinsic binding affinity, as opposed to ethyl group in ICPD62 which promotes the entropic factor, signifying the ability of chlorine to form additional interactions of non-hydrophobic nature.

5. Small alkoxy substituent on the non-resorcinol benzene ring in the ICPD compounds has only negligible effect on the intrinsic binding parameters.

1. LITERATURE OVERVIEW

1.1. Introduction to chaperones

Mammalian cells typically express over 10,000 different protein species. Synthesised in ribosomes as linear chains of up to several thousand amino acids, they need to fold into their native state in order to function. While smaller proteins can easily fold spontaneously in diluted solutions over certain period of time, it is now firmly established that in the cellular environment, with cytosolic protein concentrations reaching 300–400 $g \times L^{-1}$, many proteins require molecular chaperones in order to fold efficiently and on a biologically relevant timescale [9]. Along with the ubiquitin-proteasome and the autophagy systems that control the timely removal of irreversibly impaired proteins, chaperones are vital in ensuring proteostasis by aiding *de novo* folding and refolding of the proteins. Proteostasis disorders result in numerous diseases such as neurodegeneration, type 2 diabetes, and cancer.

In general, molecular chaperone is defined as a protein that interacts with, stabilises, or helps another protein to acquire its functionally active conformation, without being present in its final structure [10]. There are several different families of chaperones, most of them known as heat-shock proteins (HSPs) due to their upregulation in cells under stress. They are classified into structurally unrelated classes according to their molecular weight: Hsp40, Hsp60, Hsp70, Hsp90, Hsp100, and the small Hsps. Hsp70, together with Hsp40, and Hsp60 participate in early folding of the protein while Hsp100 aids protein disassembly. Hsp90 works in between, usually mediates proper function of signalling pathways, and can sometimes be a part of the active final protein complex [11].

A protein that is being aided by a chaperone is called that chaperone's client. In general, chaperones do not have specific substrates – for instance, Hsp70/Hsp40 machinery binds to any nascent peptide. However, Hsp90

interacts only with specific client proteins. Both Hsp70 and Hsp90 require a multicomponent system in order to function. In case of Hsp90, other components (co-chaperones) can regulate its selectivity towards certain clients. Moreover, Hsp90—client complexes are frequently stable enough to allow their purification using techniques such as imunoprecipitation.

1.2. Hsp90

The main focus of Hsp90 research is on the two major human cytoplasmic isoforms – the more significant inducible Hsp90α and less substantial constitutive Hsp90β. These proteins, as their name suggests, weigh approximately 90 kDa, operate mostly in cytosol, although are also located in the nucleus. Hsp90 homologs are also found in the endoplasmic reticulum (glucose related protein, Grp94) and mitochondria (TNF receptor associated protein 1, TRAP1).

The number of cytosolic Hsp90 isoforms is variable throughout organisms. Most simple eukaryotes possess only a single form of cytosolic Hsp90 (e.g., *Drosophila sp.* [12], *Caenorhabditis elegans* [13], most yeast species). Therefore *Saccharomyces cerevisiae*, a yeast species that has 2 cytosolic isoforms (constitutive Hsc82 and heat-inducible Hsp82) [14], is widely employed in Hsp90 research. Hsp90 is fairly conserved among various species. For instance, *S. cerevisiae* Hsc82 is 62 % identical and 79 % similar to human Hsp90β.

1.2.1. Hsp90 isoforms

Human Hsp90α and Hsp90β are incredibly cognate: Hsp90α is 86 % identical to Hsp90β and similar by 93% [15; 16] (Figure 1.1). Nevertheless, the nucleotide sequence of their genes diverge by a significantly higher degree, with most of the differences being located in the non-coding regions [17].

The fundamental difference between the human Hsp90 isoforms is that Hsp90β is expressed constitutively, or in other words acts as a housekeeper protein, whereas Hsp90α expression is only induced at times of stress. This is owing to the tight regulation of transcription of the *hsp90α* gene by means of 5' upstream promoter sequences that include so-called heat shock elements (HSE; highly conserved eukaryotic nucleotide sequence, characteristic to promoters of heat-inducible genes) [18; 19]. In case of elevated temperature or other type of stress, a HSF protein binds to the HSE and promotes transcription of Hsps. Several such elements exist also in *hsp90β* gene [20]. Unusually high constant *hsp90α* expression correlates with tumour progression [21], altered cell cycle regulation [22], or flawed growth factor-mediated tyrosine kinases' signalling pathway [23].

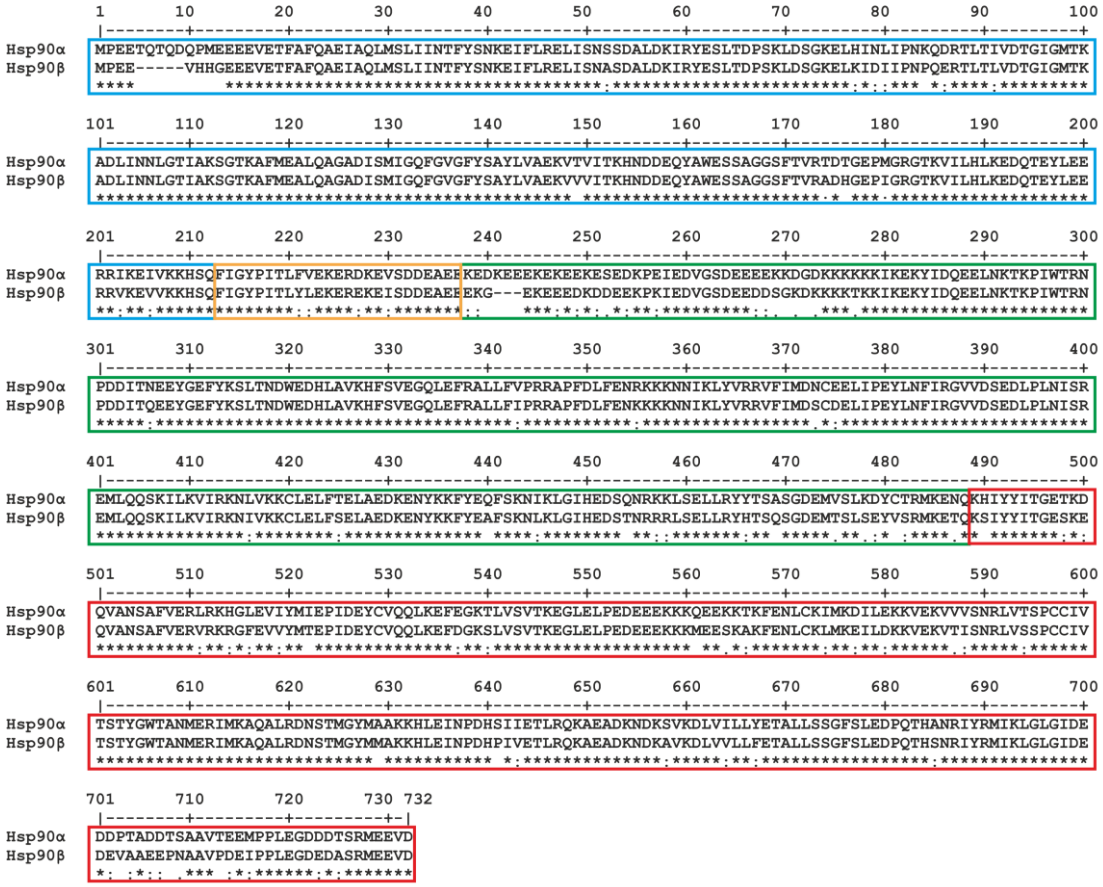

Figure 1.1. Amino acid sequence comparison of human Hsp90α and β isoforms. Domain arrangement is depicted in different colours: blue – N-domain, yellow – charged linker, green – M-domain, and red – C-domain.

In the endoplasmic reticulum there is the Grp94/Grp78 chaperone system, an analogue of the cytosolic Hsp90/Hsp70 system. It is highly selective client-wise [24] and is attributed such functions as control over Ca^{2+} balance, host defence, proteotoxic stress response, and cell adhesion. TRAP1 (also referred to as Hsp75) is another chaperone from Hsp90 family, localised predominantly in mitochondrial matrix. It is only 34% identical, 60% similar to Hsp90α [25] and more akin to the bacterial Hsp90 homolog than the human Hsp90. This chaperone is expressed constantly, though on low level (except for tumour cells) [26] but can be upregulated in response to various environmental stresses [27]. TRAP1 is involved in maintenance of mitochondrial integrity, organelle-compartmentalised protein folding, transcriptional responses to proteotoxic stress, and acquisition of resistance to drugs (such as cisplatin) [28].

1.2.2. Structure of Hsp90

A typical protein belonging to the Hsp90 family consists of 3 main domains: N-terminal (N), C-terminal (C) and the Middle (M) domains (Figure 1.2). Usually a flexible charged linker connects N-terminal and Middle domains. The N-domain is responsible for the ATP binding and hydrolysis [29]. The ATPase active centre is distinctly conserved in Hsp90 throughout evolution; however, moderate differences between species may lead to development of a species-selective Hsp90 inhibitor series [30]. The nucleotide binding pocket adopts Bergerat fold, which is characteristic to GHKL (bacterial girase, Hsp90, histidine kinase, MutL) superfamily, but differs from ATP binding sites of other kinases or chaperones of the Hsp70 family [31]. A handful of amino acids, namely, L34, N37, D79, N92, L98, G121, and F124, are directly involved in interaction with ATP. For ATP hydrolysis to occur, E33 is also required [29]. The ATPase is activated as the M-domain interacts with the γ phosphate of the ATP molecule [32]. Besides, client proteins have been reported to bind to the M-domain on multiple occasions. The key function

of C-domain is dimerization, which is essential step in the Hsp90's chaperone cycle. Moreover, C-domain contains a tetratricopeptide (TPR) receptor site, favoured by several co-chaperones that are vital for normal cellular Hsp90 function. This domain can also bind to partially folded protein in an ATP-independent manner [33]. Putative allosteric nucleotide binding sites are suggested in the C-domain [34].

Crystal structures of full length Hsp90 are available for chaperones from *Escherichia coli* (2IOP, 2IOQ) [35], yeast *S. cerevisiae* (2CG9, 2CGE) [36] and the dog endoplasmic reticulum (2O1U, 2O1V) [37].

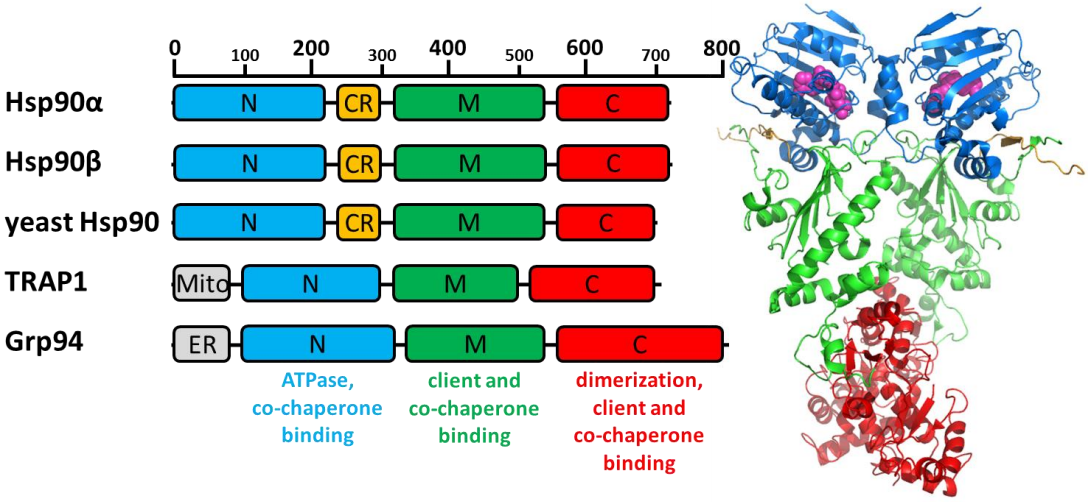

Figure 1.2. Domain structure of Hsp90. Comparison of the domain structures of human Hsp90α, Hsp90β, yeast Hsp90, human Trap1, and Grp94. N-terminal domain (also known as ATPase domain, with ATP molecule shown as purple) is marked blue both in the sequence representation and structure of full-length yeast Hsc82 (PDB ID 2CG9), as well as in Figure 1.1. Flexible charged linker is depicted in yellow, M-domain (middle) – green, C-domain (dimerisation) – red, and localisation signals in grey. Based on [20; 34].

1.2.3. Clients and functions of Hsp90

To date over 300 proteins that interact with Hsp90 are identified. Full list of known Hsp90 interacting proteins can be found at Picard Lab website [38] and online database *Hsp90Int* [39], and a recent review [40]. However, not all of the identified interacting proteins are clients; for instance, some are co-

chaperones. Searches for proteins that depend on Hsp90 by specifically inhibiting Hsp90 yield not only Hsp90 clients but also proteins that are dependent on the Hsp90 clients. Therefore in order to prove a protein to be an Hsp90 client, two requirements must be met: the protein must physically interact with Hsp90 and inhibition of Hsp90 must impair its activity. It should be noted that all currently described Hsp90 clients depend on Hsp90 even at permissive temperatures. Coupled with the distinct overexpression of Hsp90 at elevated temperatures, this suggests that the range of Hsp90 substrates might increase significantly at elevated temperatures [41].

Interestingly, despite Hsp90 reputation of having a limited clientele compared to other classes of chaperones, which bind to nascent polypeptide chains, approximately a fifth of yeast proteome is influenced by Hsp90 function [42]. This is achieved through chaperoning proteins that are hubs of many biological networks [2], namely, transcriptional factors [43-45] and kinases [46-48]. These proteins are involved in various signalling pathways and thus collectively influence a multitude of vital cellular processes. Among transcriptional factors, the steroid hormone receptors (SHRs) are the best studied class of Hsp90 model substrates. They require Hsp90 assistance mainly for constant maintenance of their activity [49]. Tumour suppressor protein p53, which is mutated in many forms of cancer [50] is also reported to interact with Hsp90 [51; 52]. Various types of kinases are also reported to associate with Hsp90. In fact, Hsp90 was first discovered as a co-precipitant of protein tyrosine kinase v-Src [53]. v-Src is the key player in transforming normal avian or mammalian cells into malignant cancer cells in case of Rous sarcoma virus. It has a much higher kinase activity and higher affinity towards Hsp90 than its cellular counterpart, c-Src [54], which is involved in cell control of cell growth and architecture, even though sequence differences between c-Src and v-Src are minor [55]. Notably, Hsp90 is necessary for maturation of c-Src and some other kinases, such as p56, but not its activity [56], while it is *vice versa* in case of SHRs. Besides the discussed regulatory proteins, Hsp90 is involved with a

great variety of other proteins, from telomerase to myosin. There is no obvious sequence or structural homology between Hsp90 clients. Different clients might bind to different sites of Hsp90 as each of the three Hsp90 domains have been implicated in client binding [57].

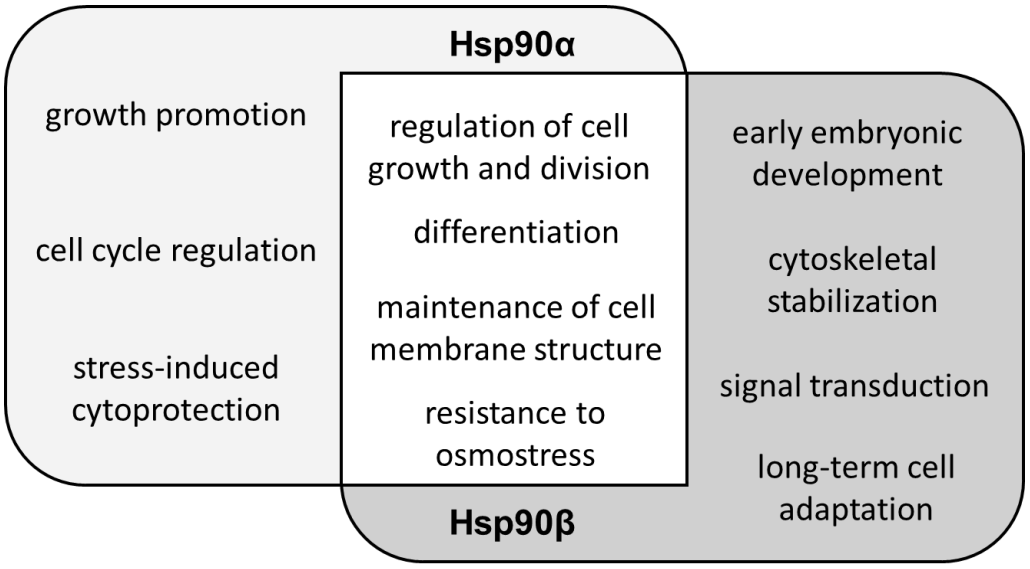

Figure 1.3. Cellular functions attributed to Hsp90α isoform (light grey), to Hsp90β (darker grey), or to both of them (white).

In the light of its numerous clientele, Hsp90 is considered to be responsible for a variety of biological functions: cell cycle regulation, maintenance of plasma membrane integrity and resistance to osmotic stress. There is no definite boundary between the functions of α and β forms on account of their structural similarity and consequent sharing of clientele. Therefore the defined differences in function (Figure 1.3) relies mostly on Hsp90α being more of an emergency service while Hsp90β plays a housekeeper's role.

An interesting example of intricate Hsp90 function is accumulation of cryptic genetic mutations under normal conditions and their release under stressful conditions. Inhibition of this chaperone significantly increases morphological variation in *Drosophila* [58] and upregulates transposon

expression [59]. It seems that Hsp90 stabilises the variation in phenotype by chaperoning Argonaute proteins [60] and thus supressing transposon activity.

1.2.4. Conformational cycle of Hsp90

Hsp90 activity as a chaperone generally must be complemented with its ATPase activity [61; 62]. Both these functions intertwine in a complex Hsp90 conformational cycle (Figure 1.4). The necessary conformational changes can be accelerated or halted by co-chaperones. Even *in vitro*, where Hsp90 is not inhibited by certain co-chaperones, the rate-limiting step of the slow Hsp90 ATPase activity (1 ATP per 20 min by human Hsp90 [63]) is the structural change, as opposed to the ATP turnover [64; 65].

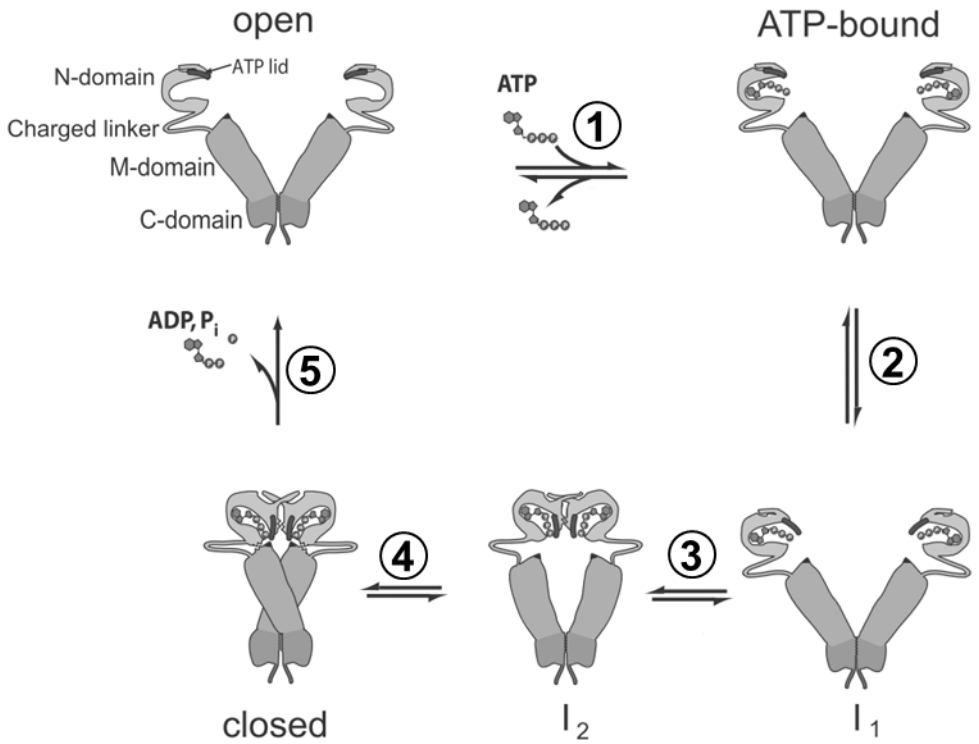

Figure 1.4. Conformational cycle of Hsp90. (1) Open Hsp90 rapidly binds ATP. (2) ATP lids slowly fall into place, forming first intermediate state, I_1. (3) Dimerization of N-domains results in formation of second intermediate state, I_2. (4) M-domain repositions in order to interact with N-domain; Hsp90 reaches the fully closed conformation. (5) ATP is hydrolysed and Hsp90 returns to the open conformation. Adapted from [66].

Hsp90 is a flexible dimer. When not bound to ATP, it adapts an open conformation, resembling a "V" shape (Figure 1.4). Upon ATP binding, first minor conformational changes occur as so-called ATP lids (flexible α-spirals) close over the bound nucleotide [67] (Figure 1.4, steps 1 and 2). At this stage a client protein can be introduced to the chaperone. The closure of ATP lids enables dimerization of the N-domains [68], which occurs in a fashion characteristic to the GHKL family (step 3). These conformational changes induce further rearrangements in the entire Hsp90, resulting in intercrossed M-domains [36; 67] that can interact with the γ-phosphate of the bound ATP (step 4). The resulting shape is a compact dimer, referred to as closed state (Figure 1.2). Finally, the ATP hydrolysis ensues and the unfolded client, as well as ADP, detach from Hsp90, which hence returns to the open state (step 5). Although the cycle was uncovered using Hsp90 from yeast (Hsp82), its relevance was confirmed for human Hsp90 [69], as well as Grp94 [37] and TRAP1 [70]. Therefore the described ATPase mechanism seems to be universally conserved in Hsp90 family. It has been suggested that Hsp90β moves through its conformational cycle slower than the α isoform and thus stays bound to the client protein for longer periods of time, though rates of ATP hydrolysis are comparable at least *in vitro* [69].

1.2.5. Regulation of Hsp90 activity

Hsp90 chaperoning is controlled in cells by a number of factors, mainly co-chaperones and post-translational modifications.

Co-chaperones

Almost every step in the Hsp90 conformational cycle can be regulated by co-chaperones. Co-chaperones may be loosely defined as proteins that participate in the function of chaperones [71]. They can deliver (or mediate

delivery of) client proteins and coordinate the chaperone cycle in a way that promotes dissociation of the client protein (usually by influencing ATPase activity). Most co-chaperones bind to Hsp90 with submicromolar affinities [72]. The evolution and abundance of such co-chaperones in complex organisms might attest for the expansion of the range of biological processes that require Hsp90 [71]. Here only a handful of plentiful Hsp90 co-chaperones are presented.

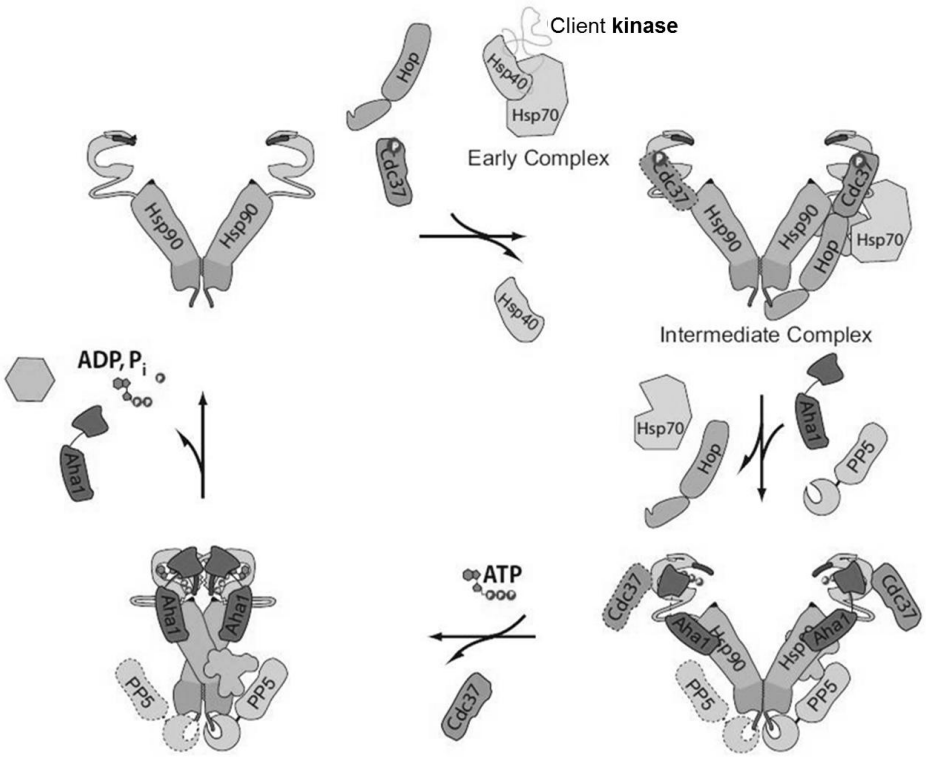

Figure 1.5. Co-chaperones regulate the Hsp90 chaperone cycle for kinases. Co-chaperones Hop and the kinase-specific Cdc37 are involved in recruiting early complex, comprised of the client kinase and Hsp70/Hsp40, to Hsp90. Hop and Hsp70/Hsp40 are expelled with the aid of co-chaperones protein phosphatase PP5 and Aha1. Later on, ATP is bound and Cdc37 can be released. Taken from [66].

Since Hsp90 can bind clients only in open conformation, the co-chaperones involved in client delivery tend to bind to the open Hsp90 and inhibit its transition to the intermediate conformations (Figure 1.5) in order to buy some time for binding of the client [73]. One of the most well-studied such co-chaperones is Hop (Sti1 in yeast). Hop binds to the open conformation of

Hsp90—ATP mainly via a MEEVD motif in the extreme C-terminus of Hsp90 [74]. It not only stabilises the open conformation, but also serves as a docking site for Hsp70 bound to clients [75]. Hop participates in maturation of SHRs [72]; kinase folding is usually also aided by a co-chaperone p50 (Cdc37) (Figure 1.5). p50 binds to the ATP lids themselves, thus jamming Hsp90 in the open state. Additionally, it suspends the ATP hydrolysis via interactions with a catalytic amino acid residue [76].

Hsp90—Hop—Hsp70—client complex is recognised by PPIase or Aha1 and PP5. Together with the nucleotide, these co-chaperones efficiently expel Hop [68]. This results in dissociation of empty Hsp70, leaving the client bound to Hsp90. Increasing ATP hydrolysis rate more than tenfold, Aha1 is the most effective known Hsp90 ATPase activator [77]. It binds to the N- and M-domains of Hsp90 and facilitates the chaperone's transition to the I_2 state [78]. Aha1 is especially critical to the activation of several specific clients such as v-Src and glucocorticoid receptor [79]. At least in case of SHRs, Aha1 is displaced by p23 (Sba1). p23 stabilises the closed 2 conformational state of Hsp90 [80] and thus delays the ATP turnover [36].

Post-translational modifications

Post-translational covalent modifications regulate Hsp90 interactions not only with its clients but with the co-chaperones as well. Hsp90 can be phosphorylated, S-nitrosylated, acetylated, ubiquitinated, or, in rare cases, oxidised. The modification sites are spread through all the length of Hsp90.

Hsp90 is considered a phosphoprotein in general. The steady-state number and locations of bound phosphoryl groups depend on cellular environment and species of the organism [81; 82]. Phosphorylation can affect the conformational cycle of Hsp90 by influencing formation of the active sites, inter-domain communication, and general flexibility [83; 84]. Kinases can subject Hsp90 to degradation, adjust its affinity towards co-chaperones or

certain clients [85]. Interestingly, most of kinases that phosphorylate Hsp90 are also Hsp90 clients [66].

Another frequent modification of Hsp90 is acetylation. This process is dynamic and tightly regulated. Generally upon acetylation the affinity of Hsp90 towards specific clients is decreased or completely terminated [86]. For instance, unless HDAC6 reverses the p300-mediated acetylation of Hsp90, function of several Hsp90 clients, including glucocorticoid and androgen receptors, is compromised [87; 88]. Furthermore, specific targeting of either HDAC6 or its target Hsp90 can result in Treg-dependent suppression of autoimmunity and transplant rejection [89].

Endothelial nitric oxide synthase (eNOS) requires association with Hsp90 for synthesis of NO. At high enough concentration of NO, S-nitrosylation of Hsp90α C597 occurs. This prevents dimerisation of Hsp90 N-domains and thus diminishes its ability to stimulate eNOS [90; 91]. Since S-nitrosylation is easily reversible [92], NO concentration is kept at a certain level.

Hsp90 function can be disrupted by ubiquitination of its lysines [93] or oxidisation of cysteines in the C-domain [94]. A more detailed overview of the complex and yet not thoroughly investigated post-translational modification system of Hsp90 can be found in several recent reviews [85; 95; 96].

1.3. Hsp90 in therapy

At first glance, Hsp90 is an unlikely drug target for treatment of any disease. First of all, this protein is pivotal to every living cell. It is highly conserved and constantly expressed so its cytosolic isoforms may constitute ~2% of the proteome in cytosol [34; 97]. It is a chaperone with several hundreds of documented interacting putative clients [38] and is involved in over a dozen cellular pathways and processes. Deletion of the protein is embryonic lethal. Moreover, there are no acknowledged disease-linked polymorphisms [98]. Considering that nowadays pharmacology aims at a

single-targeted drug that would impede a selected process and affect no other, drugging a target that is in a way responsible for many vital cellular processes is rather unusual. However, at least in the case of cancer, striking at the hub of key pathways could be the only secure way to win this battle. The majority of problems with anticancer therapy come from the flexibility of cancer cells: as the drugs block one way of their survival and prevalence, the cancer cells can rely on other means. Therefore Hsp90 might be an excellent cancer target as it suppresses most of the pathways of survival and proliferation of the cancer cells. Furthermore, in the recent years Hsp90 was noted as a putative target in other diseases, primarily neurodegenerative disorders.

1.3.1. Hsp90 in cancer

Due to unrestrained growth cancer cells are characterised by unfavourable environment for normal protein function. In general, expression of chaperones increases in cancer cells at least several times [21; 99]. In case of breast cancer, overexpression of Hsp70 and Hsp90 correlates with poor prognosis [100; 101]. The excessive Hsp90 is needed to chaperone a multitude of rapidly synthesised proteins and especially to aid the mutated proteins involved in carcinogenesis.

The specificity of Hsp90 as a druggable anticancer target lies in both its aberrant function and the overuse of Hsp90 as well as its clients in cancer cells [102]. Hsp90 in tumour cells binds tighter to its inhibitors as well as ATP and co-chaperones [103; 104]. This phenomenon might be contributed to putatively altered post-translational modification state of Hsp90 [105]. Moreover, Hsp90 inhibitors tend to accumulate in cancer cells more effectively as compared to normal tissue [106]. Furthermore, while most of the abnormal proteins and cellular pathways vary greatly between different types of cancer, Hsp90 is required for their folding, stability, or activity in most cases [107; 108].

Characteristics of a cancer cell	
Phenotype	Hsp90 client
1. Uncontrolled proliferation	MET, ERB-B2, KIT, EGFR, SRC, RAF, VEGFR, AKT, Her2, MEK, Bcr-Abl
2. Impaired apoptosis	survivin, cMET, BCR-ABL, RIP, mutant p53, SRC, Apaf-1, IGF-1R, AKT
3. Resistance to antigrowth signals	CDK4, Cyclin D, CDK6, Plk, Wee1, Myt1
4. Invasion, metastasis	cMET, urokinase, SRC, MMP-2
5. Angiogenesis	VEGF, Flt-3, MET, FAK, HIF-1α, AKT, SRC
6. Immortalization	telomerase

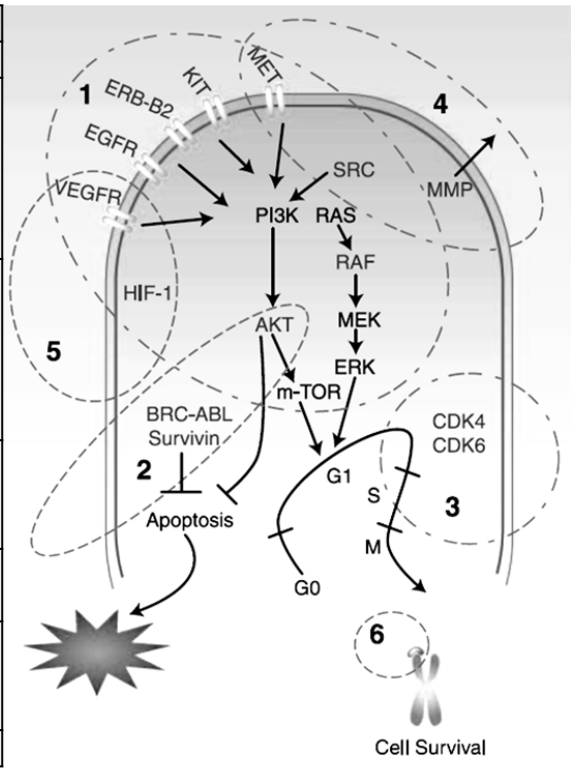

Figure 1.6. Hsp90 clients are involved in all hallmark processes of cancer: 1) uncontrolled proliferation, 2) inhibition of apoptosis, 3) resistance to antigrowth singals, 4) metastasis, 5) angiogenesis, and 6) immortalization. Based on [3; 109; 110].

There are 6 hallmarks of cancer cells discerned in literature [111]: self-sufficiency in growth signals, insensitivity to anti-growth signals, evading apoptosis, sustained angiogenesis, tissue invasion and metastasis, and limitless replicative potential. Basically, this means that cancer cells proliferate uncontrollably and indefinitely, as well as has means of spreading. As it is evident from Figure 1.6, there are Hsp90 clients involved in all these main processes of carcinogenesis. Moreover, Hsp90 also allows cancer cells to tolerate otherwise lethal mutations by stabilising mutant proteins [112]. Usually anticancer drugs target specific proteins involved in one of these processes, but there is none discovered to be able to unhinge all 6 of them simultaneously [113].

The basis for one of these hallmarks, the “immortality” of cancer cells, is the use of telomerase. Normally, fully differentiated cells cant replicate due to

loss of significant part of their telomeres [114] and only the highly proliferative cell types such as germ and somatic stem cells express telomerase to maintain their replication [115]. Almost 9 out of 10 malignant tumours display telomerase activity [116]. Hsp90 is required for assembly of functional telomerase and is a part of the functional human telomerase complex [117]. In some cases of cancer, Hsp90 is also exploited to enhance the telomerase expression [118].

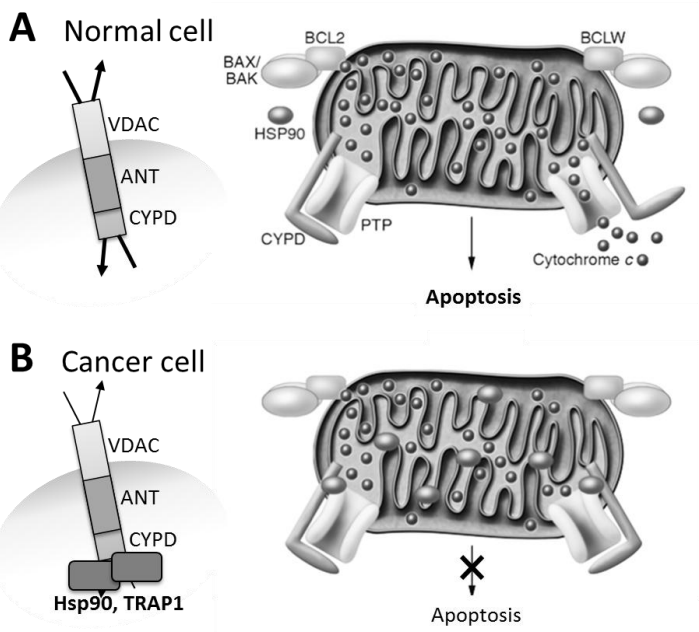

Figure 1.7. The role of Hsp90 in preventing apoptosis in cancer cells. (A) In normal cells under high stress conditions, CypD-based mitochondrial channels adapt a more permeable conformation and release cytochrome c into the cytosol, thus initiating apoptosis. (B) In cancer cells, these channels are being kept in the less permeable conformation by Hsp90 and TRAP1. Adapted from [119; 120].

A potentially immortal cell must obstruct apoptosis. Normally mitochondrial channels that contain cyclophilin D (CypD) are in low permeability conformation, allowing only little transport between matrix and cytosol [121]. But in a normal cell under considerable stress these channels assume high permeability conformation and thus let the pro-apoptotic proteins spill out of mitochondria into the cytosol [122] (Figure 1.7A). To circumvent this, both TRAP1 and Hsp90 are present in mitochondria of cancer cells [123].

These chaperones interact with each other and bind to CypD, preventing the channel from changing conformation to a more permeable and thus preventing apoptosis [123] (Figure 1.7B).

Another major trait of cancerogenesis is metastasis. Although only less than 1 in 10 000 of metastasizing cells manage to survive and set up in a new place [124], it is sufficient for establishment of discrete tumours throughout cancer patient's body. As most human cells are firmly linked to each other and to extracellular matrix by special proteins, a metastasizing cell must first detach from the tumour [125]. For this reason cancer cells are often characterised by lack of functional adhesion proteins [126]. Moreover, cancer cells employ Hsp90α secretion, which normally occurs in case of injury or other stress in order to promote cell motility and thus microphage access [127; 128], to allow weaker bonds with environment and thus metastasise more easily [129; 130]. Therefore even membrane impermeable Hsp90 inhibitors reduce metastasizing significantly [131; 132]. The disengaged cell has to reach bloodstream or lymphatic system. Tumours are capable of promoting angiogenesis, the forming of new blood vessels [133]. But even if a normal cell entered bloodstream, its nucleus would be prohibited from developing the cell while it is unattached via a certain system, characteristic to all cells. Cancer cells cheat this system by keeping a certain protein active, in such a way deceiving nucleus and continuing to grow [134].

Hsp90 involvement in cancer progression is not limited to the few here briefly described strategies. Overall, appeal of Hsp90 as anticancer drug target is not restricted only to theoretical approach, but is also evidenced by multiple Hsp90 inhibitors in Phase I-III clinical trials [135].

1.3.2. Hsp90 and neurodegenerative diseases

In recent years Hsp90 inhibitors have received attention as a possible treatment for neurodegenerative diseases. These diseases arise from CNS cell

death which is usually caused by cytotoxic accumulation of misfolded proteins [136]. This could be detained or even reversed by molecular chaperones. Thus the application of Hsp90 inhibitors in therapy of neurodegenerative diseases is rather exceptional: in this case Hsp90 is inhibited in order to increase expression of Hsp70 and other chaperones [137]. The general idea behind this strategy is as follows (Figure 1.8A). In cells client-free Hsp90 is bound to HSF-1. As the cell undergoes stress and more Hsp90 is required by its clients, Hsp90—HSF-1 complex dissipates. Free HSF-1 trimerises and is phosphorylated on its way to nucleus [138]. Such fully active HSF-1 trimer activates transcription from most of *hsp* genes, including *hsp70* [139]. In abundance ubiquitous Hsp70 is able to counteract aggregates in cells [137]. In addition, Hsp90 is reputed to stabilise even pathogenic protein mutants and hence allow formation of aggregates [140]. One of the major advantages of such neurodegenerative diseases therapy is that it potentially requires only low doses of certain Hsp90 inhibitors as there is no need to fully drug the chaperone [141].

Alzheimer's disease is the most common neurodegenerative disorder, affecting more than 10% among aged 65 years and older [142]. It manifests as memory loss, speech, and reasoning disorders. In a common disease scenario, Tau proteins dissociate from cytoskeleton and aggregate [143] (Figure 1.8B). Deprived of stabilizing Tau proteins, the microtubules, which are vital to signal transmission in neurons, begin to collapse. As these processes originate from Tau hyper-phosphorylation, mediated by Hsp90 client kinases [144; 145], treatment with Hsp90 inhibitors should work both directly (by lowering levels of phosphorylation) and indirectly (by upregulating other Hsps that can reduce aggregates). Successful results have been achieved in mouse models [146] and human neuron culture [141]. Alas, the described process is only one of many causes of Alzheimer's disease. Induced Hsp70 can aid in several other disease-linked aggregation cases (Figure 1.8C), but whether it can cope with all other aggregates, attributed to Alzheimer's disease, remains to be determined.

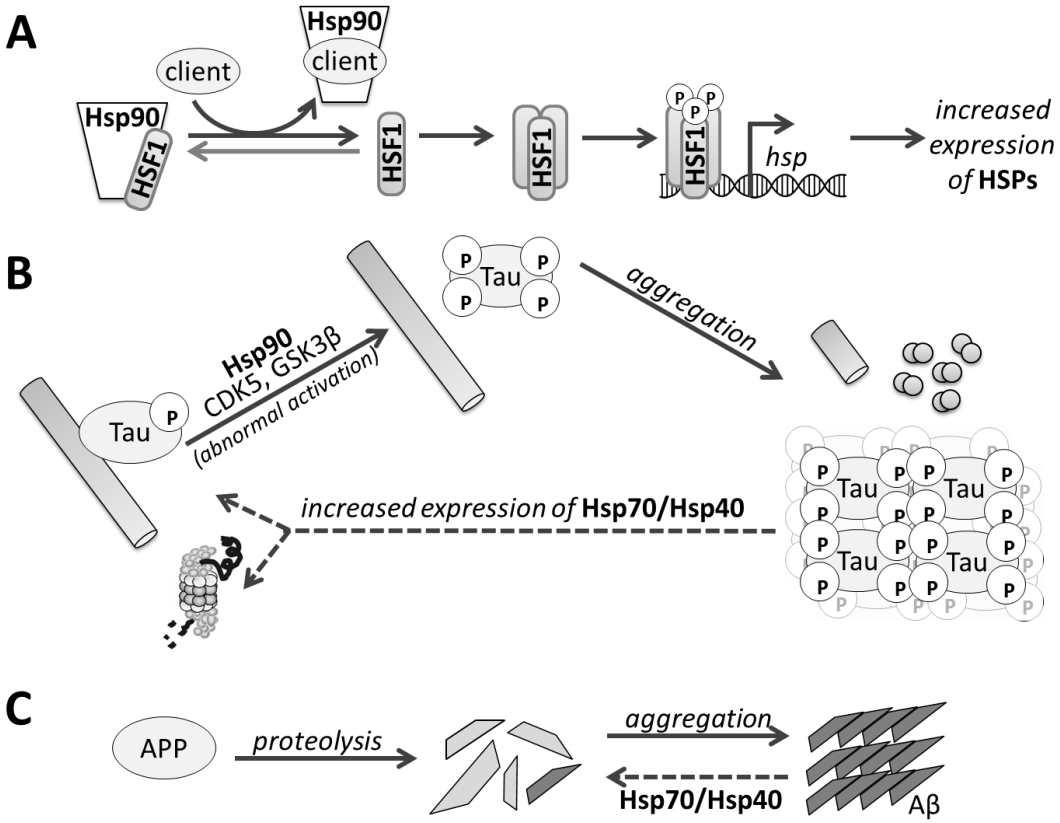

Figure 1.8. Mechanism of Alzheimer's disease progression under usual circumstances (solid arrows) and amelioration upon increased Hsp expression, caused by Hsp90 inhibition (dashed arrows). (A) HSF1 is a transcription factor that induces expression of HSPs in its trimer state. A fraction of Hsp90 prevents HSF1 from trimerising; however, when more Hsp90 is required – due to stressful protein conditions or inhibition,– more of HSF1 is released and thus the HSP expression is increased. (B) Abnormal activation of kinases CDK5 and GSK3β, both clients of Hsp90, results in increased phosphorylation of Tau. Hyperphosphorylated Tau loses its affinity to microtubules and no longer stabilises them, causing them to disassemble. Hsp90 inhibition not only restricts the hyperphosphorylation, but also increases expression of Hsp70 and Hsp40, chaperones that can increase the solubility and affinity to microtubules of Tau or commit the damaged Tau to proteasomal degradation. (C) Proteolysis of APP protein can result in peptides that are prone to aggregation (dark grey). Hsp70 and Hsp40 can disassemble these aggregates as well. Based on [147; 148].

Another widely known neurodegenerative disease is Parkinson's disease, manifesting in movement disorders. The disease develops as α-synuclein, a protein interacting with microtubules, is being significantly overexpressed in neurons, involved in transmission of motor signals. Hsp90 aids α-synuclein in oligomerisation, which finally leads to formation of Lewy bodies that cause

neuron death [149; 150]. Induced by Hsp90 inhibitors, overexpression of Hsp70 can prevent the accumulation of Lewy bodies in *Drosophila*, yeast model, and mice [151]. Parkinson's disease can be caused by mutations of several other proteins, including LRKK2 [152]. If toxic LRKK2 mutant was not stabilised by Hsp90, the protein would be simply degraded [152; 153]. Therefore in case of Parkinson's disease Hsp90 inhibitors would also achieve the goal via both direct and indirect pathways.

Overall, Hsp90 inhibitors seem to be a promising but yet clinically untested cure for neurodegenerative diseases, mainly by actuating overexpression of other Hsps that can dissolve protein aggregates. Their applications in other neurodegenerative diseases are addressed in several reviews [109; 147].

1.3.3. Hsp90 and infections

Contrarily to other discussed diseases, protozoan infections might be approached by targeting not human but protozoan Hsp90. Hsp90 is especially important for triggering important stage transitions during life cycles of such intracellular protozoan parasites like *Plasmodium* [154], *Trypanosoma*, *Leishmania* [49], and *Toxoplasma* [155]. *Plasmodium falciparum* causes the most serious form of malaria. Its Hsp90 differs from human Hsp90 by 40% of amino acid sequence [156]. The major difference is 30 amino acid long stretch of protozoan Hsp90 linker region adjoining the ATP binding domain, which might be the reason for the 6-fold higher ATPase activity of *Plasmodium* Hsp90 compared to human Hsp90 [156]. For this reason *P. falciparum* Hsp90 is more sensitive to Hsp90 inhibitors than the human homolog. As Hsp90 active centre is highly conservative among the Protozoa, its inhibitors might prove broad-spectre anti-protozoan drugs [157]. As the resistance to current specific anti-protozoan drugs advances [30], inhibitors of protozoan Hsp90 might receive much more attention in the coming years.

Hsp90 inhibitors might also be employed in treatment of lethal fungal diseases. Current fungicides are either toxic or their activity spectrum is limited, or their resistance has already emerged. Moreover, most of the few existing antifungal drugs display fungistatic but not fungicidal activities. Therefore sooner or later in a drug-suppressed fungal culture a spontaneous mutation occurs, producing a drug-resistant strain [158]. However, if the antifungal agent is coupled with a Hsp90 inhibitor, the efficacy of the drug is enhanced greatly as Hsp90 inhibitors prevent emergence of drug resistance and thus the fungicidal activity of the drug can manifest [159; 160].

Many human viruses tend to employ the cytosolic human Hsp90 for their protein folding, stabilization, or activation. Among these Hsp90-dependent pathogens are influenza A virus, poliovirus, and hepatitis C virus. Hsp90 inhibition has been proven a quite successful antiviral strategy in tissue culture in cases of various viruses [161]. Administration of Hsp90 inhibitors to animals infected with poliovirus or hepatitis C virus mitigated viral replication, with little toxicity to the infected host [162; 163].

Since chemotherapy often results in overall exhaustion which might lead to infections, the ability to not only effectively cure cancer but also combat various infections is very appealing.

1.3.4. Hsp90 and other diseases

Rheumatoid arthritis is a prevalent autoimmune inflammatory disease, characterised by aberrant infiltration of various cells into the joint synovial tissue. It often leads to disability and sometimes even mortality [164]. Rheumatoid arthritis can be compared to cancer due to abnormal cytokine and receptor signalling, angiogenesis, and cell invasion [165]. As with most here described diseases, there are no fully effective cure for rheumatoid arthritis to date [166]. Experimental data suggests that treatment with Hsp90 inhibitors interrupts several signalling pathways, induces Hsp70 expression and

suppresses angiogenesis [165]. As the cell loses active Hsp90 clients, the cytokine production decreases significantly. Hsp90 inhibitors have proven themselves in rat arthritis models [165] and were shown to be able to aid in cases of other inflammatory diseases [167].

In case of severe hereditary disease cystic fibrosis, activity of all mucus-producing glands is compromised. Majority of such patients possess a mutated protein CFTR, an ion channel, involved in Cl^- transport through membrane of epithelial cells [168]. Interestingly, although the CFTR mutant retains its activity, Hsp90 recognises it as an incorrect folding version of its client, and targets it for degradation. Was Hsp90 inhibited, degradation of mutant CFTR should be prevented and it could perform its biological function [169].

Potential clinical role for Hsp90 inhibitors has also been demonstrated in cases of cardiac diseases [170], diabetes mellitus [171], and reversible contraceptive for men [172].

1.4. Hsp90 inhibitors

Given the potential of Hsp90 inhibitors to treat such critical and widespread illnesses as cancer and neurodegenerative diseases, a number of researches are being conducted to discover a potent and non-toxic Hsp90 inhibitor. Several of such compounds have already entered clinical trials [135]. There are several strategies of blocking Hsp90 activity (Figure 1.9), the most popular being the obstruction of ATP binding to the N-domain. Others focus on disrupting co-chaperone or client interactions with Hsp90. The latter, as well as yet unexploited interference with post-translational modifications of Hsp90, could potentially be much more specific as it would prevent Hsp90-mediated maintenance of individual clients in contrast to impeding any function of Hsp90 [107]. Moreover, a couple of compounds impeding Hsp90 dimerization have been identified [173; 174].

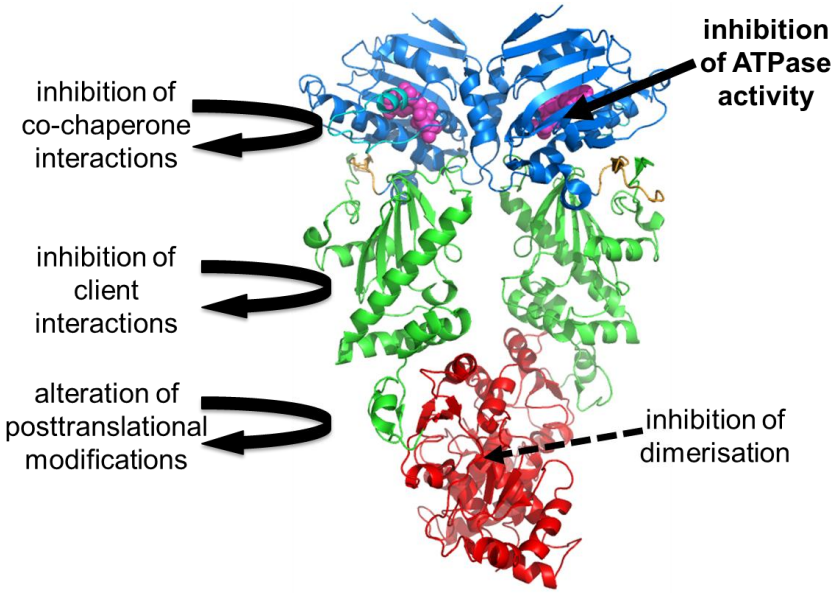

Figure 1.9. Multiple ways to impede activity of Hsp90.

1.4.1. Hsp90 inhibitors targeting the ATP binding site in N-domain

Antibiotic activity and growth-inhibitory effect on cancer culture of an asamycin compound geldanamycin (GA), naturally produced by *Streptomyces hygroscopicus*, has been known since 1970 [175] but only in mid-1990s Hsp90 has been identified as GA's molecular target [54]. GA competes with ATP for binding to the nucleotide binding site in N-domain [176], disrupts formation of the closed Hsp90 complex (see 1.2.4) [177] and thus prevents full chaperone cycling. Shortly, the same mechanism has been assigned to radicicol (RD), a natural product isolated from fungus *Monocillium nordinii* and *Monosporium bonorden* in 1953 [178]. Though invaluable to determining Hsp90 interactome and establishment of Hsp90 as anticancer target [179-181], these natural inhibitors proved too unstable, toxic, and not soluble enough for clinical development [182; 183].

First semisynthetic Hsp90 inhibitors were derivatives of GA, 17-allyl-amino-17-demethoxygeldanamycin (17-AAG) and 17-dimethylaminoethyl-amino-17-demethoxygeldanamycin (17-DMAG) (Figure 1.10). Both

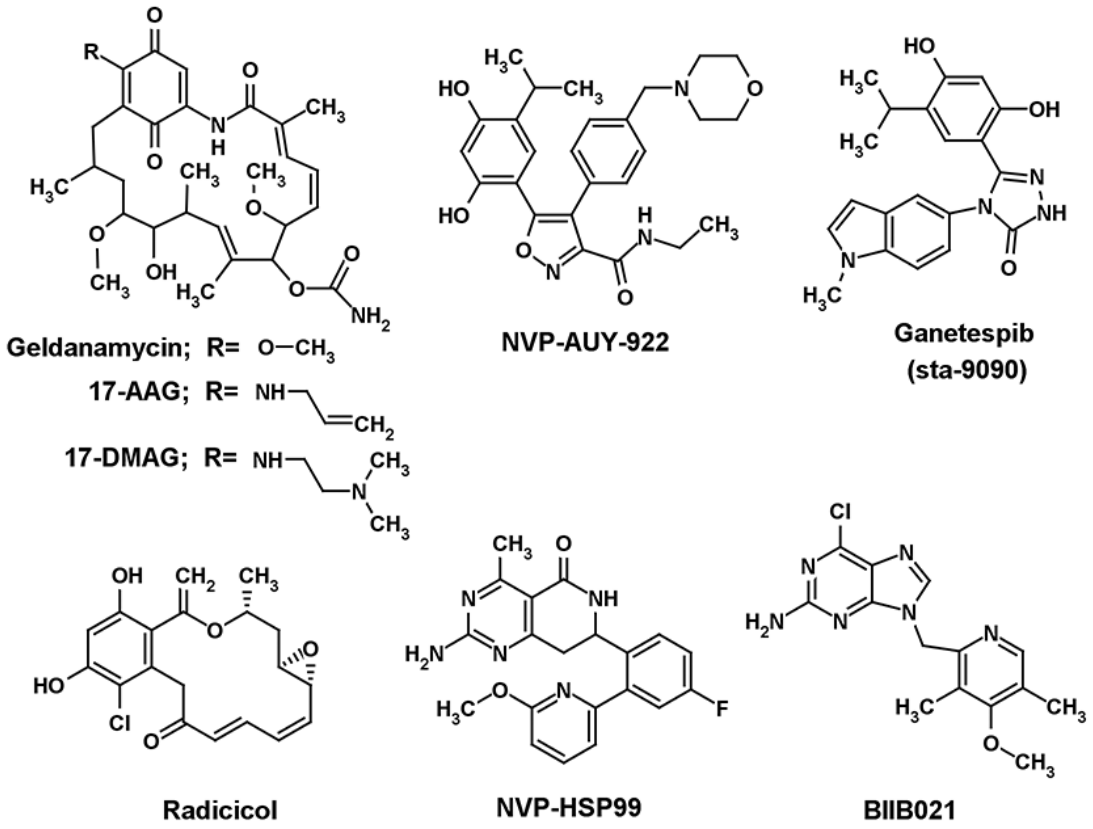

Figure 1.10. Chemical structures of various selected Hsp90 inhibitors.

compounds retained the antitumor properties of GA while exhibiting a more favourable and acceptable safety profile. The best accepted formulation of 17-AAG is tanespimycin, which has exhibited the most impressive clinical activity to date in its Phase I/II/III clinical trials (Table 1.1) [184]. The most common side-effects (such as nausea and headache) were readily managed with supportive medications. However, further development of 17-AAG was suspended in 2008 for nonclinical reasons [185]. Although it invoked several complete responses in Phase I clinical trials [186; 187], 17-DMAG also exhibited ocular toxicity even in minor doses and proved to be overall more toxic than tanespimycin [185]. Currently the soluble hydroquinone form of 17-AAG, retaspimycin (also known as IPI-504), is being tested in Phase III clinical trials (Table 1.1) [188]. However, one of the limitations of 17-AAG is its requirement for benzoquinone reduction mediated by NQO1/FT-diaphorase, which provides an opportunity for drug resistance acquisition [189; 190]. The

exhibited toxicities are partly assigned to the chemical reactivity of this benzoquinone group and not a direct consequence of Hsp90 inhibition [191].

Table 1.1. Hsp90 inhibitors in clinical trials (AML – acute lymphoblastic leukaemia; NSCLC – non-small-cell lung cancer; GIST – gastrointestinal stromal tumour; CML – chronic myeloid leukaemia; CLL – chronic lympocytic leukaemia) Based on [107; 185; 192].

	Combination therapy	Phase	Tumour responses reported
Geldanamycin analogues			
Tanespimycin (17-AAG)	-, Bortezomib Gemcitabine Paclitaxel Sorafenib	I/II/III	HER2+ breast cancer, myeloma
Alvespimycin (17-DMAG)	- Paclitaxel Transtuzumab	I	AML, myeloma, prostate, breast, ovarian cancer
Retaspimycin (IPI-504)	- Transtuzumab	I/II/III	NSCLC, GIST, breast cancer
IPI-493	-	I	-
Radicicol derivatives			
Ganetespib (STA-9090)	- Docetaxel Plerixafor Transtuzumab	I/II/III	rectal cancer, myeloma, NSCLC, CML, AML
NVP-AUY922 (VER52296)	- Bortezomib/dexamethasone Capecitabine Cetuximab Docetaxel Erlotinib hydrochl. Transtuzumab	I/II	HER2+ breast cancer, NSCLC
HSP990	-	I	-
AT-13387	- Abiraterone Crizotinib	I/II	GIST
KW-2478	Bortezomib	I/II	-
Purine derivatives			
BIIB021 (CNF 2024)	- Aromasin	I/II	CLL, HER2+ breast cancer
Debio 0932 (CUDC-305)	-	I/II	-
PU-H71	-	I/II	-
Other compounds			
SNX-5422	-	I	-

Although RD is devoid of *in vivo* activity due to its rapid degradation, its resorcinol core is the key element of a variety of synthetic Hsp90 inhibitors [193] (Figure 1.10). These can be classified into triazole, isoxazole, and other derivatives [185]. For instance, NVP-AUY922 is being evaluated in Phase I and II trials (Table 1.1), both as single-agent and in combination with other biologic agents. Ganetespib has already reached Phase III trials (Table 1.1) with clinical responses being reported in cases of a variety of cancers [185; 194]. While nausea and vomiting seem to be fairly common side-effect of Hsp90 inhibitors, the diversity and inconsistency of other significant side-effects allows assumption that such toxicities are compound-dependant and not a direct result of Hsp90 inhibition.

Crystallography studies revealed that ATP (or ADP) bound to Hsp90 adopts a unique bent shape that is not observed in high-affinity ATP-binding sites of kinases or in other chaperones [191], thus providing a chance for selectivity. Both GA and RD take on an analogous bent shape once bound to Hsp90. This feature was also exploited developing the first series of synthetic small-molecule Hsp90 inhibitors that were based on a purine scaffold [195]. These compounds demonstrate insensitivity to multidrug resistance, high aqueous solubility, and oral bioavailability [196; 197]. Several compounds of this inhibitor series have entered Phase II clinical trials (Table 1.1).

Overall clinical experience with Hsp90 inhibitors that bind to the ATP binding site in the N-domain of the chaperone is promising; however, single compound studies appear to have limited efficiency in most cases. Fortunately, it also suggests that these inhibitors might prove to be even more potent when administered together with other specific molecular inhibitors, especially targeting oncoproteins that are Hsp90 clients [107; 185]. Due to ability to trace the position of certain Hsp90 inhibitors and their lack of significant toxicity, these compounds are ideal agents for combinatorial treatments [198].

1.4.2. Alternative approaches for targeting cytosolic Hsp90

Alternative sites for Hsp90 inhibition include a non-ATP-binding region of the N-domain, the charged linker, and a putative nucleotide-binding site in the C-domain [181]. The latter can be targeted by the coumarin antibiotics, such as novobiocin [199], but they exhibit much higher affinity for topo-isomerase II than Hsp90 [200]. This has been partially improved in two novobiocin derivatives, F-4 and KU135 [201; 202]. C-domain inhibitors tend to induce Hsp genes transcription less than GA derivatives [202; 203]. C-domain of Hsp90 is also targeted by CTPR390+, rationally designed to mimic TPR motif and thus impairing Hsp90-Hsp70 interaction [204].

A natural macrocyclic product Sansalvamide A binds between N- and M-domains and thus allosterically inhibits the interactions of Hsp90 with a variety of necessary regulatory co-chaperones [205]. Another natural compound, celastrol, is unique Hsp90 inhibitor as it interferes with interactions between Hsp90 and its co-chaperone Cdc37 and thereby destabilises several Hsp90 clients while not affecting others [206].

Several widely-known anticancer agents such as taxol [207] and cisplatin [208] are also reputed to bind to Hsp90 and thus inhibit the chaperone among many other cellular macromolecular targets. However, all these drugs display only modest selectivity for cancer over normal cells [107], in contrast to the Hsp90 inhibitors that target its ATPase activity.

1.4.3. Targeting mitochondrial Hsp90

Survivin, abundant in cancer cells while absent in normal cells, inhibits apoptosis and in such a way plays a pivotal role in tumorigenesis [209]. As it requires constant stabilization by Hsp90, Plescia *et al.* engineered a cell-permeable peptidomimetic shepherdin to interact with the binding interface between survivin and Hsp90 [210]. However, its remarkable ability to induce

cancer cell death cannot be caused by survivin degradation on its own [209]. It also affects levels of several other proteins while not promoting transcription of Hsp genes [210]. Apparently, the same built-in sequence required for penetration of cell membrane, allows shepherdin to cross into the matrix of mitochondria where it can inhibit Hsp90, whose mitochondrial localization is characteristic to tumour cells, and possibly TRAP1 [123]. As these chaperones interact with CypD in mitochondria of cancer cells and thus prevents apoptosis (see 1.3.1), their inhibition leads to swift tumour cell death [123; 210; 211].

Another class of antagonists to target mitochondrial pool of Hsp90 is Gamitrinibs [212]. They were constructed by joining a lipophilic cationic moiety to 17-AAG backbone via a linker sequence [212]. As shepherdin, these compounds induce apoptosis in cancer cells while eliciting minimal effects on normal cells and not inducing overexpression of Hsp70 [209; 212]. The study of Gamitrinibs opens new opportunities for both established and yet being designed Hsp90 inhibitors as it shows that certain sequences can be added to an existing Hsp90 antagonist in order to target the mitochondrial Hsp90 pool.

1.5. Thermodynamic approach on inhibitor design

Historically drug design has been based solely on structural approaches. Nevertheless, thermodynamic methods have found increasing application for drug design and development both in academic and commercial endeavours [213; 214] as they allow understanding of the driving forces of the molecular interactions comprising the binding reaction [4]. Being able to correlate thermodynamic profiles with the structures would substantially benefit the pharmaceutical industry. However, currently there is still a very long way to go from employing structural and thermodynamic techniques simultaneously for the same set of ligands and proteins so that the data could complement each other to being able to predict all necessary parameters accurately from a single experiment.

1.5.1. Thermodynamic parameters

The thermodynamic parameters that are being determined for the binding reactions are the Gibbs energy ΔG, binding constant K_b, enthalpy ΔH, entropy ΔS, and heat capacity ΔC_p. ΔG and K_b describe the magnitude of probability of the binding event or, in other words, the ligand affinity towards the protein. However, while often pursued in drug design, high affinity is not a requirement for high selectivity and specificity [215]. The nature of the binding can be described by the balance of ΔH and ΔS. ΔH is associated with the formation and disassembly of non-covalent interactions such as hydrogen bonds. ΔS describes the overall change in the degrees of freedom in the system and thus is correlated with the hydrophobic interactions and conformational changes upon binding. In contrast to K_b (from which ΔG can be calculated according to Equation (1.1)) and ΔH, entropy cannot be measured directly and is calculated from these two parameters according to Equation (1.2).

$$\Delta G = -RT\ln K \tag{1.1}$$

$$\Delta G = \Delta H - T\Delta S \tag{1.2}$$

Hydrophobic and conformational component is also associated with ΔC_p, which is the partial derivative of the enthalpy with respect to temperature. A certain degree of hydrophobicity is required for the ligand to pass through the cell membrane into the cell cytosol; on the other hand, too high hydrophobicity leads to poorer solubility.

Binding of natural inhibitors to their targets tends to be more enthalpy-driven than that of synthetic drugs [216]. This is probably due to the relative ease of engineering additional hydrophobic contacts and/or making the compound larger and more complex, as compared to designing interactions between polar groups. The geometrical arrangement of polar groups has to be at least near to optimal so as to compensate for the entropic loss that comes from decreased mobility and desolvation of the polar groups [6]. Therefore lead compounds chosen initially for further development should have higher

enthalpy contribution to the Gibbs energy of binding [5; 6]. Moreover, it has been shown than enthalpic compounds are more likely to be selective and tend to hit less off-targets [217; 218].

The thermodynamic parameters obtained during the experiments are called the observed parameters. Their values consist not only of the binding parameters, referred to as intrinsic, but also of various potential binding-linked events: solvent rearrangement, protonation and deprotonation, and conformational changes in the interacting molecules. For instance, ligand binding to a certain pocket in the protein first has to expel the water molecules from it and to break its interactions with the solvent. While the intrinsic thermodynamic profile is not a molecular explanation for binding in itself, it provides the conceptual tool for analysing the energetics of binding from structural and chemical contexts. It is essential to note that only intrinsic parameters can be correlated to the structural data [8; 219; 220].

1.5.2. Thermodynamic techniques

Calorimetry can measure thermodynamic energetics directly and is considered to be more reliable than the methods that indirectly determine van't Hoff's enthalpy. Isothermal titration calorimetry (ITC) experiments yield the complete binding picture, encompasing ΔG, ΔH, and ΔS under relevant experimental conditions. One of the binding partners is titrated with aliquots of the other under constant temperature and the released heat is measured. Construction of a binding isotherm of interaction heat as a function of titrated ligand yields $\Delta_b H$, K_b (and therefore $\Delta_b G$), and binding stoichiometry, with $\Delta_b S$ calculated from Equation (1.2). ΔC_p is obtained by performing measurements at different temperatures. Direct determination of binding parameters makes ITC an extremely powerful and useful tool; however, it can be complicated by the binding-linked events. ITC is not a standard technique in the initial high-throughput drug screening stages due to its relatively high requirement of

material and time, but it has proven its usability in the later drug development stages [4; 215].

Differential scanning calorimetry (DSC) provides the unfolding energetics profile. It directly determines protein melting parameters: $\Delta_U H$, $\Delta_U C_p$, and melting temperature T_m. Ligand binding to the protein stabilises it and increases the T_m. Determining K_b via protein unfolding profiles enables precise estimation of a much wider range of binding constants as compared to ITC approach. On the other hand, it also involves a number of assumptions and thus should be considered carefully [4; 215]. A considerably more efficient technique exploiting the profiles of protein unfolding is the fluorescence thermal shift assay (FTSA) [221]. It yields only T_m and K_b but is significantly less time and reagent consuming. Instead of tracking heat changes in the system, it measures fluorescence of a solvatochromic dye molecule that reports on unfolded protein regions.

1.5.3. Optimisation case studies

Renin is a protease involved in production of a certain potent vasoconstrictor. Its inhibitors could be applied to treat hypertension. Combined high-throughput screening and chemistry efforts at Pfizer, USA, yielded compound 1 (Figure 1.11A). Structural approach enabled design of compounds 2 and 3 (Figure 1.11A) that would occupy the adjacent unoccupied binding pockets [222]. Thermodynamic study revealed that optimisation from compound 1 to 2 was entropically driven while compound 3 had a significantly larger enthalpy contribution. Despite higher affinity of the entropically optimised compound 2, compound 3 was superior in size and lipophilic efficiency [222]. Because of this, compound 3 was chosen for further optimisation, leading to compound 4 (Figure 1.11A). While the enantiomer compound 5 exhibited a bit lower inhibitory effect, its good bioavailability in animals prompted its selection for preclinical development [6].

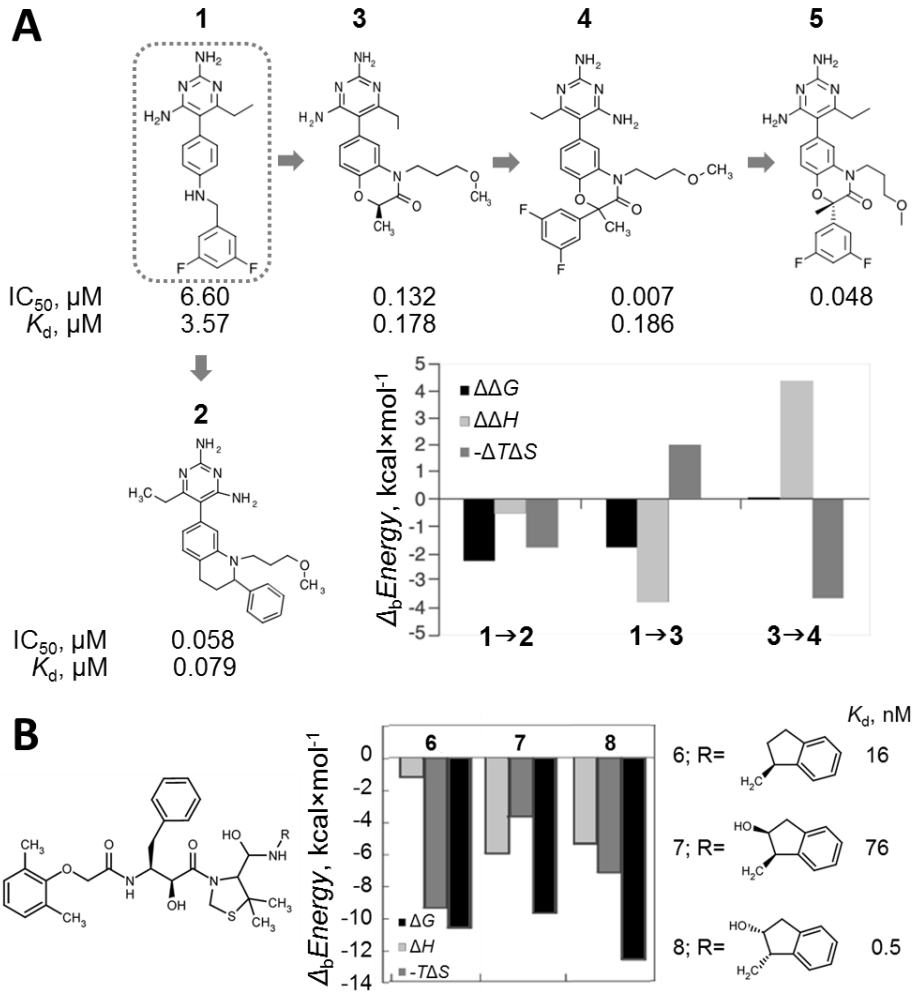

Figure 1.11. (A) Optimisation of renin inhibitors. Adapted from [6; 222]. IC_{50} is the half maximal inhibitory concentration. (B) Affinity improvement of plasmepsin II inhibitor. Adapted from [223; 224].

A study by Nezami *et al.* attempted to design an inhibitor of *P. falciparum* proteases [224]. Their main target was plasmepsin II but they sought to retain inhibitory properties towards the other 3 known proteases of this parasite as well. Addition of a hydroxyl group to compound 6 yielded compound 7 (Figure 1.11B). While compound 7 exhibited lower affinity, thermodynamic study revealed that the binding enthalpy was improved and the decrease in affinity was due to compensatory entropy loss. Therefore they tried minimising the entropy loss by changing the stereochemistry of the compound 7. The result was compound 8, which retained most of the enthalpy

contribution in compound 7 and a larger part of entropy contribution in compound 6, resulting in overall higher affinity (Figure 1.11B). This study is a good example how dissecting binding energetics into enthalpy and entropy benefits rational drug design.

2. MATERIALS AND METHODS

2.1. Materials

2.1.1. Chemicals

All chemicals used in this study were of the highest purity grade: ANS (Aldrich Chemicals, ≥ 97 %), CH_3COONa (Fluka Chemie, ≥ 99 %), DMSO (Roth, ≥ 99.5 %), H_3PO_4 (Sigma Aldrich, 85 % solution), HCl (Alfa Aesar, 36.5–38 %), HEPES (Roth, ≥ 99.5 %), $Na_2B_4O_7•10H_2O$ (Spectrum Chemical MFG corp., ≥ 99.5 %), Na_2HPO_4 (Fluka Chemie, ≥ 99 %),$Na_3PO_4•12H_2O$ (Roth, ≥ 98 %), NaCl (Roth, ≥ 99.5 %), $NaH_2PO_4•H_2O$ (Fisher Scientific, 99.4 %), NaOH (Alfa Aesar, ≥ 98 %), Tris (Sigma, ≥ 99.9 %), Tris-HCl (Sigma, ≥ 99 %).

2.2.2. Proteins

The proteins used in this study were His_6-tagged versions of the full-length human Hsp90α, its N-terminal domain Hsp90αN (1-244 amino acid residues), Hsp90β, and Hsp90βN (1-239). They were expressed in *E. coli* BL21 (DE3) and purified by means of chromatography by V. Michailovienė at the Department of Biothermodynamics and Drug Design, Institute of Biotechnology, Vilnius University. Their purity, as determined by electrophoretic analysis, was ≥ 95 %. Their molecular mass was validated by liquid chromatography coupled with mass spectrometry (LC-MS). Protein concentrations were measured spectrophotometrically (ε_{280}(Hsp90αN) = 15,930 M^{-1} cm^{-1}, ε_{280}(Hsp90α) = 62,395 M^{-1} cm^{-1}, ε_{280}(Hsp90βN) = 17,420 M^{-1} cm^{-1}).

2.2.3. Ligands

5-Aryl-4-(5-substituted-2,4-dihydroxyphenyl)-1,2,3-thiadiazole compounds (abbreviated ICPD) were synthesised as described in [225] by Prof. Dr. I. Čikotienė at the Department of Biothermodynamics and Drug Design, Institute of Biotechnology, Vilnius University, in collaboration with Vilnius University Faculty of Chemistry. They were validated using IR spectroscopy, ^{1}H and ^{13}C nuclear magnetic resonance (NMR), and MS. Their purity, as determined using MS, is as follows: ≥ 95 % for ICPD26, ≥ 80 % ICPD34, ≥ 97 % ICPD47, ≥ 95 % ICPD62.

Solid ICPD compounds were dissolved in DMSO to the final ligand concentration of 20 mM. These solutions were stored at room temperature, in dark, glass containers.

17-AAG was purchased from Selleckchem (99.88 % purity) and prepared in the same manner.

2.2.4. Buffers

Phosphate buffer: 50 mM phosphate, 100 mM NaCl. Desired pH was reached by mixing H_3PO_4, Na_2HPO_4, NaH_2PO_4, and Na_3PO_4 solutions at appropriate ratios.

Tris buffer: 50 mM Tris, 100 mM NaCl. Desired pH was reached by mixing Tris and Tris-HCl solutions at appropriate ratios.

HEPES buffer: 50 mM HEPES, 100 mM NaCl. Desired pH was reached by adding required amount of NaOH solution and diluting with water to reach the final volume.

Universal buffer: 50 mM phosphate, 50 mM CH_3COOH, 25 mM $Na_2B_4O_7$, 100 mM NaCl. Desired pH was reached by mixing appropriate ratio of H_3PO_4, Na_2HPO_4, NaH_2PO_4, and Na_3PO_4 solutions.

2.2. Methods

2.2.1. Isothermal titration calorimetry

Isothermal titration calorimetry (ITC) experiments were conducted using VP-ITC calorimeter (MicroCal, Inc.). Protein solutions (2–6 μM) were loaded into its cell (active cell volume of 1.4315 ml). Ligand solutions (20–60 μM) were loaded into the 300 μl titration syringe. Protein solution was titrated by injecting 10 μl of ligand solution 25-30 times at 3–4 minute intervals. The stirring speed was set to 260 rpm. Experiments were carried out at constant temperature in 7–43 °C temperature range. The ligand solutions were prepared in the same buffer as protein solutions, with concentration of DMSO not exceeding 2 % (v/v; usually 1 %).

Most titration experiments were repeated at least twice. Some experiments, such as titrations at borderlining pH values, were performed once. Experiments at standard conditions of pH and temperatures were repeated at least three times.

In cases of pH values in which buffer capacity of the utilised buffer is insufficient to support the required pH value, pH-meter with a microelectrode was used to confirm and adjust pH of the solutions being loaded into the calorimeter.

The obtained raw ITC data was processed using ITC module in the *MicroCal Origin 5.0* software and the observed values of binding constant (K_{b_obs}) and binding enthalpy ($\Delta_b H_{obs}$), as well as concentration correction factor *n*, for the given experiment were calculated. Error of *n* determination is ±5 % [226], in case of $\Delta_b H$ and K_b – ~10 %.

Using this software, the raw data is converted into a sigmoidal binding isotherm. Wiseman *et al.* noted that the shape of such a binding isotherm depends on K_b and the concentration of the protein [227] and proposed *c* value (also known as Wiseman parameter) to describe this shape:

$$c = nK_{\mathrm{b}}P_{\mathrm{t}}, \tag{2.1}$$

where n is the number of binding sites per protein; and P_{t} is the total protein concentration. It is estimated that c value must be between approximately 5 and 500 for an accurate ITC titration fit [228; 229]. K_{b} is calculated from the steepness of the ITC titration curve and a binding isotherm of higher c value is simply too steep. In contrast, $\Delta_{\mathrm{b}}H$ can still be determined quite accurately even in cases of higher c value but is not so precise when c value is below 5.

2.2.2. Fluorescence thermal shift assay

Fluorescence thermal shift assays (FTSA; also known as TSA, DSF, and ThermoFluor) were performed using Corbett Rotor-Gene 6000 (Qiagen Rotor-Gene Q) spectrofluorimeter. The prepared protein concentration was 5 or 10 µM and the ligand concentrations varied from 0 to 200 µM. FTSA experiments were carried out in Phosphate or Universal buffer. DMSO was added to accommodate up to 2 % of solution volume. Total solution volume was 10 or 20 µl.

During a FTSA experiment, the intrinsic protein fluorescence or the fluorescence of a solvatochromic dye is being monitored. In our experiments, we used 50 µM of a fluorescent dye 8-anilino-1-naphthalenesulfonate (ANS) to enhance the sensitivity. This concentration was chosen as yielding satisfactory signal intensity while not affecting protein binding to other ligands or protein stability. The samples were excited with 365 ± 20 nm UV light and ANS fluorescence emission was registered at 460 ± 15 nm. The changes in fluorescence yield reflect on the temperature-induced protein transition from native (N) to unfolded (U) state. This transition can be affected by a ligand (L) which stabilises or destabilises the protein upon binding:

$$\mathrm{U} + \mathrm{L_f} \overset{K_{\mathrm{U}}}{\rightleftharpoons} \mathrm{N} + \mathrm{L_f} \overset{K_{\mathrm{b}}}{\rightleftharpoons} \mathrm{NL_b} \tag{2.2}$$

The two equilibrium constants here are the protein unfolding constant, K_U, and ligand binding constant, K_b. They can be described as follows:

$$K_U = \frac{[U]}{[N]} = e^{-\Delta_U G/RT}, \quad (2.3)$$

$$K_b = \frac{[NL_b]}{[N][L_f]} = e^{-\Delta G_b/RT}, \quad (2.4)$$

where $\Delta_U G$ and $\Delta_b G$ are the Gibbs energies of unfolding and binding, respectively; L_f stands for free ligand; L_b – ligand that is bound to the protein; R is the universal gas constant; and T is the absolute temperature (K). During the thermal denaturation of the protein, it gradually unfolds, exposing previously hidden regions to the solution. ANS interacts with the hydrophobic regions of the protein. In the hydrophobic environment the fluorescence of ANS significantly increases as it is no longer quenched by the water [230; 231].

The protein stability curve is obtained by gradually increasing the temperature to denature the protein and monitoring the dye fluorescence at each temperature step. In our experiments the samples were heated from 25 to 95 °C at a rate of 1 ºC/min. The unfolding of Hsp90N proteins yielded a single transition, confirming that the single-domain protein preparations were homogeneous. The midpoint of the protein stability curve is referred to as the melting temperature, T_m. At this temperature half of protein molecules are unfolded and the other half remain in their native state.

T_m values were determined by fitting the experimentally obtained protein melting curves according to Equation (2.5) [232]:

$$y(T) = y_N + \frac{y_U - y_N}{1 + e^{-\Delta_U G/RT}} = y_U + \frac{y_N - y_U}{1 + e^{-\Delta_U G/RT}}, \quad (2.5)$$

where $y(T)$ is the observed fluorescence as a function of temperature; y_N is the fluorescence yield of the dye bound to folded protein; and y_U is the fluorescence yield of the dye bound to unfolded protein. Both y_N and y_U are functions of temperature, with slopes of m_N and m_U, respectively:

$$y_{\mathrm{N}}(T) = y_{\mathrm{N},T_{\mathrm{m}}} + m_{\mathrm{N}}(T - T_{\mathrm{m}}), \quad (2.6)$$

$$y_{\mathrm{U}}(T) = y_{\mathrm{U},T_{\mathrm{m}}} + m_{\mathrm{U}}(T - T_{\mathrm{m}}), \quad (2.7)$$

The Gibbs energy of unfolding ($\Delta_{\mathrm{U}}G$) can be expressed as in Equations (1.1) and (1.2). The temperature dependence of both $\Delta_{\mathrm{U}}H$ and $\Delta_{\mathrm{U}}S$ is defined by the heat capacity change (ΔC_{p}). As it is assumed that ΔC_{p} is temperature-independent over the temperature range studied [233], the Gibbs energy (of unfolding, $\Delta_{\mathrm{U}}G$, or of binding, $\Delta_{\mathrm{b}}G$) can be described as

$$\Delta G = [\Delta H(T_{\mathrm{R}}) + \Delta C_p(T - T_{\mathrm{R}})] - T[\Delta S(T_{\mathrm{R}}) + \Delta C_p \ln\frac{T}{T_{\mathrm{R}}}], \quad (2.8)$$

where T_{R} is any reference temperature. At $T_{\mathrm{R}} = T_{\mathrm{m}}$, $\Delta_{\mathrm{U}}G = 0$ and hence $\Delta_{\mathrm{U}}S = \Delta_{\mathrm{U}}H / T_m$. The value of ΔC_{p} for Hsp90 was estimated according to the correlation of protein $\Delta_{\mathrm{U}}C_{\mathrm{p}}$ with the number of residues [233]. $\Delta_{\mathrm{U}}H$ was determined previously for Hsp90 in [234].

The equipment allows T_{m} determination with ± 0.5 °C accuracy but its reproducibility within a single set of experiments is ± 0.02 °C. The error values presented in this work are the standard errors of several experiments.

In order to determine the Hsp90 binding constants for studied inhibitors, a series of experiments with varying ligand concentrations were conducted. Increasing concentration of the compound shifted the protein denaturation temperature T_{m} increasingly upwards depending on the binding affinity. For ligands binding to the native conformation of the protein (as in our case), the T_{m} dependency on the added amount of ligand can be described by Equation (2.9) [232]:

$$L_{\mathrm{t}} = (K_{\mathrm{U}} - 1)(\frac{P_{\mathrm{t}}}{2K_{\mathrm{U}}} + \frac{1}{K_{\mathrm{b}}}), \quad (2.9)$$

where L_t is the total concentration of the added ligand; P_t is the total protein concentration; K_{b} and K_{U} are the equilibrium constants, which are described by Equations (2.3) and (2.4) in relation to T_{m}. By varying the parameters in Equation (2.9), the model is fitted to the experimental data points and the binding constant K_{b} is obtained.

2.2.3. Differential scanning calorimetry

Differential scanning calorimetry (DSC) experiments were carried out using MC-2 scanning calorimeter (MicroCal, Inc.), raising temperature at 1 °C/min rate. Protein concentration in the 1.1551 ml cell was 10 μM, ligand concentration – 100 μM. The reference cell contained the equivalent solution without the protein. The obtained raw DSC data was processed by means of DSC module in the *MicroCal Origin 5.0* software.

2.2.4. Analysis of the linked protonation events

pK_a values for ICPD compounds have been calculated using *MarvinSketch* software [235]. Relevant amino acid pK_a values have been computed using *H++* online tool [236] according to the structural data. Simulation was carried out assuming 0.1 M salt and pH 7.5.

A theoretical treatment demonstrating the use of ITC measurements to dissect proton linkage from ligand binding was given by Murphy and co-workers [8; 237]. If a protein has a single ligand-binding site and a single proton uptake is linked to the binding process (i.e., a proton is taken from the buffer solution), then there are four linked processes described by the thermodynamic parameters, namely: i) unprotonated ligand binding to the unprotonated protein form; ii) ligand binding to the protonated protein form or protonated ligand binding to the protein; iii) proton binding to unliganded protein form or unbound ligand; iv) proton binding to the ligand-protein complex. Ligand binding affecting and shifting the pK_a of any ionizable group on a protein molecule is characteristic for binding-linked protonation events. At the pH at which proton uptake or release into the buffer is required for the binding, the observed binding constant K_{b_obs} is diminished as additional energy is required to bind and release protein at unfavourable conditions. For

binding-linked protonation events, the relation of K_{b_obs} to the intrinsic binding constant K_{b_intr} can be described by Equation (2.10):

$$K_{\mathrm{obs}} = K_{\mathrm{intr}} \frac{1 + 10^{\mathrm{pH} - \mathrm{p}K_{\mathrm{a}}{}^{\mathrm{b}}}}{1 + 10^{\mathrm{pH} - \mathrm{p}K_{\mathrm{a}}{}^{\mathrm{f}}}}, \tag{2.10}$$

$K_a^{\,b}$ and $K_a^{\,f}$ are the proton dissociation constants from the protein-ligand complex and free protein (or ligand), respectively. The net change in the number of protons bound by the protein (or ligand) upon binding (n) is the difference between the fractional saturation of protons in the free and bound states:

$$n = f_{\mathrm{p}}{}^{\mathrm{b}} - f_{\mathrm{p}}{}^{\mathrm{f}} = \frac{10^{pK_{\mathrm{a}}{}^{\mathrm{b}} - \mathrm{pH}}}{1 + 10^{pK_{\mathrm{a}}{}^{\mathrm{b}} - \mathrm{pH}}} - \frac{10^{pK_{\mathrm{a}}{}^{\mathrm{f}} - \mathrm{pH}}}{1 + 10^{pK_{\mathrm{a}}{}^{\mathrm{f}} - \mathrm{pH}}} \tag{2.11}$$

By means of ITC, n value can be determined as it contributes to the observed binding enthalpy ($\Delta_b H_{obs}$):

$$\Delta_{\mathrm{b}} H_{\mathrm{obs}} = \Delta_{\mathrm{b}} H_{\mathrm{debuff}} + n \Delta_{\mathrm{b}} H_{\mathrm{buffer}} \tag{2.12}$$

$\Delta_b H_{\mathrm{debuff}}$ is the theoretical enthalpy that would be observed in a buffer that has ionization enthalpy ($\Delta_b H_{buffer}$) equal to zero. Therefore it encompasses both the intrinsic binding enthalpy ($\Delta_b H_{intr}$), the ionization enthalpy of the protein or ligand, and possibly energies contributed from other binding-linked events. When protonation is the only binding-linked event, the intrinsic enthalpy can be calculated from the relationship:

$$\Delta_{\mathrm{b}} H_{\mathrm{intr}} = \Delta_{\mathrm{b}} H_{\mathrm{obs}} - n(\Delta_{\mathrm{b}} H_{\mathrm{complex}} + \Delta_{\mathrm{b}} H_{\mathrm{buffer}}) \tag{2.13}$$

2.2.5. Structural analysis

The crystal structures of Hsp90—ICPD complexes, analysed in this work, were obtained by Dr. S. M. Roe and Dr. C. Prodromou at University of Sussex, United Kingdom, as described in [238]. They are deposited in Protein Data Bank (PDB) with IDs 2YI0, 2YI5, 2YI6, and 2YI7. These and other relevant structures were visualised using *Discovery Studio Visualizer 4.5* [239] and

PyMol [240] software. The colour code employed in the figures is as follows: red for O, yellow for S, blue for N, green for Cl, while C colouring is indicated in the figure legends. Superimposition of structures has been performed using *PyMol*.

2.2.6. Cellular assays

Compound effect on cancer cells was tested by determining cell growth, death, and survival as a function of compound concentration. Dr. J. Matulienė and Dr. V. Petrikaitė at Vilnius University Institute of Biotechnology, Lithuania, performed tetrazolium/formazan assays [241] in U2OS (osteosarcoma) and HeLa (cervival carcinoma) cell lines to determine EC_{50} values for the ICPD compounds. EC_{50} denotes the concentration of the drug at which half of its maximum effect is observed on the cell survival. Dr. S.Y. Sharp at the Institute of Cancer Research, United Kingdom, employed sulforhodamine B (SRB) assay [189] to evaluate the growth inhibition (GI_{50} – drug concentration required to reduce cell growth rate to 50 % of the maximum rate) by ICPD compounds in HCT116 cells. The experiments have been conducted several times to obtain the average values presented in this work. Detailed descriptions of cell cultures and their cultivation can be found in [225] and [238], respectively.

Dr. S.Y. Sharp also performed a Western blotting analysis on selected protein expression in HCT116 cells upon treatment with ICPD compounds. Protein extracts were prepared and Western blotting was carried out as previously described [189].

3. RESULTS

3.1. ICPD compounds

ATP-dependent protein folding and stabilisation by Hsp90 is essential for development and progression of various cancers. There are two groups of natural inhibitors that bind to the ATP-binding pocket located in the N-terminal domain: radicicol (RD) and geldanamycin (GA). However, both of them exhibit several properties that impede their clinical applications. Therefore structurally similar compounds are being researched in order to find a non-toxic and effective Hsp90 inhibitor [242].

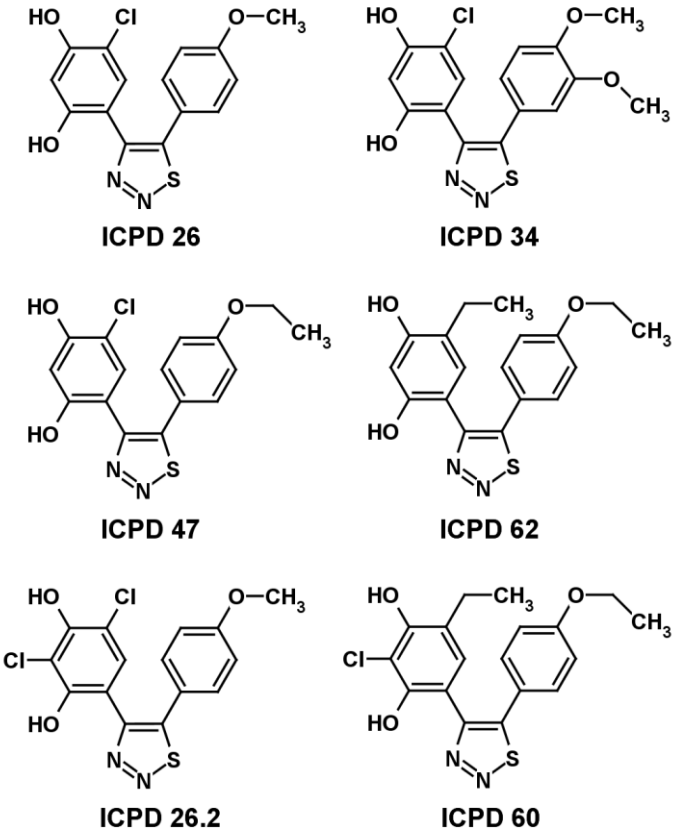

Figure 3.1. Chemical structures of compounds belonging to the ICPD series, the object of this study.

A variety of resorcinol-type compounds, including diarylpyrazole [243] and diarylisoxazole [244; 245] derivatives, have been synthesised by multiple research groups and tested for Hsp90 inhibition. Several of Hsp90 inhibitors, developed in such fashion, have advanced to clinical trials. We developed a series of resorcinol-type compounds, bearing thiadiazole moiety (aryl-dihydroxyphenyl-thiadiazoles, referred to as ICPD) and had them synthesised at Vilnius University. Their chemical structures are shown in Figure 3.1.

Even with the existing achievements, full thermodynamic description of the ligand binding to Hsp90 is rather fragmented despite its importance for structure-based drug development [246; 247]. It is well established that there is some correlation between the thermodynamic characteristics of binding and structural parameters. The binding enthalpy primarily reflects the strength of the ligand—protein interaction in comparison to protein—solvent and ligand—solvent interactions. Hydrophobic interactions and conformational changes are attributed to the binding entropy [220]. The Gibbs energy, being a function of both these parameters and hence describing the strength of the interaction, does not provide enough insight into the underlying reasons for binding. Therefore ligands should not be evaluated based on only one of these parameters and all of them have to be taken into account [5; 248; 249].

In this study we employed two independent methods, ITC and thermal denaturation profile studies (FTSA and DSC), to characterise thermodynamic parameters of the binding of ICPD compounds to the N-terminal domain of recombinant human Hsp90α and Hsp90β (termed Hsp90αN and Hsp90βN, respectively).

3.2. Isothermal titration calorimetry of ICPD compound binding to Hsp90

Our primary method for analysing the energetics of ICPD compound binding to Hsp90 was ITC. This method enables to determine all of the

fundamental thermodynamic parameters of the binding reaction: K_b, enthalpy, entropy, and heat capacity [246; 250].

3.2.1. Hsp90N as a representative of full-length Hsp90 in ICPD binding experiments

The target of the ICPD compounds is the ATP-binding pocket, located in the N-terminal domain of Hsp90. Since the isolated N-terminal domain of Hsp90 (termed Hsp90N) is easier to produce in required quantities than full-length Hsp90, we first tested whether Hsp90N is a suitable representative of full-length recombinant human Hsp90 in ICPD binding experiments. Additional benefit of using Hsp90N is that FTSA experiments (that we employ to verify and expand ITC data) are significantly better suited for single-domain proteins.

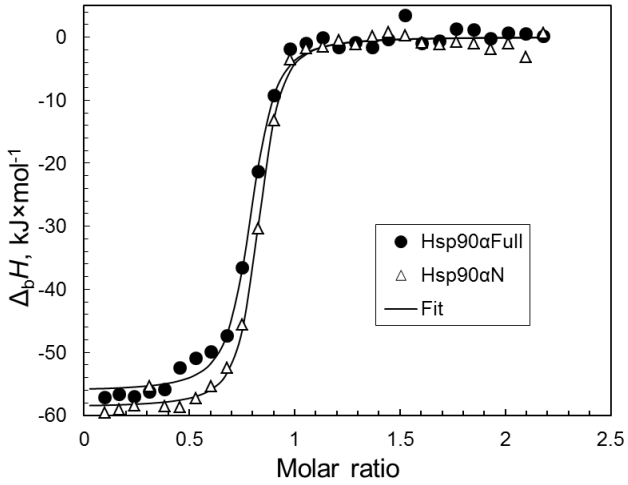

Figure 3.2. Integrated ITC curves for ICPD47 binding to full-length Hsp90α protein (black dots) and to Hsp90αN (white triangles). Differences between the N-terminal and full-length protein binding were within the experimental error. The experiment was conducted in Phosphate buffer of pH 7.5 at 37 °C with 6 μM protein.

We used ITC to determine the thermodynamic parameters of the binding of ICPD47 to Hsp90α, Hsp90αN, Hsp90β, and Hsp90βN over a range of temperatures at pH 7.5. Figure 3.2 compares the integrated ITC curves of

ICPD47 binding to Hsp90αN and full-length Hsp90α. Additional data can be found in Table 3.1. There was essentially no difference in the binding curve observed with the Hsp90N and the full length Hsp90 protein, in cases of both isoforms. Our data supports that ICPD47 binds to the N-terminal domain of Hsp90. As the thermodynamics of ICPD compounds binding to full-length Hsp90 is well represented by Hsp90N in our experiments, further in this study we used primarily Hsp90N.

3.2.2. Observed thermodynamic parameters for ICPD binding to Hsp90

We measured the energetics of 6 ICPD compounds binding to Hsp90N using ITC. Initial experiments revealed that 2 of them, ICPD26.2 and ICPD60, do not bind to Hsp90N. The 4 ICPD compounds that do bind to Hsp90N were investigated in more detail. We conducted a series of experiments over a range of temperatures, pH, and buffers in order to evaluate various events that could be linked to the binding. Understanding of such events is essential in order to interpret how exactly the binding occurs and link it to the structure of the compounds. Table 3.1 lists representative ITC data for the series of ICPD binding to Hsp90. Representative raw data of Hsp90αN titration with ICPD47 in HEPES buffer, pH 7.5, at 37 °C is shown in Figure 3.3. Consistently to all other data presented here, the observed binding enthalpy change ($\Delta_b H_{obs}$) was exothermic. The binding reaction exhibited a steep slope of the ITC curve, which indicates tight binding. For instance, in Phosphate buffer, pH 7.5, at 37 °C the K_{b_obs} values for these ICPD compounds varied from 1.8×10^7 to 1.8×10^8 M^{-1}, with ICPD34 exhibiting notably weaker binding than the other 3 ICPD compounds. These values indicate significantly stronger binding to Hsp90 than reported for its natural substrate ATP (K_{b_obs} = 7.6×10^3 M^{-1} at 25 °C, pH 7.4) [29; 249]. Moreover, this trend persisted under other experimental conditions as well.

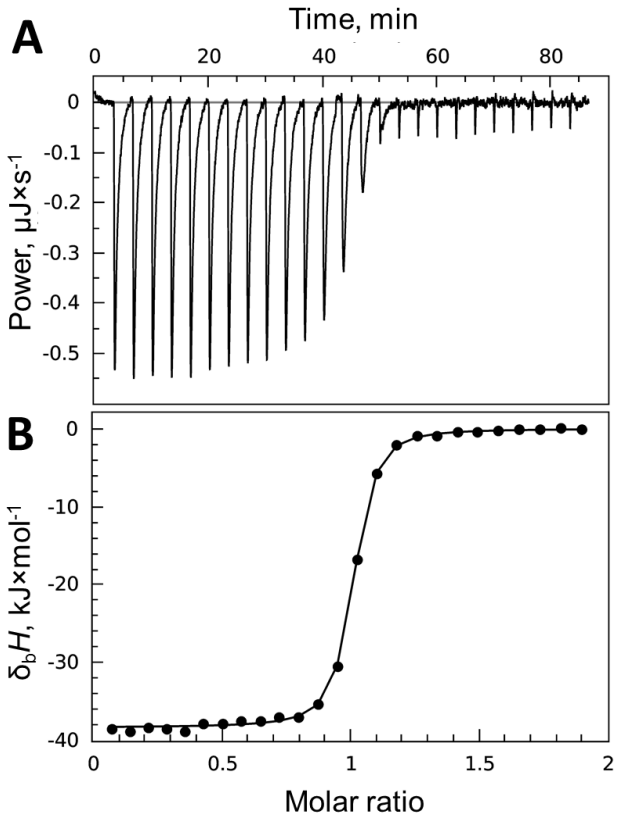

Figure 3.3. Representative ITC data of ICPD compound binding to Hsp90. Both the titration data (upper panel) and the integrated data (lower panel) curves of 60 μM ICPD47 binding to 6 μM Hsp90αN in HEPES buffer, pH 7.5, at 37 °C are displayed.

Reliability of K_b values, determined by means of ITC, can be estimated using *c* value (see 2.2.1). The 4 studied ICPD compounds bound to the tested Hsp90 constructs with the stoichiometry of one inhibitor molecule per one N-terminal ATP-binding site of the protein within the error of ITC measurements. Therefore under our experimental conditions of 6 μM protein, we can accurately measure the observed binding constants of only up to about 8×10^7 M^{-1}. The strongest binding ICPD compounds, ICPD47 and ICPD62, are around this borderline under the discussed conditions. At lower pH the binding is even tighter and thus exceeds the limit of accurate K_b evaluation. Therefore, in order to increase the precision and verify the binding constants, an additional alternative method was required. The observed enthalpy, on the other hand, is measured accurately by ITC even if the binding is too strong to reliably evaluate K_b.

Table 3.1. Summary of selected representative ITC data for the binding of ICPD compounds to recombinant human Hsp90 as a function of pH, temperature, and buffer (Phosphate (Phos.), HEPES, and Tris) ionization enthalpy.

ICPD	*T*, °C	pH	Buffer	$K_b \times 10^7$, M^{-1}	$\Delta_b H_{obs}$, $kJ \times mol^{-1}$	ICPD	*T*, °C	pH	Buffer	$K_b \times 10^7$, M^{-1}	$\Delta_b H_{obs}$, $kJ \times mol^{-1}$
Hsp90αN						**Hsp90αN**					
ICPD47	37	6.0	Phos.	13.7	-40.1	ICPD62	12	7.5	Phos.	25.7	-14.1
	37	6.5	Phos.	24.2	-39.9		25	7.5	Phos.	513	-19.4
	37	7.0	Phos.	14.7	-40.7		37	7.5	Phos.	57.1	-28.5
	37	7.5	Phos.	9.19	-50.2		43	7.5	Phos.	117	-36.6
	37	8.0	Phos.	6.89	-40.1		7	7.5	Tris	519	-10.8
	37	8.5	Phos.	2.20	-43.8		12	7.5	Tris	301	-14.2
	37	9.0	Phos.	1.27	-60.8		25	7.5	Tris	77.5	-17.0
	37	9.5	Phos.	0.90	-50.9		37	7.5	Tris	48.5	-25.5
	37	10.0	Phos.	0.25	-49.8		43	7.5	Tris	6.72	-34.2
	37	10.5	Phos.	0.14	-51.5	ICPD34	7	7.5	HEPES	36.4	-23.5
	37	11.0	Phos.	0.06	-26.5		12	7.5	HEPES	16.2	-25.7
	37	11.5	Phos.	0.01	-34.4		25	7.5	HEPES	5.66	-31.6
	37	12.0	Phos.	0	0		43	7.5	HEPES	1.87	-44.4
	37	6.0	Tris	10.7	-35.9		7	7.5	Phos.	11.0	-31.2
	37	6.5	Tris	35.2	-33.4		12	7.5	Phos.	19.9	-28.8
	37	7.0	Tris	9.16	-30.8		25	7.5	Phos.	7.89	-38.4
	37	7.5	Tris	9.19	-28.0		37	7.5	Phos.	2.53	-45.8
	37	8.0	Tris	4.48	-21.3		43	7.5	Phos.	1.82	-53.3
	37	8.5	Tris	1.16	-22.6		7	7.5	Tris	62.8	-11.7
	37	9.0	Tris	1.13	-26.1		12	7.5	Tris	24.2	-14.3
	37	9.5	Tris	0.18	-29.7		25	7.5	Tris	7.89	-21.0
	37	10.0	Tris	0.20	-23.1		37	7.5	Tris	2.30	-26.7
	12	7.5	HEPES	20.0	-29.1	ICPD26	12	7.5	HEPES	32.0	-28.4
	25	7.5	HEPES	12.5	-28.6		25	7.5	HEPES	27.4	-36.9
	37	7.5	HEPES	10.2	-38.3		37	7.5	HEPES	10.0	-42.2
	43	7.5	HEPES	7.55	-44.1		43	7.5	HEPES	5.70	-53.2
	12	7.5	Phos.	13.2	-33.7		25	7.5	Phos.	13.2	-42.0
	25	7.5	Phos.	13.9	-41.1		37	7.5	Phos.	6.16	-48.4
	37	7.5	Phos.	9.27	-51.8		43	7.5	Phos.	5.55	-61.6
	43	7.5	Phos.	4.62	-65.4		12	7.5	Tris	16.2	-16.2
	12	7.5	Tris	12.3	-14.7		25	7.5	Tris	15.3	-27.0
	25	7.5	Tris	14.9	-25.0		37	7.5	Tris	12.0	-36.6
	37	7.5	Tris	10.0	-32.9		43	7.5	Tris	15.2	-44.8
	43	7.5	Tris	12.2	-47.8	**Hsp90αFull**					
ICPD62	7	7.5	HEPES	16.4	-13.9	ICPD47	12	7.5	HEPES	16.5	-32.6
	12	7.5	HEPES	192	-18.3		25	7.5	HEPES	16.2	-35.4
	25	7.5	HEPES	370	-21.2		37	7.5	HEPES	11.9	-39.0
	37	7.5	HEPES	11.0	-25.5		43	7.5	HEPES	13.4	-44.1
	43	7.5	HEPES	30.5	-34.8		12	7.5	Phos.	24.7	-33.7
	7	7.5	Phos.	322	-11.9		25	7.5	Phos.	20.8	-42.1

(continued on next page)

(Table 3.1, *continued from previous page*)

ICPD	*T*, °C	pH	Buffer	$K_b \times 10^7$, M^{-1}	$\Delta_b H_{obs}$, $kJ \times mol^{-1}$	ICPD	*T*, °C	pH	Buffer	$K_b \times 10^7$, M^{-1}	$\Delta_b H_{obs}$, $kJ \times mol^{-1}$
Hsp90αFull						**Hsp90βN**					
ICPD47	37	7.5	Phos.	12.0	-50.2	ICPD62	37	7.5	Tris	4.33	-19.8
	43	7.5	Phos.	6.40	-60.6	ICPD34	12	7.5	HEPES	9.30	-26.0
	12	7.5	Tris	77.7	-18.7		25	7.5	HEPES	2.04	-30.9
	25	7.5	Tris	31.8	-25.7		37	7.5	HEPES	0.90	-39.8
	37	7.5	Tris	28.6	-35.9		12	7.5	Phos.	5.51	-31.1
	43	7.5	Tris	12.0	-40.5		25	7.5	Phos.	2.00	-38.2
Hsp90βN							37	7.5	Phos.	0.78	-48.8
ICPD47	12	7.5	HEPES	5.24	-27.8		12	7.5	Tris	5.78	-17.2
	37	7.5	HEPES	2.28	-49.4		25	7.5	Tris	2.42	-21.3
	12	7.5	Phos.	5.71	-35.1		37	7.5	Tris	0.30	-34.7
	25	7.5	Phos.	5.59	-42.5	ICPD26	12	7.5	HEPES	6.49	-27.1
	37	7.5	Phos.	2.46	-52.1		25	7.5	HEPES	2.27	-30.9
	12	7.5	Tris	5.46	-17.4		37	7.5	HEPES	1.47	-37.3
	37	7.5	Tris	2.73	-27.7		12	7.5	Phos.	10.2	-30.3
ICPD62	12	7.5	HEPES	8.88	-14.1		25	7.5	Phos.	2.36	-38.7
	25	7.5	HEPES	6.13	-16.7		37	7.5	Phos.	1.48	-45.7
	37	7.5	HEPES	3.23	-19.9		12	7.5	Tris	16.3	-15.4
	12	7.5	Phos.	17.1	-12.6		25	7.5	Tris	4.84	-20.1
	25	7.5	Phos.	14.0	-16.0		37	7.5	Tris	1.54	-25.6
	37	7.5	Phos.	2.35	-23.3	**Hsp90βFull**					
	12	7.5	Tris	58.3	-11.8	ICPD47	37	7.5	Phos.	1.47	-55.7

3.3. Evaluating ICPD binding from protein denaturation profiles

While ITC struggles to reliably quantify K_b that exceeds certain limits, protein denaturation-based methods, like FTSA and DSC, can be used for determining K_{b_obs} values for any non-covalent ligand binding to a protein, regardless of the K_b magnitude [251; 252]. However, these methods cannot yield the observed enthalpy of the binding reaction. Therefore, ITC and FTSA/DSC methods complement each other for increased precision of the measurements [232].

Both FTSA and DSC measures K_b by determining the effect the ligand has on the melting temperature of the protein [232; 251]. Soluble single-domain globular proteins melt with a single transition that is affected by the bound ligands. However, the full-length Hsp90 is a multi-domain protein that

yields a complicated multi-peak melting transition profile which makes its analysis not straightforward if possible at all. On the other hand, Hsp90N construct yields a single transition profile that can be employed to study inhibitor binding to Hsp90. Since ITC data confirmed that ICPD compounds bind to Hsp90N in the same manner as to Hsp90, we used Hsp90N in FTSA and DSC experiments.

DSC is much older and thus better established method in pharmacology than FTSA [253-255]. However, it is exceedingly costly both time- and reagent-wise. Therefore we conducted our experiments by means of FTSA and tested several cases by means of DSC.

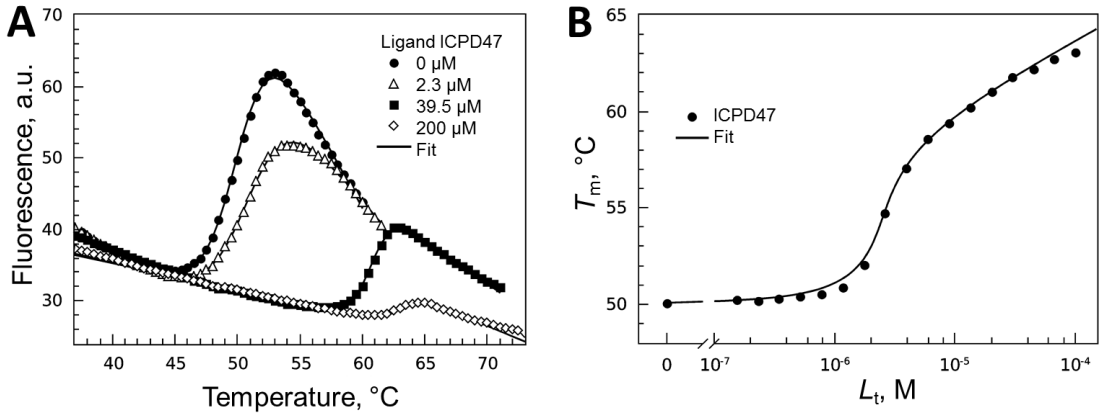

Figure 3.4. Representative FTSA data of ICPD compound binding to Hsp90N. (A) The raw fluorescence FTSA data of ICPD47 binding to 10 μM Hsp90αN at pH 7.5. The Hsp90αN thermal denaturation transitions (T_m) were increasingly shifted upwards as the concentration of ICPD47 increased. (B) Determined T_m values plotted as a function of ICPD47 concentration.

By means of FTSA, we determined K_b for the 4 ICPD compounds binding to Hsp90N over a range of pH and buffers in order to crosscheck and revise the corresponding ITC data. For each pH, we performed a set of experiments at several different ligand concentrations. Several examples from such set for ICPD47 at pH 7.5 are displayed in Figure 3.4A. During a FTSA experiment, the fluorescence of the dye that binds to the exposed unfolded protein's hydrophobic regions (ANS in this case) is measured as a function of temperature. In case of 10 μM Hsp90N under the given experimental

conditions (see 2.2.2) without any ligand added, a steep increase in fluorescence is observed at approximately 50 °C (49.5±0.1 °C for Hsp90α, 49.1±0.2 °C for Hsp90βN). This peak signifies the unfolding of the protein which results in exposure of previously hidden hydrophobic surfaces. Addition of ICPD47 shifted the transition midpoint towards higher temperatures because the ligand stabilised Hsp90N upon binding. The T_m shift observed in DSC experiments (Figure 3.5) was identical to the one observed using FTSA.

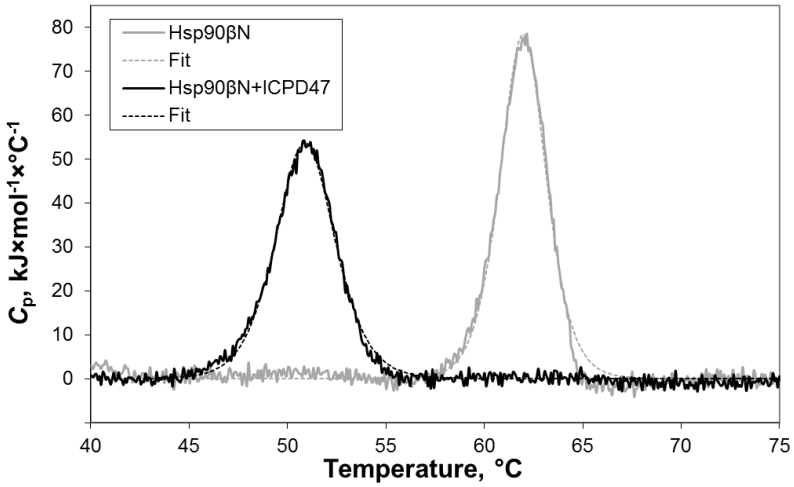

Figure 3.5. Denaturation of Hsp90βN protein in the unliganded state (black line) and in the presence of ICPD47 (grey line) during a DSC experiment. The dashed lines represent fits.

By fitting the protein melting curves obtained from FTSA experiments according to Equation (2.5), we determined protein melting temperatures (T_m) at various inhibitor concentrations. Plotting the resultant transition midpoints as a function of added ligand concentration yielded a ligand-dosing curve (Figure 3.4B) for each tested pH. The K_{b_obs} values were obtained by fitting these datapoints according to Equation (2.9).

As can be seen in Figure 3.6 and Table 3.2, all 4 ICPD compounds bind significantly tighter to Hsp90αN at pH 7.5 (at 37 °C) than a classic Hsp90 inhibitor 17-AAG and thus exhibit a larger protein T_m shift. ICPD26.2 (and ICPD60) does not bind to Hsp90 and thus does not shift its T_m. According to this FTSA data, the ICPD compounds can be ranked from the strongest binder

to the weakest as follows: ICPD62 > ICPD47 > ICPD26 > ICPD34. This tendency is characteristic not only to pH 7.5 but also persists at other tested pH values. Moreover, this trend also continues in experiments conducted with Hsp90βN. In general, Hsp90N T_m shift exceeds 10 °C at excess concentrations of the analysed ICPD compounds, signifying strong binding.

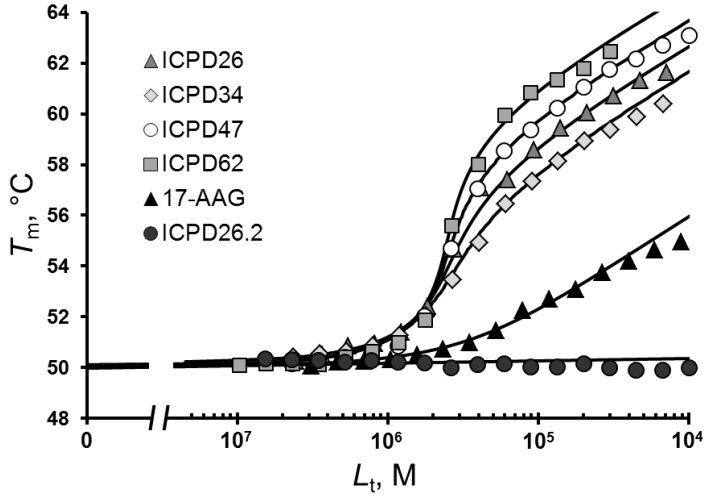

Figure 3.6. T_m of 5 μM Hsp90αN, as obtained by means of FTSA at pH 7.5, as a function of the concentration of various added ligands. Note that ICPD62 shifts the T_m to the greatest extent and thus its K_{b_obs} (though not K_{b_intr}) is largest.

Table 3.2. K_{b_obs}, as obtained by means of FTSA. The values are displayed in M^{-1}. ± denotes the error calculated from multiple experiments.

Compound	Hsp90αN	Hsp90βN
ICPD26	7.6×10^7 ±0.03×	1.0×10^7 ±0.17×
ICPD34	2.5×10^7 ±0.19×	4.8×10^6 ±0.25×
ICPD47	8.8×10^7 ±0.17×	2.3×10^7 ±0.28×
ICPD62	1.7×10^8 ±0.16×	4.7×10^7 ±0.10×
17-AAG	5.8×10^5 ±0.17×	n.d.

3.4. Interpretation of binding-linked protonation events

Observed parameter is a sum of the intrinsic parameter and contributions from various binding-linked phenomena. The most common events that are coupled with protein—ligand binding is (de)protonation and conformational

changes [256]. The analysis of binding-linked protonation events was done as previously described [8; 237; 257].

3.4.1. ICPD binding to Hsp90N is coupled with a single protonation event

Early on in our ITC experiments we noticed that the observed enthalpies of binding were highly dependent on the buffer used (Figure 3.7A, Table 3.1). For example, the observed enthalpy at pH 7.5 was approximately -28 kJ×mol^{-1} in Tris buffer, -38 kJ×mol^{-1} in HEPES buffer, and -42 kJ×mol^{-1} in Phosphate buffer. The key distinction between the buffers is their significantly different deprotonation enthalpies. Therefore such discrepancy in observed binding enthalpies suggests one or more binding-linked (de)protonation events.

In general, binding of small molecules to a protein may change the local environment of labile protons of either species. This can result in the labile group having a different pK_a in the free and bound states due to different surrounding interactions. By manipulating pH, we can affect the ionisation of the free ligand and protein: at low pH the predominant state is protonated while at higher pH the deprotonated state is more prevalent. Therefore we analysed observed enthalpies for ICPD47 and other compounds as a function of pH (Figure 3.7B). There is only one transition point in the buffer-dependent $\Delta_b H_{obs}$ curves (~ -40 kJ×mol^{-1}) that is visible within the pH interval at which significant fraction of protein is not denatured. This indicates that only a single protonation event is linked to the ICPD inhibitor binding to Hsp90. We assumed that it is the ICPD47 that binds to Hsp90 while being in the protonated state rather than contributing the protonation effect to the protein itself. Experiments with both ICPD26 and ICPD34 compounds yielded similar results and conclusions. The results were the same both for Hsp90αN and Hsp90βN.

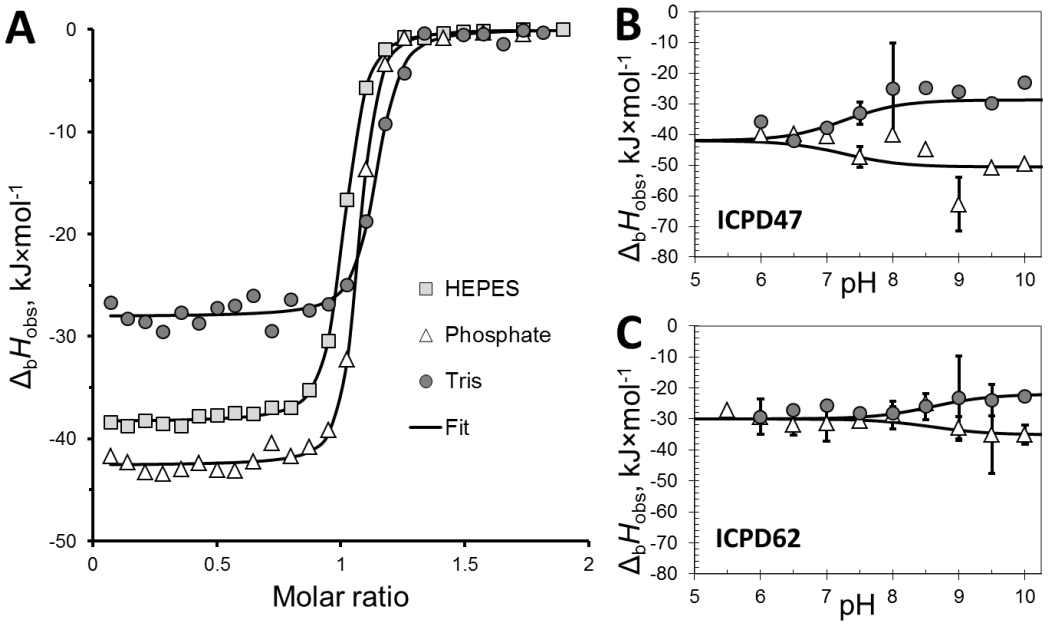

Figure 3.7. The pH and buffer effects on ICPD compounds binding to Hsp90N. (A) Fitted integrated ITC curves for ICPD47 binding to Hsp90αN in three different buffers. (B) The observed enthalpies of ICPD47 binding to Hsp90αN as a function of pH in the two buffers that differ the most in their protonation enthalpies (Phosphate and Tris). (C) The observed enthalpies of ICPD62 binding to Hsp90αN as a function of pH in Phosphate and Tris buffers. The error bars depict standard error of several experiments. In all panels data for HEPES buffer is depicted in grey squares, for Phosphate – white triangles, and for Tris – dark grey circles.

ICPD62 displayed a slightly different profile (Figure 3.7C). While it still exhibited a pH dependence that suggests a single protonation event, ICPD62 remained at protonated state even at pH 7.5. This distinction can be easily explained by the structural differences between the ligands. There are two hydroxyl groups in the ICPD compounds that could participate in the (de)protonation event that is evident in our experiments. While others contain chlorine situated in a position that is *ortho* and *para* in respect of the hydroxyl groups, ICPD62 there accommodates an ethyl residue. The difference in electron withdrawing capacity of these residues results in contrasting effects on the protonation state of the hydroxyl groups. According to calculations conducted with *Marvin* software [235], the *para*-hydroxyl group has similar pK_a in all 4 ICPD compounds; however, the *ortho*-hydroxyl residue is much more prone to be protonated in ICPD62 as compared to the chlorine-containing

compounds (pK_a ~9.9 *versus* pK_a ~7.3). This indicates that the *ortho*-hydroxyl residue has to be protonated for binding event to occur, while the protonation state of the *para*-hydroxyl residue is less likely to affect the binding to Hsp90.

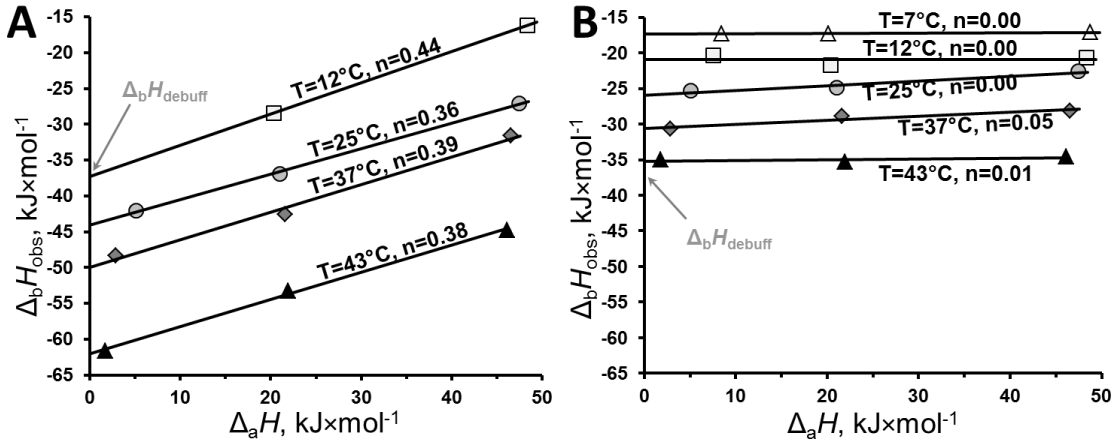

Figure 3.8. The observed enthalpies of (A) ICPD47 and (B) ICPD62 binding to Hsp90αN at pH 7.5 as a function of buffer deprotonation enthalpy (Δ_aH) at various temperatures. Δ_bH_{debuff} – enthalpy that would be observed in a buffer with deprotonation enthalpy equal to 0.

The observed enthalpies of binding plotted as a function of buffer deprotonation enthalpy [258] yielded the number of protons being uptaken from that particular solution upon inhibitor binding at various temperatures (Figure 3.8). The trendlines are linear fits, with their slopes equal to the net number of exchanged protons (*n*). The fraction number of protons bound per ICPD molecule suggests that a portion of ligands is already in the protonated state at this particular pH. The net number of exchanged protons depended primarily on solution pH and not on temperature. The enthalpies obtained from this plot are the sum of both the intrinsic binding enthalpy and heat of protonation of protein/ligand functional groups; however, they do not include buffer deprotonation enthalpy. Intrinsic binding enthalpy can be calculated from the ligand protonation enthalpy and the number of exchanged protons or estimated as the ΔH at the intersection point in Figure 3.7B.

3.4.2. pH-dependence of the binding constant

ICPD compound interaction with Hsp90 was progressively weaker with increasing alkalinity of the solution. The observed binding constant, as determined both by ITC and FTSA, diminished by approximately 1 order of magnitude with each pH unit (Figure 3.9). This tendency was characteristic to all ICPD compounds, except for ICPD62. As we established that the ICPD compounds have to be in their protonated state to bind to Hsp90, these results seem self-explanatory: the higher pH, the more prevalent is the deprotonated state of the ligand. In accordance with binding enthalpy data, ICPD62 exhibited the decrease in K_{b_obs} at greater pH than the other ICPD compounds.

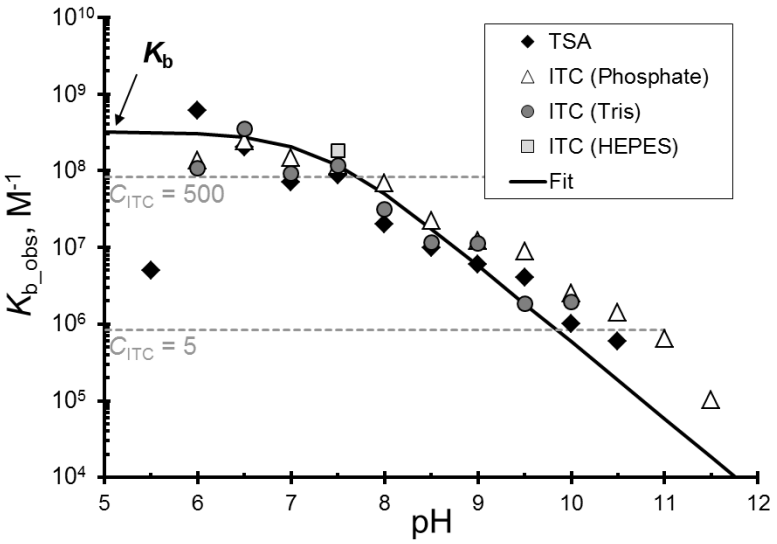

Figure 3.9. pH dependence of K_{b_obs} for ICPD47 and Hsp90αN. The line is fitted according to Equation (2.10). Note that the ITC data does not provide accurate measure of the binding constant at pH below 7.5 because the binding is too tight, as indicated by the dashed line representing the ITC *c* factor, equal to 500. At pH below 6.0 even FTSA data is significantly compromised as the protein is unstable.

3.4.3. Model of the binding-linked protonation event

Figure 3.10 illustrates the protonation of the hydroxyl group of ICPD47 at high pH upon binding to Hsp90. The enthalpic contributions to all linked

reactions, including buffer deprotonation and compound protonation, are shown. As can be seen in the figure, these linked reactions make large enthalpic contributions. They have to be accounted for in order to dissect the intrinsic binding parameters.

The intrinsic binding enthalpy can be obtained from Figure 3.7B or calculated as the difference between the binding enthalpy that would be observed at a buffer with deprotonation enthalpy of 0 (evaluated from Figure 3.8A) and the enthalpy of protonation of the ICPD47 hydroxyl group (obtained by fitting all titration data). The same protonation event model is applicable to the other 3 ICPD compounds.

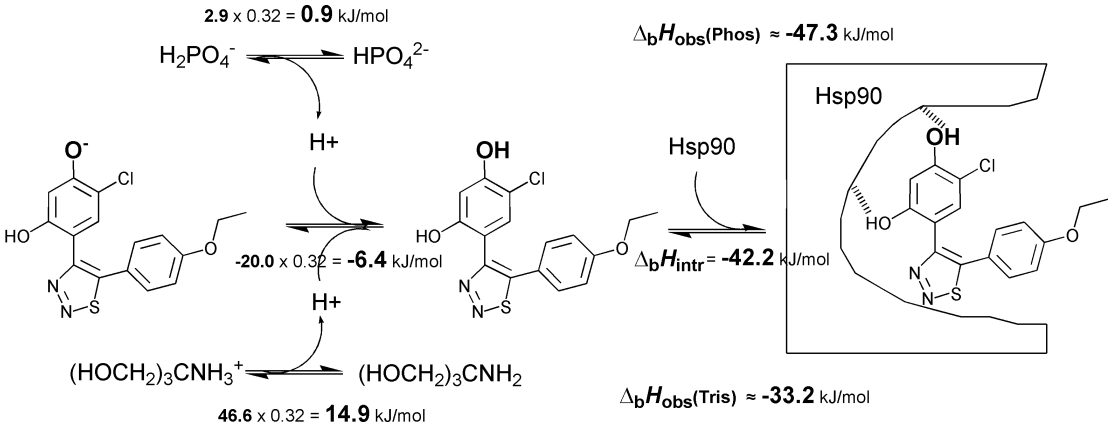

Figure 3.10. Enthalpic contributions of the binding-linked reactions: the protonation of the compound (ICPD47) hydroxyl group (bold), buffer ionization, and the intrinsic enthalpy of binding.

3.5. Intrinsic binding of ICPD compounds to Hsp90 protein

The thermodynamic parameters that are directly obtained during experiments are called observed as their values include not only intrinsic parameters of the binding event but also various binding-linked events. While observed values can be used to evaluate the strength of binding under the chosen conditions, only the intrinsic binding parameters can be used to correlate with the structural features of the protein-ligand complex. Deeper

understanding of the molecular interactions of the binding event is essential in selecting the best compounds for further development [248].

The most common binding-linked event is (de)protonation of the ligand and consequently buffer, and it can be evaluated from a series of comprehensive ITC experiments (see 3.4). However, binding-linked conformational changes can only be observed by means of structural analysis.

3.5.1. Structural analysis of Hsp90—ICPD complexes

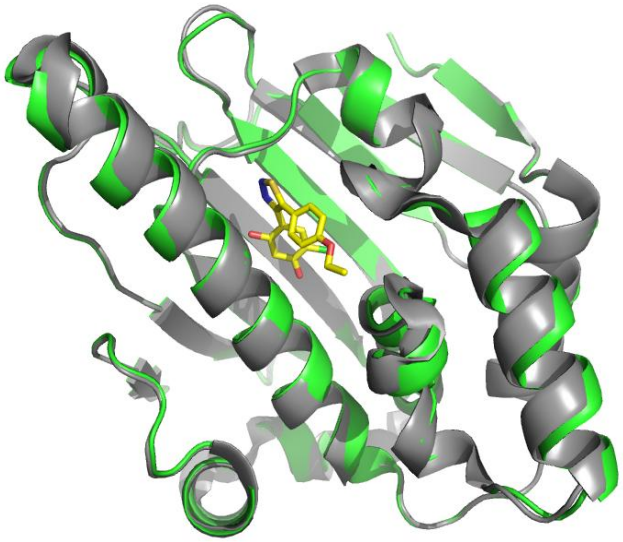

Figure 3.11. Superimposition of ICPD47-bound human Hsp90αN (green cartoon; ICPD47 is yellow sticks) with the structure of unbound protein (grey cartoon; PDB ID 3T0H). The overall r.m.s.d. of the two N-terminal domains is 0.24 Å (0.23 Å for ICPD24-bound, 0.40 Å for ICPD34-bound, and 0.16 Å for ICPD62-bound protein structure comparison to unbound Hsp90αN).

C. Prodromou and colleagues at the Institute of Cancer Research (United Kingdom) performed X-ray crystallography studies on Hsp90—ICPD complexes and obtained the structures revealing ICPD26, ICPD34, ICPD47, and ICPD62 bound to human Hsp90αN (Figure 3.11). As expected, all these 4 ICPD compounds bound to Hsp90 in a similar manner which shares conservative interactions with other resorcinol group ligands such as the naturally occurring RD (PDB ID 1bgq [259]) or synthetic inhibitors such as 4-

chloro-6-(4-piperazin-1-yl-1h-pyrazol-3-yl)-benzene-1,2-diol (PDB ID 2CCS [260]). Contacts between Hsp90 and ICPD compounds are described in more detail in Section 3.7.

The crystal structure of Hsp90αN—ICPD shows only minor differences in comparison to apo Hsp90αN (Figure 3.11). This is in agreement with the data Nilapwar *et al* obtained on Hsp90αN interaction with GA and 17-AAG by means of circular dichroism spectroscopy and NMR [249]. Given this data, the influence of potential binding-linked conformational changes can be considered negligible.

3.5.2. Values of intrinsic thermodynamic parameters of Hsp90—ICPD interaction

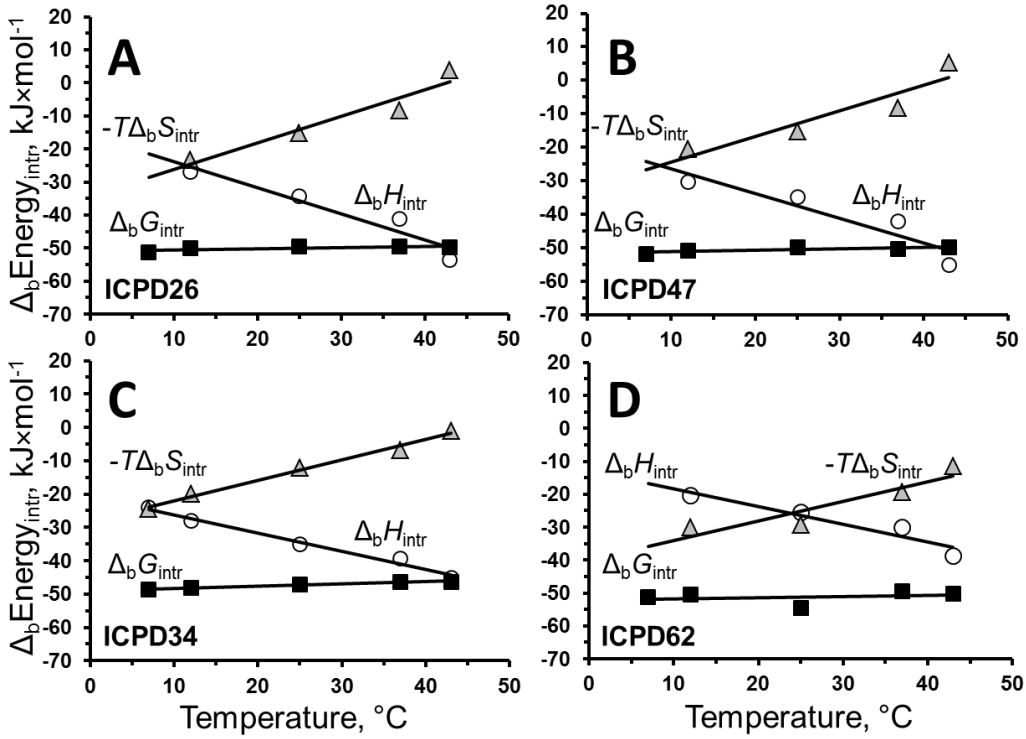

Figure 3.12. The intrinsic thermodynamic parameters of (A) ICPD26, (B) ICPD47, (C) ICPD34, and (D) ICPD62 binding to Hsp90αN as a function of temperature. Δ_bG_{intr} datapoints are depicted as black squares, Δ_bH_{intr} – white circles, and $-T\Delta_bS_{intr}$ – grey triangles.

Figure 3.12 displays the intrinsic thermodynamic parameters that we obtained for ICPD compounds binding to Hsp90 as a function of temperature. The slopes of the intrinsic binding enthalpies as a function of temperature provide the heat capacities of binding ($\Delta_b C_p$) of binding. $\Delta_b C_p$ values of all tested ICPD compounds binding to Hsp90αN are within the range of -540 to -660 $J \times mol^{-1} \times K^{-1}$. Negative heat capacity is a signature of hydrophobic binding reactions and these particular values are akin to GA analogues 17-AAG and 17-DMAG [249] as well as RD [234] binding to Hsp90.

The intrinsic thermodynamic parameters at physiologically significant temperature of 37 °C are listed in Table 3.3. All 4 ICPD compounds bind to the inducible Hsp90α approximately 4.5 times tighter than to the constitutive Hsp90β. Similar differences in affinity to the two human Hsp90 isoforms have been previously reported for RD [234] and GA [261]. The only distinction in the ATP-binding pockets of these two isoforms is the A47 residue in Hsp90β instead of the S52 residue in Hsp90α.

In cases of both isoforms, the ICPD compounds can be ranked from the strongest binder to the weakest as follows: ICPD47 > ICPD26 ~ ICPD62 > ICPD34.

Table 3.3. The intrinsic thermodynamic parameters of ICPD compounds binding to Hsp90N at 37 °C, pH 7.5. ± denotes the errors that were evaluated fitting data of multiple experiments.

ICPD	Protein	$\Delta_b H_{intr}$, $kJ \times mol^{-1}$	K_{b_intr}, M^{-1}	K_{d_intr}, nM	$\Delta_b G_{intr}$, $kJ \times mol^{-1}$	$-T\Delta_b S_{intr}$, $kJ \times mol^{-1}$	$\Delta_b C_p$, $J \times mol^{-1} \times K^{-1}$
26	Hsp90αN	-41.1	2.21×10^8	4.5	-49.5	-8.4	-790
	Hsp90βN	-38.0	3.9×10^7	25.9	-45.1	-7.0	-650
34	Hsp90αN	-39.5	6.6×10^7	15.1	-46.4	-7.0	-550
	Hsp90βN	-39.5	1.9×10^7	52.1	-43.3	-3.7	-640
47	Hsp90αN	-42.2	3.15×10^8	3.2	-50.5	-8.3	-730
	Hsp90βN	-43.2	7.3×10^7	13.8	-46.7	-3.5	-700
62	Hsp90αN	-30.1	2.18×10^8	4.6	-49.5	-19.4	-540
	Hsp90βN	-26.8	4.7×10^7	21.4	-45.5	-18.8	-340
		±1.7	±1.5×	±1.5×	±1.1	±2.0	±125

It has been noticed that synthetic drugs tend to have greater favourable entropy contribution to the Gibbs energy of binding than natural ligands [216]. While entropy gains are easier to achieve via addition of hydrophobic residues, such improvement is limited as solubility needs to be taken into account as well [248]. Therefore the primary focus of optimisation should be enthalpy. For easier comparison of energetic contributions to ICPD compound binding to Hsp90, the intrinsic values are depicted as bars in Figure 3.13. In case of ICPD26, ICPD34, and ICPD47, enthalpy contributes from 80 % to 90 % of the binding free energy. However, the binding of ICPD62 to Hsp90N was driven by both enthalpy and entropy in nearly equal parts.

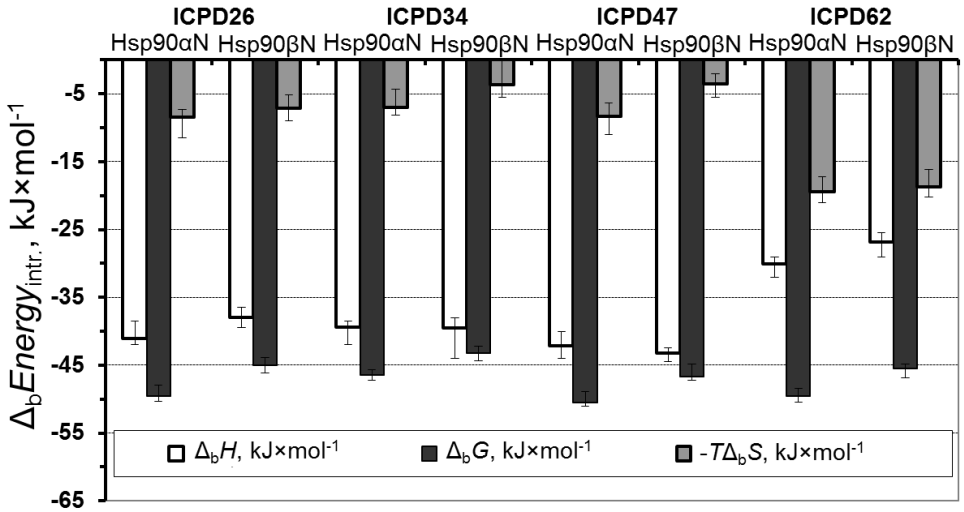

Figure 3.13. Bar chart comparing relative contributions of intrinsic enthalpies (white bars) and intrinsic entropies (grey) to the intrinsic Gibbs energies (black) of binding of ICPD compounds to Hsp90N at 37°C.

3.6. Structure–affinity relationship for ICPD compounds

Ability to predict the thermodynamic parameters associated with binding and the affinity of the interaction itself from a high-resolution structure would potentially make pharmaceutical research less taxing financially and time-wise [7]. As current set of bioinformatics tools are not up for the task [6; 7],

correlations of molecular structure with thermodynamics have to be made by obtaining all the possible data in order to lay foundation for future estimations.

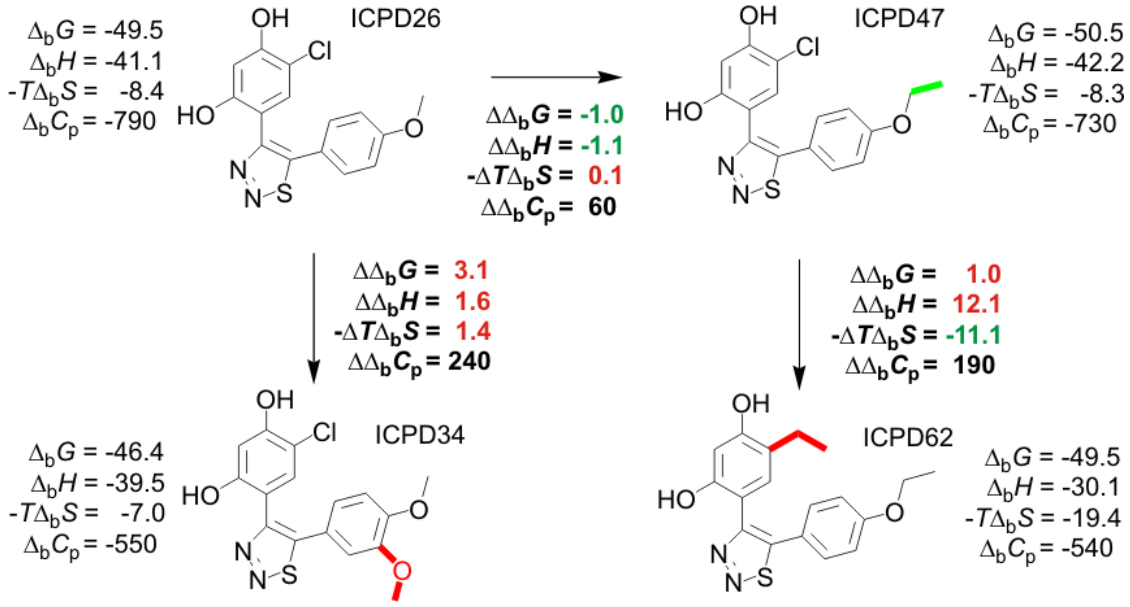

Figure 3.14. Comparison of functional group contributions to the intrinsic binding parameters. Groups promoting $\Delta_b G_{intr}$ are shown in bold green while those disfavouring binding – in bold red. Same colour coding applies to the values of binding parameters. $\Delta_b G_{intr}$, $\Delta_b H_{intr}$, and $-T\Delta_b S_{intr}$ values are presented in kJ×mol^{-1} (with uncertainties of ±1.1, ±1.7, and ±2.0, respectively), $\Delta_b C_p$ – in J×mol^{-1}×K^{-1} (with uncertainty of ±125).

First of all we correlated the disparities of all intrinsic thermodynamic parameters of ICPD compound binding to Hsp90N with the differences in the functional groups of ICPD compounds (Figure 3.14). Addition of a second methoxy group in ICPD34, as compared to ICPD26, results in a minor loss of favourable enthalpy contribution. The extra methylene group in ICPD47, as compared to ICPD26, has little effect on the binding Gibbs energy. The change of chlorine atom in ICPD47 to the ethyl group in ICPD62 results in significant entropy gain; however, it is outweighed by a large decrease in binding enthalpy. Notably, the observed binding constant, as determined by FTSA, was greater for ICPD62 than ICPD47. This highlights the possible discrepancies between the observed and intrinsic binding parameters that can lead to erroneous conclusions about the contributions of the functional groups to the

binding energetics if the intrinsic thermodynamic parameters are not determined.

The crystal structures of Hsp90—ICPD compounds (see Section 3.5.1), determined in collaboration with C. Prodromou and his team, provide valuable insight into the actual contacts between the protein and ligands (Figure 3.15). Resorcinol group participates in a crucial network of hydrogen bonding with highly conserved amino-acid residues L48, S52, D93, G97, and T184 of the ATP-binding site, as previously seen in cases of pyrazole and isoxazole resorcinol inhibitors [244; 262; 263]. Some of the hydrophobic interactions are also conserved, for instance, those with N51, A55, M98, and F138.

All 4 studied ICPD compounds position themselves almost identically in the ATP-binding pocket of human Hsp90α (Figure 3.15B). Several water molecules are involved in an extensive network that anchors the thiadiazole ring in the binding pocket of Hsp90 (Figure 3.15A). Additional methoxy residue in ICPD34 forces the benzene ring to adapt a slightly different conformation in regards to the thiadiazole ring. However, this change has only minor effect on the intrinsic energetics of the binding as the benzene ring is located at the entrance of the binding pocket (Figure 3.15A).

The chlorine, present in 3 determined structures, makes hydrophobic contacts with F138 and L107. In case of ICPD62, ethyl group is capable of forming interactions with these amino acids as well. The binding pocket area, in which these residues reside, is of hydrophobic nature. Interestingly, the ICPD compounds containing chlorine are characterised by significantly higher enthalpic contributions to the intrinsic binding affinity. From a chemical standpoint, chlorine is an electron withdrawing group while ethyl is electron donating group and thus could impact the strength of the hydrogen bonds formed by the *ortho* and *para* hydroxyl groups. Nevertheless, there is no apparent difference in the orientation of ICPD47 and ICPD62 (Figure 3.15B) nor their principal interactions with Hsp90αN that could be easily predicted from the structural data. However, the quality of the structures does not allow

reliable determination of the possible small discrepancies in the hydrogen bond geometry that could account for the difference in $\Delta_b H_{intr}$.

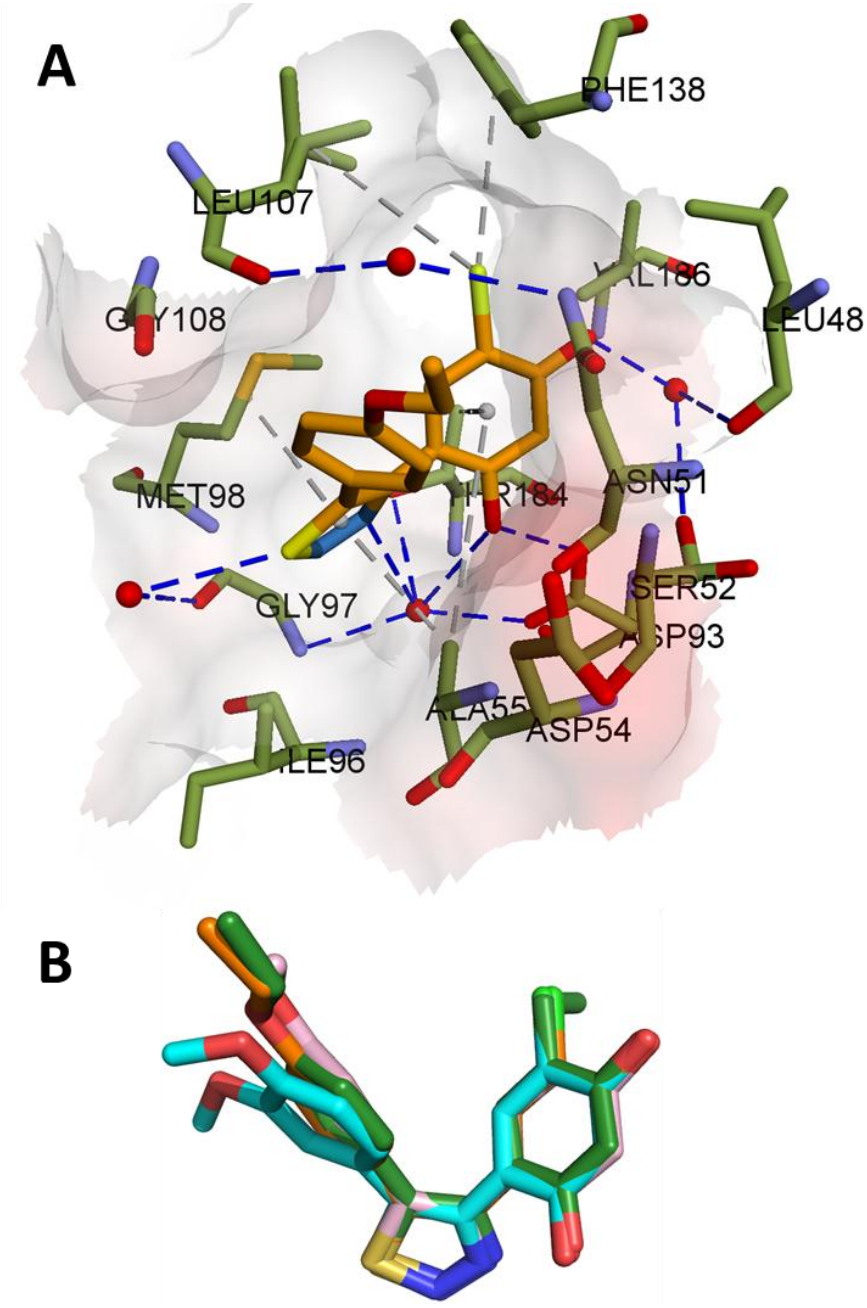

Figure 3.15. (A) ICPD47 (orange sticks) bound to the NTP-binding pocket of human Hsp90αN (protein surface is coloured according to its interpolated charge while amino acids are represented by green sticks). Blue dashed lines represent hydrogen bonds, grey ones – hydrophobic interactions. (B) Comparison of orientations of the 4 ICPD compounds bound to Hsp90αN. ICPD47 is depicted as yellow sticks, ICPD26 in pink, ICPD34 in cyan, and ICPD62 in green.

An alternative explanation of such energy profiles could lie in the unique electronic properties of halogens (excluding fluorine) when bound to aryl or similar moieties [264-266]. In addition to hydrophobic contacts, halogens are able to establish electrostatic interactions such as with the π electrons of phenylalanine [265]. Moreover, chlorine can form hydrogen bonds with C-H under certain circumstances [266; 267]. The lengths of such bonds typically are 3.0 Å or more (over 4.0 Å as well) [267], which would be in agreement with the distances between chlorine of ICPD compounds and aliphatic carbons of L107 and F138. While weak, such bonds are specific [264] and could be the source of the enthalpy gain. The increased entropy in ICPD62 could be partially explained by the higher lability of ethyl group, as compared to chlorine.

The tested ICPD compounds contain two hydroxyl groups. Due to its estimated pK_a, we predicted the hydroxyl group adjacent to chlorine being the participant of the binding-linked protonation event (see Section 3.5). According to the structural data, this hydroxyl group participates in a network of hydrogen bond interactions that involve water while the other hydroxyl group forms a direct hydrogen bond with D93 (Figure 3.15). pK_a of the side chain of aspartic acid is generally considered to be 3.96 [268]; however, its local environment in the protein can affect this property significantly. We used a bioinformatics tool *H++* [236] to compute pK_a(D93) from the structural data. This method estimated pK_a of the deeply buried aspartate at approximately 0.7, indicating that the side chain carboxyl group of D93 should be fully deprotonated under all experimental conditions described in this work. Since the pK_a estimated for the most labile group is approximately 7.3 for ICPD26, ICPD34, and ICPD47 and ~8.6 for ICPD62, we can safely conclude that it is the ligand and not the protein that participates in the binding-linked protonation event.

Notably, the hydroxyl group in *ortho* position from chlorine forms a hydrogen bond with a water molecule that is held in place by L48 and S52 in

Hsp90αN (Figure 3.15A). Instead of this serine, Hsp90β contains alanine that is not able to form a corresponding hydrogen bond. This can explain the overall lower affinity of Hsp90β to the ICPD compounds, as compared to Hsp90αN.

3.7. ICPD compounds as Hsp90 inhibitors

3.7.1. Effect of ICPD compounds on cancer cells

ICPD compound effect on human cancer cell growth was tested in three selected cancer cell lines: U2OS (osteosarcoma), HeLa (cervival carcinoma), and HCT116 (colorectal carcinoma) (Table 3.4 and Figure 3.16). The experiments were performed and interpreted by Dr. J. Matulienė, Dr. V. Petrikaitė (Vilnius University Institute of Biotechnology, Lithuania), and Dr. S.Y. Sharp (Institute of Cancer Research, United Kingdom). ICPD26, ICPD34, and ICPD47 exhibit similar growth inhibition level while significantly lower concentration of ICPD62 causes cell death. ICPD60, which is structurally similar albeit practically does not bind to Hsp90 (see Section 3.2 and 3.3), exhibits cell growth inhibiting effect only at higher concentrations. In contrast to the 4 ICPD compounds that do bind to Hsp90, we did not observe total cell population death when treated with ICPD60 under the experimental conditions.

Table 3.4. ICPD compound inhibitory activity on cancer cells. The values presented are EC_{50} mean ± standard error of assays done in multiplicate. All values are displayed in μM.

Cell line / Compound	U2OS	HeLa	HCT116
ICPD26	5.6±0.4	2.35±0.02	3.2±0.7
ICPD34	7.2±0.5	3.13±0.09	4.6±0.4
ICPD47	8.3±0.7	3.76±0.33	4.6±0.4
ICPD60	24.2±0.1	19.5±1.7	n.d.
ICPD62	0.70±0.04	0.79±0.02	n.d.

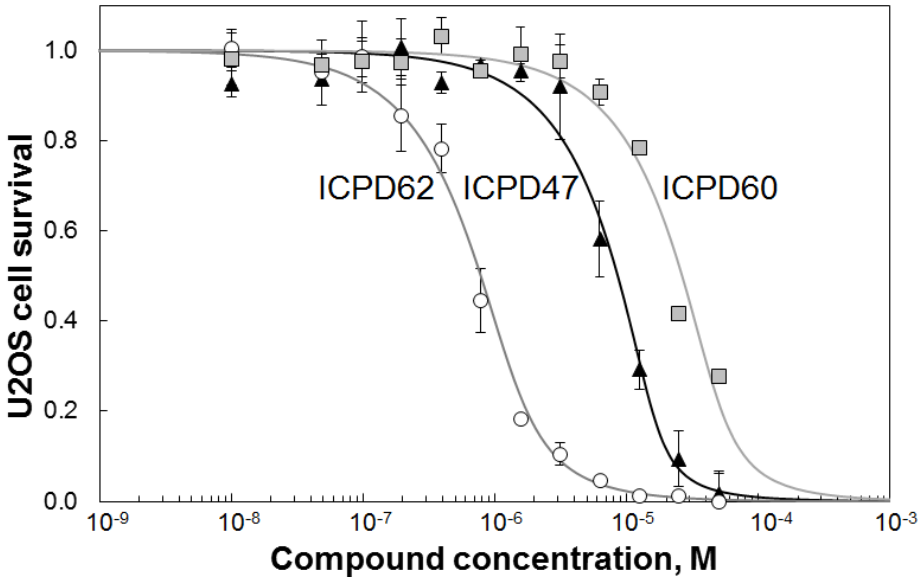

Figure 3.16. Normalised U2OS cancer cell line survival as a function of compound (ICPD47, ICPD60, and ICPD62) concentration. The error bars depict standard error of at least two experiments. As denoted, ICPD62 is depicted as white circles, ICPD47 – black triangles, and ICPD60 – grey squares.

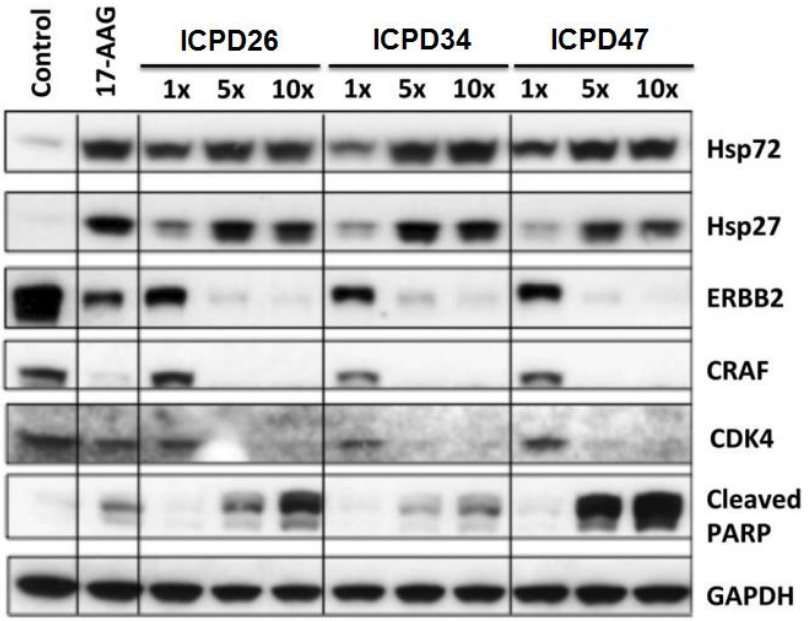

Figure 3.17. The biomarker signature of Hsp90 inhibition in HCT116 cells. Western blot analysis was performed on cells being treated with 1×, 5×, or 10× GI_{50} concentrations for 24 h. For positive control, the cells were treated with 17-AAG, while GAPDH was used as loading control. [238]

In order to confirm that the observed growth inhibition was caused by the ICPD compounds inhibiting Hsp90, Dr. S.Y. Sharp performed analysis of

several selected well established Hsp90 inhibition biomarkers in HCT166 cells (Figure 3.17). Treatment of these cells with ICPD compounds resulted in elevated expression of heat shock proteins (Hsp72 and Hsp27) and depletion of selected client proteins (CRAF, ERBB2, and CDK4), both explicit indications of Hsp90 inhibition. Moreover, the observed increased level of cleaved PARP indicates induction of apoptosis. Overall this data show that the 4 ICPD compounds analysed in this work do inhibit Hsp90 in cancer cells *in vitro* and thus causes cancer cell death.

3.7.2. Future directions

Hsp90 is a promising target for anticancer drugs and might be exploited in treatment of some other diseases (see Section 1.3). While several Hsp90 inhibitors have been assessed in clinical trials, most were discontinued due to various undesirable side-effects. Since the side-effects seem to vary, they are mostly caused by the compounds rather than the Hsp90 inhibition itself. Based on the obtained thermodynamic and structural data, the series of ICPD compounds could be expanded by probing new possible interactions.

The discrepancy between the significantly larger cell growth inhibitory effect of ICPD62 and similar K_{b_intr} values, as compared to the other 3 analysed ICPD compounds, could be attributed to higher cell membrane permeability. In general, electrically neutral molecules pass through the hydrophobic cell membrane more easily than charged ones. The ethyl group in ICPD62 that substituted chlorine is not only of hydrophobic nature itself but also highly promotes protonated state of the adjacent hydroxyl group at pH characteristic to cell medium. However, this also results in an undesirable loss of enthalpy contribution to the binding, thus impeding further compound optimisation. Therefore the mostly enthalpically driven binding of ICPD26 and ICPD47 to Hsp90N could be augmented by increasing their hydrophobicity without impairing their hydrophilic interactions with the active site of Hsp90.

However, occurrences of Hsp90 surface mutations that grant the protein resistance to certain inhibitors have been noticed [269; 270]. Therefore the less bulky nature of the ICPD compounds and a simple interaction set with the conservative Hsp90 residues might prove an advantage over some of the larger compounds as cancer cell genes tend to mutate and could potentially acquire resistance.

Notably, the tested compounds bound to both Hsp90α and Hsp90β with similar tendencies albeit their affinity to Hsp90β was slightly lower in all cases. Overall, we have shown here that the ICPD compounds are enthalpically optimised single-digit nanomolar binders of Hsp90 that may represent a therapeutically very useful class of Hsp90 inhibitors. The current *in vitro* characterisation of ICPD compounds makes them viable candidates for initial xenograft experiments and further clinical trials. Given the enthalpic nature of their binding, some of the studied ICPD compounds could be further developed to improve their cell membrane permeability and binding to Hsp90.

CONCLUSIONS

1. ICPD compounds are tight binders of both human Hsp90α and Hsp90β isoforms with observed K_b ranging from 4.8×10^6 to 1.65×10^8 M^{-1}, tighter than the classic inhibitor 17-AAG.

2. Affinity of ICPD compounds to Hsp90α is 4 to 6 times higher than to Hsp90β.

3. Protonation of hydroxyl group in ICPD compounds is essential for binding to Hsp90.

4. Intrinsically, binding of ICPD26, ICPD34, and ICPD47 to Hsp90 is driven mostly (~84 %) by enthalpy which makes them suitable candidates for further drug development while ICPD62 binding is driven by enthalpy and entropy in roughly equal parts.

5. Chlorine in the ICPD compounds increases enthalpic contribution to the intrinsic binding affinity, as opposed to ethyl group in ICPD62 which promotes the entropic factor, signifying the ability of chlorine to form additional interactions of non-hydrophobic nature.

6. Small alkoxy substituent on the non-resorcinol benzene ring in the ICPD compounds has only negligible effect on the intrinsic binding parameters.

LIST OF PUBLICATIONS

The thesis is based on the following original publications:

1. Sharp SY, Roe SM, **Kazlauskas E**, Cikotienė I, Workman P, Matulis D, Prodromou C. Co-crystalization and in vitro biological characterization of 5-aryl-4-(5-substituted-2-4-dihydroxyphenyl)-1,2,3-thiadiazole Hsp90 inhibitors. *PLoS One*. 2012;7(9):e44642.

2. **Kazlauskas E**, Petrikaitė V, Michailovienė V, Revuckienė J, Matulienė J, Grinius L, Matulis D. Thermodynamics of aryl-dihydroxyphenyl-thiadiazole binding to human Hsp90. *PLoS One*. 2012;7(5):e36899.

3. Cikotiene I, **Kazlauskas E**, Matuliene J, Michailoviene V, Torresan J, Jachno J, Matulis D. 5-Aryl-4-(5-substituted-2,4-dihydroxyphenyl)-1,2,3-thiadiazoles as inhibitors of Hsp90 chaperone. *Bioorg Med Chem Lett*. 2009;19(4):1089-92.

Patents:

Matulis D., Cikotiene I., **Kazlauskas E**., Matuliene J. 5-aryl-4-(5-substituted 2,4-dihydroxyphenyl)-1,2,3-thiadiazoles as inhibitors of Hsp90 chaperone and the intermediates for production thereof. US 831413220. 2012-12-20

Matulis D., Cikotiene I., **Kazlauskas E**., Matuliene J. 5-aryl-4-(5-substituted 2,4-dihydroxyphenyl)-1,2,3-thiadiazoles as inhibitors of Hsp90 chaperone and the intermediates for production thereof. EP 2268626 B1. 2012-02-01

D. Matulis, I. Čikotienė, **E.Kazlauskas**, J.Matulienė. 5-aril-4-(5-pakeistieji 2,4-dihidroksifenil)-1,2,3-tiacilazolai kaip Hsp90 šaperono slopikliai ir tarpiniai junginiai jiems gauti. LT 5623 B. 2010-01-25

Other publications:

1. Dudutienė V, Matulienė J, Smirnov A, Timm DD, Zubrienė A, Baranauskienė L, Morkūnaite V, Smirnovienė J, Michailovienė V, Juozapaitienė V, Mickevičiūtė A, Kazokaitė J, Bakšytė S, Kasiliauskaitė A, Jachno J, Revuckienė J, Kišonaitė M, Pilipuitytė V, Ivanauskaitė E, Milinavičiūtė G, Smirnovas V, Petrikaitė V, Kairys V, Petrauskas V, Norvaišas P, Lingė D, Gibieža P, Capkauskaitė E, Zakšauskas A, **Kazlauskas E**, Manakova E, Gražulis S, Ladbury JE, Matulis D. Discovery and characterization of novel selective inhibitors of carbonic anhydrase IX. *J Med Chem*. 2014;57(22):9435-46.

2. Giessrigl B, Krieger S, Rosner M, Huttary N, Saiko P, Alami M, Messaoudi S, Peyrat JF, Maciuk A, Gollinger M, Kopf S, **Kazlauskas E**, Mazal P, Szekeres T, Hengstschläger M, Matulis D, Jäger W, Krupitza G. Hsp90 stabilizes Cdc25A and counteracts heat shock-mediated Cdc25A degradation and cell-cycle attenuation in pancreatic carcinoma cells. *Hum Mol Genet*. 2012;21(21):4615-27.

3. Zubriene A, **Kazlauskas E**, Baranauskiene L, Petrauskas V, Matulis D. Isothermal titration calorimetry and thermal shift assay in drug design. *Eur Pharm Rev* 2011;16:56-59.

Conference presentations[1]:

1. Zubrienė A., Baranauskienė L., **Kazlauskas E.**, Petrauskas V., Matulis D. Thermodynamics of Anticancer Drug Lead Binding to Target Proteins by Thermal Shift Assay. Signature discovery. Nottingham, Great Britain, 2014 10 08.

2. Petrikaitė V., Brukštus A., **Kazlauskas E.**, Petrikas H., Čikotienė I., Matulienė J., Matulis D. Synthesis of 6-(5-aryl-1,2,3-thiadiazol-4-yl)-4-

[1] Underlined name indicates conferences which I attended personally.

isopropylbenzene-1,3-dioles as Hsp90 inhibitors and their activity on human tumor cell lines. COST-TD0905. Athens, Greece, 2014 05 04–08.

3. Brukštus A., **Kazlauskas E.**, Petrikas H., Petrikaitė V., Čikotienė I., Matulis D. Synthesis and Biological Evaluation of 6-(5-Aryl-1,2,3-thiadiazol-4-yl)-4-isopropylbenzene-1,3-dioles as Inhibitors of Hsp90. Chemistry and Chemical Technology. Kaunas, Lithuania, 2014 04 25.

4. Petrikaitė V., **Kazlauskas E.**, Matulis D. Thermodynamics of Aryl-dihydroxyphenyl-thiadiazole Inhibitor Series Binding to Molecular Chaperone Hsp90. COST TD0905. Vilnius, Lithuania, 2013 10 30–31.

5. Zubrienė A., Baranauskienė L., **Kazlauskas E.**, Petrauskas E., Matulis D. Thermodynamics of anticancer drug lead binding to target proteins by thermal shift assay. NovAliX Conference 2013. Biophysics in drug discovery. Strasbourg, France, 2013 10 15–18.

6. **Kazlauskas E.**, Petrikaitė V., Matulis D. Thermodynamics of Aryl-dihydroxyphenyl-thiadiazole Inhibitor Series Binding to Molecular Chaperone Hsp90. 2nd Central and Eastern European Conference on Thermal Analysis and Calorimetry. Vilnius, Lithuania, 2013 08 27–30.

7. Zubrienė A., Gylytė J., Morkūnaitė V., **Kazlauskas E.**, Baranauskienė L., Čapkauskaitė E., Dudutienė V., Jogaitė V., Michailovienė V., Kazokaitė J., Kasiliauskaitė A., Petrikaitė V., Petrauskas V., Matulienė J., Matulis D. Thermodynamics of anticancer drug lead binding to target proteins by thermal shift assay. 9th European Biophysics Congress. Lisbon, Portugal, 2013 07 13–18.

8. Zubrienė A., Baranauskienė L., **Kazlauskas E.**, Gylytė J., Timm D., Morkūnaitė V., Kišonaitė M., Čapkauskaitė E., Dudutienė V., Jogaitė V., Kazokaitė J., Kasiliauskaitė A., Michailovienė V., Mickevičiūtė A., Bakšytė S., Petrikaitė V., Petrauskas V., Smirnov A., Manakova L., Gražulis S., Kairys V., Matulienė J., Matulis D. The Pitfalls of Drug Lead IC_{50} and Binding Measurements to Target Proteins. COST CM0804. Izmir, Turkey, 2013 05 05–09.

9. **Kazlauskas E.**, Matulis D. Thermodynamics of aryl-dihydroxyphenyl-thiazole binding to HSP90. 6th International Conference on the Hsp90 Chaperone Machine. Les Diablerets, Switzerland, 2012 09 19–23.

10.Petrikaite V., **Kazlauskas E.**, Matuliene J., Matulis D. Development of Hsp90 inhibitors as anticancer compounds. Animal Models and Their Value in Predicting Efficacy and Toxicity. New York, USA, 2011 09 15–16.

11.Zubrienė A., Baranauskienė L., **Kazlauskas E.**, Toleikis Z., Matulis D. Drug Binding Energetics by Titration Calorimetry, Thermal and Pressure Shift Assay. The 1st Central and Eastern European Conference on Thermal Analysis and Calorimetry. Craiova, Romania, 2011 09 07–10.

12.Zubrienė A., **Kazlauskas E.**, Michailovienė V., Matulis D. Towards intrinsic binding thermodynamics. 8th European Biophysics Congress. Budapest, Hungary, 2011 08 23–27.

13.Petrikaite V., **Kazlauskas E.**, Matuliene J., Matulis D. Anticancer activity and ADMET properties of resorcinol-bearing lead compounds. Drug Discovery and Selection. Lyon, France, 2011 07 06–08.

14.Petrikaitė V., **Kazlauskas E.**, Matulienė J., Matulis D. Rezorcinolio darinių priešvėžinis aktyvumas ir farmakokinetinių savybių tyrimas. Pasaulio lietuvių mokslo ir kūrybos simpoziumas. Kaunas, Lietuva, 2011 07 03–04.

15.Petrikaite V., **Kazlauskas E.**, Matuliene J., Matulis D. Pharmacokinetics and toxicity of resorcinol-bearing lead compounds. Frontiers in Medicinal Chemistry. Stockholm, Sweden, 2011 06 19–21.

16.Petrauskas V., Zubrienė A., **Kazlauskas E.**, Baranauskienė L., Matulis D. Intrinsic Binding Parameters as a Necessity to Correlate Energetics with Structure. 19th Biennial Meeting of the International Society for Molecular Recognition. Tavira, Portugal, 2011 06 16–19.

17.Zubrienė A., Baranauskienė L., **Kazlauskas E.**, Čapkauskaitė E., Dudutienė V., Toleikis Z., Jogaitė V., Chaleckis R., Michailovienė V., Šližytė J., Torresan J., Petrikaitė V., Petrauskas V., Matulienė J., Matulis D.

Thermodynamic-structure correlation of drug lead binding to target proteins. The 66th Calorimetry Conference. Oahu, Hawaii, USA, 2011 06 12–17.

18.Zubrienė A., **Kazlauskas E.**, Baranauskienė L., Petrauskas V., Matulis D. Towards the intrinsic lead binding thermodynamics. COST TD0905. Split, Croatia, 2011 04 29–30.

19.Petrikaitė V., **Kazlauskas E.**, Zubriene A., Michailoviene V., Matuliene J., Matulis D. Anticancer activity and ADME/Tox properties of resorcinol-bearing Hsp90 inhibitors. ADMET Europe. Munich, Germany, 2011 03 28-29.

20.Zubrienė A., Baranauskienė L., **Kazlauskas E.**, Toleikis Z., Chaleckis R., Michailovienė V., Petrikaitė V., Čapkauskaitė E., Dudutienė V., Matulienė J., Matulis D. Resorcinol-Bearing Hsp90 inhibitors as anticancer agents. COST Action TD0905 Epigenetics - Bench to Bedside. Brno, Czech, 2010 11 22–25.

21.Zubrienė A., Maier M.E., Sasse F., **Kazlauskas E.**, Toleikis Z., Chaleckis R., Michailovienė V., Petrikaitė V., Grinius L., Matulienė J., Matulis D., Radicicol, a natural compound and an efficient inhibitor of Hsp90, as a lead for anticancer drug design. COST Action CM0804, Workshop "Natural Products as Drugs and Leads to Drugs". Crete, Greece, 2010 10 12–15.

22.Zubrienė A., **Kazlauskas E.**, Chaleckis R., Michailovienė V., Matulienė J., Matulis D. Thermodynamics of radicicol binding to human Hsp90 alpha and beta isoforms. 5th International Conference on the Hsp90 Chaperone Machine. Les Diablerets, Switzerland, 2010 09 29–10 03.

23.Cimmperman P., Zubrienė A., Baranauskienė L., **Kazlauskas E.**, Matulienė J., Matulis D. Determination of protein-ligand binding thermodynamics by thermal shift assay. European Biophysics Congress. Genoa, Italy, 2009 07 11–15.

24.Baranauskiene L., **Kazlauskas E.**, Cikotiene I., Matuliene J., Zubriene A., Jachno J., Torresan J., Michailoviene V., Cimmperman P., Grazulis S., Matulis D. Carbonic anhydrase and Hsp90 inhibitor binding measurements by

thermal shift assay, titration calorimetry, and X-ray crystallography. INSTRUCT meeting. Budapest, Hungary, 2009 03 29–31.

25.**Kazlauskas E.**, Čikotienė I., Matulienė J., Zubrienė A., Grinius L., Jachno J., Torresan J., Michailovienė V., Petrikaitė V., Matulis D. Resorcinol Class Hsp90 Inhibitors Binding Thermodynamics and the Effect on Cancerous Cells. 4th International Conference on the Hsp90 Chaperone Machine. Seeon, Germany, 2008 10 02–06.

26.Matulis D., **Kazlauskas E.**, Baranauskienė L., Čikotienė I., Dudutienė V., Matulienė J., Zubrienė A., Jachno J., Torresan J., Michailovienė V., Cimmperman P., Lingė D., Zaveckas M., Petrikaitė V., Šebėka H., Grinius L. Chaperone Hsp90 and carbonic anhydrase IX inhibitors as anticancer agents. 7th ScanBalt Forum & Biomaterial Days. Vilnius, Lithuania, 2008 09 24–26.

ACKNOWLEDGEMENTS

I would like to express my deepest gratitude to the people who made this work possible.

First of all, I thank my supervisor Prof. Dr. D. Matulis for the opportunity to work in his team, discussions, boundless optimism, and multiple encouragements towards doctoral thesis defence.

I thank V. Michailovienė and students under her supervision for the steady supply of Hsp90 proteins, Prof. Dr. I. Čikotienė for the ICPD compounds, Dr. J. Matulienė for initial Hsp90 expression plasmids and cell assays, Dr. S. Y. Sharp (The Institute of Cancer Research, London) for cell assays, Dr. S. M. Roe and Dr. C. Prodromou (University of Sussex) for the crystal structures.

I am grateful to all my colleagues at the Department of Biothermodynamics and Drug Design, especially Dr. L. Baranauskienė for many discussions and advice, Dr. A. Zubrienė for valuable discussions and suggestions about this work, Dr. V. Petrikaitė for help with interpretation of cell assay data and other discussions, Dr. V. Petrauskas for healthy critique of this work, and Dr. V. Kairys for revision of this thesis.

I also thank Dr. Mindaugas Zaremba and Dr. Saulius Serva for the reviews of this doctoral thesis.

I wish to thank my chemistry teacher J. Lagunavičius who consolidated my decision to study biochemistry and Dr. G. Sasnauskas for guidance during my first years in a biochemical laboratory.

My greatest thanks are to my parents for their concern, support, and the love for nature, instilled from my early days. A special thanks to my dearest wife Miglė for understanding. I would also like to thank my many pets and plants, and my trusted DnD party for their moral support.

LITERATURE

[1] CancerResearch UK (accessed in 2016) www.cancerresearchuk.org, "Cancer risk statistics".

[2] Taipale M, Jarosz DF, Lindquist S (2010) HSP90 at the hub of protein homeostasis: emerging mechanistic insights. *Nat Rev Mol Cell Biol* 11: 515-528

[3] Banerji U (2009) Heat shock protein 90 as a drug target: some like it hot. *Clin Cancer Res* 15: 9-14

[4] Garbett NC, Chaires JB (2012) Thermodynamic studies for drug design and screening. *Expert Opin Drug Discov* 7: 299-314

[5] Freire E (2008) Do enthalpy and entropy distinguish first in class from best in class? *Drug Discov Today* 13: 869-874

[6] Ferenczy GG, Keseru GM (2015) The impact of binding thermodynamics on medicinal chemistry optimizations. *Future Med Chem* 7: 1285-1303

[7] Ladbury JE (2010) Calorimetry as a tool for understanding biomolecular interactions and an aid to drug design. *Biochem Soc Trans* 38: 888-893

[8] Baker BM, Murphy KP (1997) Dissecting the energetics of a protein-protein interaction: the binding of ovomucoid third domain to elastase. *J Mol Biol* 268: 557-569

[9] Hartl FU, Bracher A, Hayer-Hartl M (2011) Molecular chaperones in protein folding and proteostasis. *Nature* 475: 324-332

[10] Hartl FU (1996) Molecular chaperones in cellular protein folding. *Nature* 381: 571-579

[11] Saibil H (2013) Chaperone machines for protein folding, unfolding and disaggregation. *Nat Rev Mol Cell Biol* 14: 630-642

[12] Cutforth T, Rubin GM (1994) Mutations in Hsp83 and cdc37 impair signaling by the sevenless receptor tyrosine kinase in Drosophila. *Cell* 77: 1027-1036

[13] Birnby DA, Link EM, Vowels JJ, Tian H, Colacurcio PL, Thomas JH (2000) A transmembrane guanylyl cyclase (DAF-11) and Hsp90 (DAF-21) regulate a common set of chemosensory behaviors in caenorhabditis elegans. *Genetics* 155: 85-104

[14] Borkovich KA, Farrelly FW, Finkelstein DB, Taulien J, Lindquist S (1989) hsp82 is an essential protein that is required in higher concentrations for growth of cells at higher temperatures. *Mol Cell Biol* 9: 3919-3930

[15] Gupta RS (1995) Phylogenetic analysis of the 90 kD heat shock family of protein sequences and an examination of the relationship among animals, plants, and fungi species. *Mol Biol Evol* 12: 1063-1073

[16] Millson SH, Truman AW, Racz A, Hu B, Panaretou B, Nuttall J, Mollapour M, Soti C, Piper PW (2007) Expressed as the sole Hsp90 of yeast, the alpha and beta isoforms of human Hsp90 differ with regard to their capacities for activation of certain client proteins, whereas only Hsp90beta generates sensitivity to the Hsp90 inhibitor radicicol. *FEBS J* 274: 4453-4463

[17] Csermely P, Schnaider T, Soti C, Prohaszka Z, Nardai G (1998) The 90-kDa molecular chaperone family: structure, function, and clinical applications. A comprehensive review. *Pharmacol Ther* 79: 129-168

[18] Durkin AS, Maglott DR, Vamvakopoulos NC, Zoghbi HY, Nierman WC (1993) Assignment of an intron-containing human heat-shock protein gene (hsp90 beta, HSPCB) to chromosome 6 near TCTE1 (6p21) and two intronless pseudogenes to chromosomes 4 and 15 by polymerase chain reaction amplification from a panel of hybrid cell lines. *Genomics* 18: 452-454

[19] Pelham HR (1982) A regulatory upstream promoter element in the Drosophila hsp 70 heat-shock gene. *Cell* 30: 517-528

[20] Sreedhar AS, Kalmar E, Csermely P, Shen YF (2004) Hsp90 isoforms: functions, expression and clinical importance. *FEBS Lett* 562: 11-15

[21] Yufu Y, Nishimura J, Nawata H (1992) High constitutive expression of heat shock protein 90 alpha in human acute leukemia cells. *Leuk Res* 16: 597-605

[22] Jerome V, Leger J, Devin J, Baulieu EE, Catelli MG (1991) Growth factors acting via tyrosine kinase receptors induce HSP90 alpha gene expression. *Growth Factors* 4: 317-327

[23] Bertram J, Palfner K, Hiddemann W, Kneba M (1996) Increase of P-glycoprotein-mediated drug resistance by hsp 90 beta. *Anticancer Drugs* 7: 838-845

[24] Marzec M, Eletto D, Argon Y (2012) GRP94: An HSP90-like protein specialized for protein folding and quality control in the endoplasmic reticulum. *Biochim Biophys Acta* 1823: 774-787

[25] Song HY, Dunbar JD, Zhang YX, Guo D, Donner DB (1995) Identification of a protein with homology to hsp90 that binds the type 1 tumor necrosis factor receptor. *J Biol Chem* 270: 3574-3581

[26] Coller HA, Grandori C, Tamayo P, Colbert T, Lander ES, Eisenman RN, Golub TR (2000) Expression analysis with oligonucleotide microarrays reveals that MYC regulates genes involved in growth, cell cycle, signaling, and adhesion. *Proc Natl Acad Sci U S A* 97: 3260-3265

[27] Zhang Y, Jiang DS, Yan L, Cheng KJ, Bian ZY, Lin GS (2011) HSP75 protects against cardiac hypertrophy and fibrosis. *J Cell Biochem* 112: 1787-1794

[28] Costantino E, Maddalena F, Calise S, Piscazzi A, Tirino V, Fersini A, Ambrosi A, Neri V, Esposito F, Landriscina M (2009) TRAP1, a novel mitochondrial chaperone responsible for multi-drug resistance and protection from apoptotis in human colorectal carcinoma cells. *Cancer Lett* 279: 39-46

[29] Prodromou C, Roe SM, O'Brien R, Ladbury JE, Piper PW, Pearl LH (1997) Identification and structural characterization of the ATP/ADP-binding site in the Hsp90 molecular chaperone. *Cell* 90: 65-75

[30] Roy N, Nageshan RK, Ranade S, Tatu U (2012) Heat shock protein 90 from neglected protozoan parasites. *Biochim Biophys Acta* 1823: 707-711

[31] Dutta R, Inouye M (2000) GHKL, an emergent ATPase/kinase superfamily. *Trends Biochem Sci* 25: 24-28

[32] Meyer P, Prodromou C, Hu B, Vaughan C, Roe SM, Panaretou B, Piper PW, Pearl LH (2003) Structural and functional analysis of the middle segment of hsp90: implications for ATP hydrolysis and client protein and cochaperone interactions. *Mol Cell* 11: 647-658

[33] Young JC, Schneider C, Hartl FU (1997) In vitro evidence that hsp90 contains two independent chaperone sites. *FEBS Lett* 418: 139-143

[34] Whitesell L, Lindquist SL (2005) HSP90 and the chaperoning of cancer. *Nat Rev Cancer* 5: 761-772

[35] Shiau AK, Harris SF, Southworth DR, Agard DA (2006) Structural Analysis of E. coli hsp90 reveals dramatic nucleotide-dependent conformational rearrangements. *Cell* 127: 329-340

[36] Ali MM, Roe SM, Vaughan CK, Meyer P, Panaretou B, Piper PW, Prodromou C, Pearl LH (2006) Crystal structure of an Hsp90-nucleotide-p23/Sba1 closed chaperone complex. *Nature* 440: 1013-1017

[37] Dollins DE, Warren JJ, Immormino RM, Gewirth DT (2007) Structures of GRP94-nucleotide complexes reveal mechanistic differences between the hsp90 chaperones. *Mol Cell* 28: 41-56

[38] Picard D. (2015) www.picard.ch, "Table of Hsp90 interactors".

[39] Echeverria PC, Bernthaler A, Dupuis P, Mayer B, Picard D (2011) An interaction network predicted from public data as a discovery tool: application to the Hsp90 molecular chaperone machine. *PLoS One* 6: e26044

[40] Hartson SD, Matts RL (2012) Approaches for defining the Hsp90-dependent proteome. *Biochim Biophys Acta* 1823: 656-667

[41] Richter K, Meinlschmidt B, Buchner J (2005) Hsp90: From Dispensable Heat Shock Protein to Global Player. In *Protein Folding Handbook*, Buchner J, Kiefhaber T (eds), Vol. II, 23. Weinheim, Germany: Wiley-VCH Verlag GmbH

[42] Breitkreutz BJ, Stark C, Reguly T, Boucher L, Breitkreutz A, Livstone M, Oughtred R, Lackner DH, Bahler J, Wood V, Dolinski K, Tyers M (2008) The BioGRID Interaction Database: 2008 update. *Nucleic Acids Res* 36: D637-640

[43] Joab I, Radanyi C, Renoir M, Buchou T, Catelli MG, Binart N, Mester J, Baulieu EE (1984) Common non-hormone binding component in non-transformed chick oviduct receptors of four steroid hormones. *Nature* 308: 850-853

[44] Wilhelmsson A, Cuthill S, Denis M, Wikstrom AC, Gustafsson JA, Poellinger L (1990) The specific DNA binding activity of the dioxin receptor is modulated by the 90 kd heat shock protein. *EMBO J* 9: 69-76

[45] Sanchez ER, Toft DO, Schlesinger MJ, Pratt WB (1985) Evidence that the 90-kDa phosphoprotein associated with the untransformed L-cell glucocorticoid receptor is a murine heat shock protein. *J Biol Chem* 260: 12398-12401

[46] Aligue R, Akhavan-Niak H, Russell P (1994) A role for Hsp90 in cell cycle control: Wee1 tyrosine kinase activity requires interaction with Hsp90. *EMBO J* 13: 6099-6106

[47] Oppermann H, Levinson W, Bishop JM (1981) A cellular protein that associates with the transforming protein of Rous sarcoma virus is also a heat-shock protein. *Proc Natl Acad Sci U S A* 78: 1067-1071

[48] Stancato LF, Chow YH, Hutchison KA, Perdew GH, Jove R, Pratt WB (1993) Raf exists in a native heterocomplex with hsp90 and p50 that can be reconstituted in a cell-free system. *J Biol Chem* 268: 21711-21716

[49] Wegele H, Muller L, Buchner J (2004) Hsp70 and Hsp90--a relay team for protein folding. *Rev Physiol Biochem Pharmacol* 151: 1-44

[50] Muller PA, Vousden KH (2013) p53 mutations in cancer. *Nat Cell Biol* 15: 2-8

[51] Sepehrnia B, Paz IB, Dasgupta G, Momand J (1996) Heat shock protein 84 forms a complex with mutant p53 protein predominantly within a cytoplasmic compartment of the cell. *J Biol Chem* 271: 15084-15090

[52] Blagosklonny MV, Toretsky J, Bohen S, Neckers L (1996) Mutant conformation of p53 translated in vitro or in vivo requires functional HSP90. *Proc Natl Acad Sci U S A* 93: 8379-8383

[53] Brugge JS, Erikson E, Erikson RL (1981) The specific interaction of the Rous sarcoma virus transforming protein, pp60src, with two cellular proteins. *Cell* 25: 363-372

[54] Whitesell L, Mimnaugh EG, De Costa B, Myers CE, Neckers LM (1994) Inhibition of heat shock protein HSP90-pp60v-src heteroprotein complex formation by benzoquinone ansamycins: essential role for stress proteins in oncogenic transformation. *Proc Natl Acad Sci U S A* 91: 8324-8328

[55] Murphy SM, Bergman M, Morgan DO (1993) Suppression of c-Src activity by C-terminal Src kinase involves the c-Src SH2 and SH3 domains: analysis with Saccharomyces cerevisiae. *Mol Cell Biol* 13: 5290-5300

[56] Bijlmakers MJ, Marsh M (2000) Hsp90 is essential for the synthesis and subsequent membrane association, but not the maintenance, of the Src-kinase p56(lck). *Mol Biol Cell* 11: 1585-1595

[57] Pratt WB, Toft DO (2003) Regulation of signaling protein function and trafficking by the hsp90/hsp70-based chaperone machinery. *Exp Biol Med (Maywood)* 228: 111-133

[58] Rutherford SL, Lindquist S (1998) Hsp90 as a capacitor for morphological evolution. *Nature* 396: 336-342

[59] Specchia V, Piacentini L, Tritto P, Fanti L, D'Alessandro R, Palumbo G, Pimpinelli S, Bozzetti MP (2010) Hsp90 prevents phenotypic variation by suppressing the mutagenic activity of transposons. *Nature* 463: 662-665

[60] Liu J, Carmell MA, Rivas FV, Marsden CG, Thomson JM, Song JJ, Hammond SM, Joshua-Tor L, Hannon GJ (2004) Argonaute2 is the catalytic engine of mammalian RNAi. *Science* 305: 1437-1441

[61] Obermann WM, Sondermann H, Russo AA, Pavletich NP, Hartl FU (1998) In vivo function of Hsp90 is dependent on ATP binding and ATP hydrolysis. *J Cell Biol* 143: 901-910

[62] Panaretou B, Prodromou C, Roe SM, O'Brien R, Ladbury JE, Piper PW, Pearl LH (1998) ATP binding and hydrolysis are essential to the function of the Hsp90 molecular chaperone in vivo. *EMBO J* 17: 4829-4836

[63] McLaughlin SH, Smith HW, Jackson SE (2002) Stimulation of the weak ATPase activity of human hsp90 by a client protein. *J Mol Biol* 315: 787-798

[64] Weikl T, Muschler P, Richter K, Veit T, Reinstein J, Buchner J (2000) C-terminal regions of Hsp90 are important for trapping the nucleotide during the ATPase cycle. *J Mol Biol* 303: 583-592

[65] Graf C, Stankiewicz M, Kramer G, Mayer MP (2009) Spatially and kinetically resolved changes in the conformational dynamics of the Hsp90 chaperone machine. *EMBO J* 28: 602-613

[66] Li J, Buchner J (2013) Structure, function and regulation of the hsp90 machinery. *Biomed J* 36: 106-117

[67] Richter K, Moser S, Hagn F, Friedrich R, Hainzl O, Heller M, Schlee S, Kessler H, Reinstein J, Buchner J (2006) Intrinsic inhibition of the Hsp90 ATPase activity. *J Biol Chem* 281: 11301-11311

[68] Li J, Richter K, Reinstein J, Buchner J (2013) Integration of the accelerator Aha1 in the Hsp90 co-chaperone cycle. *Nat Struct Mol Biol* 20: 326-331

[69] Richter K, Soroka J, Skalniak L, Leskovar A, Hessling M, Reinstein J, Buchner J (2008) Conserved conformational changes in the ATPase cycle of human Hsp90. *J Biol Chem* 283: 17757-17765

[70] Leskovar A, Wegele H, Werbeck ND, Buchner J, Reinstein J (2008) The ATPase cycle of the mitochondrial Hsp90 analog Trap1. *J Biol Chem* 283: 11677-11688

[71] Caplan AJ (2003) What is a co-chaperone? *Cell Stress Chaperones* 8: 105-107

[72] Wandinger SK, Richter K, Buchner J (2008) The Hsp90 chaperone machinery. *J Biol Chem* 283: 18473-18477

[73] Prodromou C, Siligardi G, O'Brien R, Woolfson DN, Regan L, Panaretou B, Ladbury JE, Piper PW, Pearl LH (1999) Regulation of Hsp90 ATPase activity by tetratricopeptide repeat (TPR)-domain co-chaperones. *EMBO J* 18: 754-762

[74] Scheufler C, Brinker A, Bourenkov G, Pegoraro S, Moroder L, Bartunik H, Hartl FU, Moarefi I (2000) Structure of TPR domain-peptide complexes: critical elements in the assembly of the Hsp70-Hsp90 multichaperone machine. *Cell* 101: 199-210

[75] Johnson BD, Schumacher RJ, Ross ED, Toft DO (1998) Hop modulates Hsp70/Hsp90 interactions in protein folding. *J Biol Chem* 273: 3679-3686

[76] Roe SM, Ali MM, Meyer P, Vaughan CK, Panaretou B, Piper PW, Prodromou C, Pearl LH (2004) The Mechanism of Hsp90 regulation by the protein kinase-specific cochaperone p50(cdc37). *Cell* 116: 87-98

[77] Panaretou B, Siligardi G, Meyer P, Maloney A, Sullivan JK, Singh S, Millson SH, Clarke PA, Naaby-Hansen S, Stein R, Cramer R, Mollapour M, Workman P, Piper PW, Pearl LH, Prodromou C (2002) Activation of the ATPase activity of hsp90 by the stress-regulated cochaperone aha1. *Mol Cell* 10: 1307-1318

[78] Hessling M, Richter K, Buchner J (2009) Dissection of the ATP-induced conformational cycle of the molecular chaperone Hsp90. *Nat Struct Mol Biol* 16: 287-293

[79] Lotz GP, Lin H, Harst A, Obermann WM (2003) Aha1 binds to the middle domain of Hsp90, contributes to client protein activation, and stimulates the ATPase activity of the molecular chaperone. *J Biol Chem* 278: 17228-17235

[80] Siligardi G, Hu B, Panaretou B, Piper PW, Pearl LH, Prodromou C (2004) Co-chaperone regulation of conformational switching in the Hsp90 ATPase cycle. *J Biol Chem* 279: 51989-51998

[81] Mollapour M, Tsutsumi S, Neckers L (2010) Hsp90 phosphorylation, Wee1 and the cell cycle. *Cell Cycle* 9: 2310-2316

[82] Legagneux V, Morange M, Bensaude O (1991) Heat shock increases turnover of 90 kDa heat shock protein phosphate groups in HeLa cells. *FEBS Lett* 291: 359-362

[83] Mollapour M, Tsutsumi S, Truman AW, Xu W, Vaughan CK, Beebe K, Konstantinova A, Vourganti S, Panaretou B, Piper PW, Trepel JB, Prodromou C, Pearl LH, Neckers L (2011) Threonine 22 phosphorylation attenuates Hsp90 interaction with cochaperones and affects its chaperone activity. *Mol Cell* 41: 672-681

[84] Soroka J, Wandinger SK, Mausbacher N, Schreiber T, Richter K, Daub H, Buchner J (2012) Conformational switching of the molecular chaperone Hsp90 via regulated phosphorylation. *Mol Cell* 45: 517-528

[85] Mollapour M, Neckers L (2012) Post-translational modifications of Hsp90 and their contributions to chaperone regulation. *Biochim Biophys Acta* 1823: 648-655

[86] Scroggins BT, Robzyk K, Wang D, Marcu MG, Tsutsumi S, Beebe K, Cotter RJ, Felts S, Toft D, Karnitz L, Rosen N, Neckers L (2007) An acetylation site in the middle domain of Hsp90 regulates chaperone function. *Mol Cell* 25: 151-159

[87] Kovacs JJ, Murphy PJ, Gaillard S, Zhao X, Wu JT, Nicchitta CV, Yoshida M, Toft DO, Pratt WB, Yao TP (2005) HDAC6 regulates Hsp90 acetylation and chaperone-dependent activation of glucocorticoid receptor. *Mol Cell* 18: 601-607

[88] Murphy PJ, Morishima Y, Kovacs JJ, Yao TP, Pratt WB (2005) Regulation of the dynamics of hsp90 action on the glucocorticoid receptor by acetylation/deacetylation of the chaperone. *J Biol Chem* 280: 33792-33799

[89] de Zoeten EF, Wang L, Butler K, Beier UH, Akimova T, Sai H, Bradner JE, Mazitschek R, Kozikowski AP, Matthias P, Hancock WW (2011) Histone deacetylase 6 and heat shock protein 90 control the functions of Foxp3(+) T-regulatory cells. *Mol Cell Biol* 31: 2066-2078

[90] Martinez-Ruiz A, Villanueva L, Gonzalez de Orduna C, Lopez-Ferrer D, Higueras MA, Tarin C, Rodriguez-Crespo I, Vazquez J, Lamas S (2005) S-nitrosylation of Hsp90 promotes the inhibition of its ATPase and endothelial nitric oxide synthase regulatory activities. *Proc Natl Acad Sci U S A* 102: 8525-8530

[91] Retzlaff M, Stahl M, Eberl HC, Lagleder S, Beck J, Kessler H, Buchner J (2009) Hsp90 is regulated by a switch point in the C-terminal domain. *EMBO Rep* 10: 1147-1153

[92] Scroggins BT, Neckers L (2009) Just say NO: nitric oxide regulation of Hsp90. *EMBO Rep* 10: 1093-1094

[93] Blank M, Mandel M, Keisari Y, Meruelo D, Lavie G (2003) Enhanced ubiquitinylation of heat shock protein 90 as a potential mechanism for mitotic cell death in cancer cells induced with hypericin. *Cancer Res* 63: 8241-8247

[94] Chen WY, Chang FR, Huang ZY, Chen JH, Wu YC, Wu CC (2008) Tubocapsenolide A, a novel withanolide, inhibits proliferation and induces apoptosis in MDA-MB-231 cells by thiol oxidation of heat shock proteins. *J Biol Chem* 283: 17184-17193

[95] Mollapour M, Tsutsumi S, Kim YS, Trepel J, Neckers L (2011) Casein kinase 2 phosphorylation of Hsp90 threonine 22 modulates chaperone function and drug sensitivity. *Oncotarget* 2: 407-417

[96] Prodromou C (2012) The 'active life' of Hsp90 complexes. *Biochim Biophys Acta* 1823: 614-623

[97] Goetz MP, Toft DO, Ames MM, Erlichman C (2003) The Hsp90 chaperone complex as a novel target for cancer therapy. *Ann Oncol* 14: 1169-1176

[98] Urban JD, Budinsky RA, Rowlands JC (2012) An evaluation of single nucleotide polymorphisms in the human heat shock protein 90 kDa alpha and beta isoforms. *Drug Metab Pharmacokinet* 27: 268-278

[99] Conroy SE, Sasieni PD, Fentiman I, Latchman DS (1998) Autoantibodies to the 90kDa heat shock protein and poor survival in breast cancer patients. *Eur J Cancer* 34: 942-943

[100] Jameel A, Skilton RA, Campbell TA, Chander SK, Coombes RC, Luqmani YA (1992) Clinical and biological significance of HSP89 alpha in human breast cancer. *Int J Cancer* 50: 409-415

[101] McCarthy MM, Pick E, Kluger Y, Gould-Rothberg B, Lazova R, Camp RL, Rimm DL, Kluger HM (2008) HSP90 as a marker of progression in melanoma. *Ann Oncol* 19: 590-594

[102] Blagg BS, Kerr TD (2006) Hsp90 inhibitors: small molecules that transform the Hsp90 protein folding machinery into a catalyst for protein degradation. *Med Res Rev* 26: 310-338

[103] Kamal A, Thao L, Sensintaffar J, Zhang L, Boehm MF, Fritz LC, Burrows FJ (2003) A high-affinity conformation of Hsp90 confers tumour selectivity on Hsp90 inhibitors. *Nature* 425: 407-410

[104] Maroney AC, Marugan JJ, Mezzasalma TM, Barnakov AN, Garrabrant TA, Weaner LE, Jones WJ, Barnakova LA, Koblish HK, Todd MJ, Masucci JA, Deckman IC, Galemmo RA, Jr., Johnson DL (2006) Dihydroquinone ansamycins: toward resolving the conflict between low in vitro affinity and high cellular potency of geldanamycin derivatives. *Biochemistry* 45: 5678-5685

[105] Neckers L (2007) Heat shock protein 90: the cancer chaperone. *J Biosci* 32: 517-530

[106] Chiosis G, Huezo H, Rosen N, Mimnaugh E, Whitesell L, Neckers L (2003) 17AAG: low target binding affinity and potent cell activity--finding an explanation. *Mol Cancer Ther* 2: 123-129

[107] Patki JM, Pawar SS (2013) HSP90: Chaperone-me-not. *Pathol Oncol Res*

[108] Chiosis G, Neckers L (2006) Tumor selectivity of Hsp90 inhibitors: the explanation remains elusive. *ACS Chem Biol* 1: 279-284

[109] Peterson LB, Blagg BS (2009) To fold or not to fold: modulation and consequences of Hsp90 inhibition. *Future Med Chem* 1: 267-283

[110] Workman P, Burrows F, Neckers L, Rosen N (2007) Drugging the cancer chaperone HSP90: combinatorial therapeutic exploitation of oncogene addiction and tumor stress. *Ann N Y Acad Sci* 1113: 202-216

[111] Hanahan D, Weinberg RA (2000) The hallmarks of cancer. *Cell* 100: 57-70

[112] Li Y, Zhang T, Schwartz SJ, Sun D (2009) New developments in Hsp90 inhibitors as anti-cancer therapeutics: mechanisms, clinical perspective and more potential. *Drug Resist Updat* 12: 17-27

[113] McCarty MF (2004) Targeting multiple signaling pathways as a strategy for managing prostate cancer: multifocal signal modulation therapy. *Integr Cancer Ther* 3: 349-380

[114] Hemann MT, Strong MA, Hao LY, Greider CW (2001) The shortest telomere, not average telomere length, is critical for cell viability and chromosome stability. *Cell* 107: 67-77

[115] Flores I, Benetti R, Blasco MA (2006) Telomerase regulation and stem cell behaviour. *Curr Opin Cell Biol* 18: 254-260

[116] Cech TR (2004) Beginning to understand the end of the chromosome. *Cell* 116: 273-279

[117] Keppler BR, Grady AT, Jarstfer MB (2006) The biochemical role of the heat shock protein 90 chaperone complex in establishing human telomerase activity. *J Biol Chem* 281: 19840-19848

[118] Kim RH, Kim R, Chen W, Hu S, Shin KH, Park NH, Kang MK (2008) Association of hsp90 to the hTERT promoter is necessary for hTERT expression in human oral cancer cells. *Carcinogenesis* 29: 2425-2431

[119] Atay C, Ugurlu S, Ozoren N (2009) Shock the heat shock network. *J Clin Invest* 119: 445-448

[120] Fulda S, Galluzzi L, Kroemer G (2010) Targeting mitochondria for cancer therapy. *Nat Rev Drug Discov* 9: 447-464

[121] Kroemer G, Galluzzi L, Brenner C (2007) Mitochondrial membrane permeabilization in cell death. *Physiol Rev* 87: 99-163

[122] Green DR, Kroemer G (2004) The pathophysiology of mitochondrial cell death. *Science* 305: 626-629

[123] Kang BH, Plescia J, Dohi T, Rosa J, Doxsey SJ, Altieri DC (2007) Regulation of tumor cell mitochondrial homeostasis by an organelle-specific Hsp90 chaperone network. *Cell* 131: 257-270

[124] Chambers AF, Groom AC, MacDonald IC (2002) Dissemination and growth of cancer cells in metastatic sites. *Nat Rev Cancer* 2: 563-572

[125] Felding-Habermann B (2003) Integrin adhesion receptors in tumor metastasis. *Clin Exp Metastasis* 20: 203-213

[126] Tsutsumi S, Beebe K, Neckers L (2009) Impact of heat-shock protein 90 on cancer metastasis. *Future Oncol* 5: 679-688

[127] Li W, Sahu D, Tsen F (2012) Secreted heat shock protein-90 (Hsp90) in wound healing and cancer. *Biochim Biophys Acta* 1823: 730-741

[128] Cheng CF, Sahu D, Tsen F, Zhao Z, Fan J, Kim R, Wang X, O'Brien K, Li Y, Kuang Y, Chen M, Woodley DT, Li W (2011) A fragment of secreted Hsp90alpha carries properties that enable it to accelerate effectively both acute and diabetic wound healing in mice. *J Clin Invest* 121: 4348-4361

[129] Chen JS, Hsu YM, Chen CC, Chen LL, Lee CC, Huang TS (2010) Secreted heat shock protein 90alpha induces colorectal cancer cell invasion through CD91/LRP-1 and NF-kappaB-mediated integrin alphaV expression. *J Biol Chem* 285: 25458-25466

[130] Sahu D, Zhao Z, Tsen F, Cheng CF, Park R, Situ AJ, Dai J, Eginli A, Shams S, Chen M, Ulmer TS, Conti P, Woodley DT, Li W (2012) A potentially common peptide target in secreted heat shock protein-90alpha for hypoxia-inducible factor-1alpha-positive tumors. *Mol Biol Cell* 23: 602-613

[131] Tsutsumi S, Scroggins B, Koga F, Lee MJ, Trepel J, Felts S, Carreras C, Neckers L (2008) A small molecule cell-impermeant Hsp90 antagonist inhibits tumor cell motility and invasion. *Oncogene* 27: 2478-2487

[132] Stellas D, El Hamidieh A, Patsavoudi E (2010) Monoclonal antibody 4C5 prevents activation of MMP2 and MMP9 by disrupting their interaction with extracellular HSP90 and inhibits formation of metastatic breast cancer cell deposits. *BMC Cell Biol* 11: 51

[133] Saaristo A, Karpanen T, Alitalo K (2000) Mechanisms of angiogenesis and their use in the inhibition of tumor growth and metastasis. *Oncogene* 19: 6122-6129

[134] Carstens CP, Kramer A, Fahl WE (1996) Adhesion-dependent control of cyclin E/cdk2 activity and cell cycle progression in normal cells but not in Ha-ras transformed NRK cells. *Exp Cell Res* 229: 86-92

[135] ClinicalTrials.gov ([cited 2016]) [Internet]. *National Library of Medicine at the National Institutes of Health*: Available from: https://clinicaltrials.gov/

[136] Ross CA, Poirier MA (2004) Protein aggregation and neurodegenerative disease. *Nat Med* 10 Suppl: S10-17

[137] Klettner A (2004) The induction of heat shock proteins as a potential strategy to treat neurodegenerative disorders. *Drug News Perspect* 17: 299-306

[138] Zou J, Guo Y, Guettouche T, Smith DF, Voellmy R (1998) Repression of heat shock transcription factor HSF1 activation by HSP90 (HSP90 complex) that forms a stress-sensitive complex with HSF1. *Cell* 94: 471-480

[139] Anckar J, Sistonen L (2007) Heat shock factor 1 as a coordinator of stress and developmental pathways. *Adv Exp Med Biol* 594: 78-88

[140] Luo W, Rodina A, Chiosis G (2008) Heat shock protein 90: translation from cancer to Alzheimer's disease treatment? *BMC Neurosci* 9 Suppl 2: S7

[141] Dickey CA, Eriksen J, Kamal A, Burrows F, Kasibhatla S, Eckman CB, Hutton M, Petrucelli L (2005) Development of a high throughput drug screening assay for the detection of changes in tau levels -- proof of concept with HSP90 inhibitors. *Curr Alzheimer Res* 2: 231-238

[142] Mattson MP (2004) Pathways towards and away from Alzheimer's disease. *Nature* 430: 631-639

[143] Muchowski PJ, Wacker JL (2005) Modulation of neurodegeneration by molecular chaperones. *Nat Rev Neurosci* 6: 11-22

[144] Dou F, Chang X, Ma D (2007) Hsp90 maintains the stability and function of the Tau phosphorylating kinase GSK3β. *Int J Mol Sci* 8: 51-60

[145] Rademakers R, Sleegers K, Theuns J, Van den Broeck M, Bel Kacem S, Nilsson LG, Adolfsson R, van Duijn CM, Van Broeckhoven C, Cruts M (2005) Association of cyclin-dependent kinase 5 and neuronal activators p35 and p39 complex in early-onset Alzheimer's disease. *Neurobiol Aging* 26: 1145-1151

[146] Dou F, Netzer WJ, Tanemura K, Li F, Hartl FU, Takashima A, Gouras GK, Greengard P, Xu H (2003) Chaperones increase association of tau protein with microtubules. *Proc Natl Acad Sci U S A* 100: 721-726

[147] Luo W, Sun W, Taldone T, Rodina A, Chiosis G (2010) Heat shock protein 90 in neurodegenerative diseases. *Mol Neurodegener* 5: 24

[148] Neef DW, Jaeger AM, Thiele DJ (2011) Heat shock transcription factor 1 as a therapeutic target in neurodegenerative diseases. *Nat Rev Drug Discov* 10: 930-944

[149] Gomez-Tortosa E, Newell K, Irizarry MC, Albert M, Growdon JH, Hyman BT (1999) Clinical and quantitative pathologic correlates of dementia with Lewy bodies. *Neurology* 53: 1284-1291

[150] McKeith IG, Galasko D, Kosaka K, Perry EK, Dickson DW, Hansen LA, Salmon DP, Lowe J, Mirra SS, Byrne EJ, Lennox G, Quinn NP, Edwardson JA, Ince PG, Bergeron C, Burns A, Miller BL, Lovestone S, Collerton D, Jansen EN, Ballard C, de Vos RA, Wilcock GK, Jellinger KA, Perry RH (1996) Consensus guidelines for the clinical and pathologic diagnosis of dementia with Lewy bodies (DLB): report of the consortium on DLB international workshop. *Neurology* 47: 1113-1124

[151] Luk KC, Mills IP, Trojanowski JQ, Lee VM (2008) Interactions between Hsp70 and the hydrophobic core of alpha-synuclein inhibit fibril assembly. *Biochemistry* 47: 12614-12625

[152] Hurtado-Lorenzo A, Anand VS (2008) Heat shock protein 90 modulates LRRK2 stability: potential implications for Parkinson's disease treatment. *J Neurosci* 28: 6757-6759

[153] Wang L, Xie C, Greggio E, Parisiadou L, Shim H, Sun L, Chandran J, Lin X, Lai C, Yang WJ, Moore DJ, Dawson TM, Dawson VL, Chiosis G, Cookson MR, Cai H (2008) The chaperone activity of heat shock protein 90 is critical for maintaining the stability of leucine-rich repeat kinase 2. *J Neurosci* 28: 3384-3391

[154] Banumathy G, Singh V, Pavithra SR, Tatu U (2003) Heat shock protein 90 function is essential for Plasmodium falciparum growth in human erythrocytes. *J Biol Chem* 278: 18336-18345

[155] Echeverria PC, Matrajt M, Harb OS, Zappia MP, Costas MA, Roos DS, Dubremetz JF, Angel SO (2005) Toxoplasma gondii Hsp90 is a potential drug target whose expression and subcellular localization are developmentally regulated. *J Mol Biol* 350: 723-734

[156] Pallavi R, Roy N, Nageshan RK, Talukdar P, Pavithra SR, Reddy R, Venketesh S, Kumar R, Gupta AK, Singh RK, Yadav SC, Tatu U (2010) Heat shock protein 90 as a drug target against protozoan infections: biochemical characterization of HSP90 from Plasmodium falciparum and Trypanosoma evansi and evaluation of its inhibitor as a candidate drug. *J Biol Chem* 285: 37964-37975

[157] Shonhai A (2010) Plasmodial heat shock proteins: targets for chemotherapy. *FEMS Immunol Med Microbiol* 58: 61-74

[158] Cowen LE, Singh SD, Kohler JR, Collins C, Zaas AK, Schell WA, Aziz H, Mylonakis E, Perfect JR, Whitesell L, Lindquist S (2009) Harnessing Hsp90 function as a powerful, broadly effective therapeutic strategy for fungal infectious disease. *Proc Natl Acad Sci U S A* 106: 2818-2823

[159] Cowen LE, Lindquist S (2005) Hsp90 potentiates the rapid evolution of new traits: drug resistance in diverse fungi. *Science* 309: 2185-2189

[160] Semighini CP, Heitman J (2009) Dynamic duo takes down fungal villains. *Proc Natl Acad Sci U S A* 106: 2971-2972

[161] Geller R, Taguwa S, Frydman J (2012) Broad action of Hsp90 as a host chaperone required for viral replication. *Biochim Biophys Acta* 1823: 698-706

[162] Nakagawa S, Umehara T, Matsuda C, Kuge S, Sudoh M, Kohara M (2007) Hsp90 inhibitors suppress HCV replication in replicon cells and humanized liver mice. *Biochem Biophys Res Commun* 353: 882-888

[163] Geller R, Vignuzzi M, Andino R, Frydman J (2007) Evolutionary constraints on chaperone-mediated folding provide an antiviral approach refractory to development of drug resistance. *Genes Dev* 21: 195-205

[164] Firestein GS (2003) Evolving concepts of rheumatoid arthritis. *Nature* 423: 356-361

[165] Rice JW, Veal JM, Fadden RP, Barabasz AF, Partridge JM, Barta TE, Dubois LG, Huang KH, Mabbett SR, Silinski MA, Steed PM, Hall SE (2008) Small molecule inhibitors of Hsp90 potently affect inflammatory disease pathways and exhibit activity in models of rheumatoid arthritis. *Arthritis Rheum* 58: 3765-3775

[166] Smolen JS, Aletaha D, Koeller M, Weisman MH, Emery P (2007) New therapies for treatment of rheumatoid arthritis. *Lancet* 370: 1861-1874

[167] Choi SR, Lee SA, Kim YJ, Ok CY, Lee HJ, Hahm KB (2009) Role of heat shock proteins in gastric inflammation and ulcer healing. *J Physiol Pharmacol* 60 Suppl 7: 5-17

[168] Childers M, Eckel G, Himmel A, Caldwell J (2007) A new model of cystic fibrosis pathology: lack of transport of glutathione and its thiocyanate conjugates. *Med Hypotheses* 68: 101-112

[169] Coppinger JA, Hutt DM, Razvi A, Koulov AV, Pankow S, Yates JR, 3rd, Balch WE (2012) A chaperone trap contributes to the onset of cystic fibrosis. *PLoS One* 7: e37682

[170] Griffin TM, Valdez TV, Mestril R (2004) Radicicol activates heat shock protein expression and cardioprotection in neonatal rat cardiomyocytes. *Am J Physiol Heart Circ Physiol* 287: H1081-1088

[171] Li C, Dobrowsky RT (2012) Targeting Molecular Chaperones in Diabetic Peripheral Neuropathy. In *Peripheral Neuropathy - Advances in Diagnostic and Therapeutic Approaches*, Hayat G (ed). InTech

[172] Tash JS, Chakrasali R, Jakkaraj SR, Hughes J, Smith SK, Hornbaker K, Heckert LL, Ozturk SB, Hadden MK, Kinzy TG, Blagg BS, Georg GI (2008) Gamendazole, an orally active indazole carboxylic acid male contraceptive agent, targets HSP90AB1 (HSP90BETA) and EEF1A1 (eEF1A), and stimulates Il1a transcription in rat Sertoli cells. *Biol Reprod* 78: 1139-1152

[173] Matts RL, Dixit A, Peterson LB, Sun L, Voruganti S, Kalyanaraman P, Hartson SD, Verkhivker GM, Blagg BS (2011) Elucidation of the Hsp90 C-terminal inhibitor binding site. *ACS Chem Biol* 6: 800-807

[174] Strocchia M, Terracciano S, Chini MG, Vassallo A, Vaccaro MC, Dal Piaz F, Leone A, Riccio R, Bruno I, Bifulco G (2015) Targeting the Hsp90 C-terminal domain by the chemically accessible dihydropyrimidinone scaffold. *Chem Commun (Camb)* 51: 3850-3853

[175] DeBoer C, Meulman PA, Wnuk RJ, Peterson DH (1970) Geldanamycin, a new antibiotic. *J Antibiot (Tokyo)* 23: 442-447

[176] Stebbins CE, Russo AA, Schneider C, Rosen N, Hartl FU, Pavletich NP (1997) Crystal structure of an Hsp90-geldanamycin complex: targeting of a protein chaperone by an antitumor agent. *Cell* 89: 239-250

[177] Zuehlke A, Johnson JL (2010) Hsp90 and co-chaperones twist the functions of diverse client proteins. *Biopolymers* 93: 211-217

[178] Sharma SV, Agatsuma T, Nakano H (1998) Targeting of the protein chaperone, HSP90, by the transformation suppressing agent, radicicol. *Oncogene* 16: 2639-2645

[179] Workman P, Collins I (2010) Probing the probes: fitness factors for small molecule tools. *Chem Biol* 17: 561-577

[180] Neckers L (2006) Using natural product inhibitors to validate Hsp90 as a molecular target in cancer. *Curr Top Med Chem* 6: 1163-1171

[181] Travers J, Sharp S, Workman P (2012) HSP90 inhibition: two-pronged exploitation of cancer dependencies. *Drug Discov Today* 17: 242-252

[182] Neckers L, Workman P (2012) Hsp90 molecular chaperone inhibitors: are we there yet? *Clin Cancer Res* 18: 64-76

[183] Supko JG, Hickman RL, Grever MR, Malspeis L (1995) Preclinical pharmacologic evaluation of geldanamycin as an antitumor agent. *Cancer Chemother Pharmacol* 36: 305-315

[184] Modi S, Stopeck A, Linden H, Solit D, Chandarlapaty S, Rosen N, D'Andrea G, Dickler M, Moynahan ME, Sugarman S, Ma W, Patil S, Norton L, Hannah AL, Hudis C (2011) HSP90 inhibition is effective in breast cancer: a phase II trial of tanespimycin (17-AAG) plus trastuzumab in patients with HER2-positive metastatic breast cancer progressing on trastuzumab. *Clin Cancer Res* 17: 5132-5139

[185] Jhaveri K, Modi S (2012) HSP90 inhibitors for cancer therapy and overcoming drug resistance. *Adv Pharmacol* 65: 471-517

[186] Lancet JE, Gojo I, Burton M, Quinn M, Tighe SM, Kersey K, Zhong Z, Albitar MX, Bhalla K, Hannah AL, Baer MR (2010) Phase I study of the heat shock protein 90 inhibitor alvespimycin (KOS-1022, 17-DMAG) administered intravenously twice weekly to patients with acute myeloid leukemia. *Leukemia* 24: 699-705

[187] Pacey S, Wilson RH, Walton M, Eatock MM, Hardcastle A, Zetterlund A, Arkenau HT, Moreno-Farre J, Banerji U, Roels B, Peachey H, Aherne W, de Bono JS, Raynaud F, Workman P, Judson I (2011) A phase I study of the heat shock protein 90 inhibitor alvespimycin (17-DMAG) given intravenously to patients with advanced solid tumors. *Clin Cancer Res* 17: 1561-1570

[188] Modi S, Saura C, Henderson C, Lin NU, Mahtani R, Goddard J, Rodenas E, Hudis C, O'Shaughnessy J, Baselga J (2013) A multicenter trial evaluating retaspimycin HCL (IPI-504) plus trastuzumab in patients with advanced or metastatic HER2-positive breast cancer. *Breast Cancer Res Treat* 139: 107-113

[189] Kelland LR, Sharp SY, Rogers PM, Myers TG, Workman P (1999) DT-Diaphorase expression and tumor cell sensitivity to 17-allylamino, 17-demethoxygeldanamycin, an inhibitor of heat shock protein 90. *J Natl Cancer Inst* 91: 1940-1949

[190] Gaspar N, Sharp SY, Pacey S, Jones C, Walton M, Vassal G, Eccles S, Pearson A, Workman P (2009) Acquired resistance to 17-allylamino-17-demethoxygeldanamycin (17-AAG, tanespimycin) in glioblastoma cells. *Cancer Res* 69: 1966-1975

[191] Solit DB, Chiosis G (2008) Development and application of Hsp90 inhibitors. *Drug Discov Today* 13: 38-43

[192] Garcia-Carbonero R, Carnero A, Paz-Ares L (2013) Inhibition of HSP90 molecular chaperones: moving into the clinic. *Lancet Oncol* 14: e358-369

[193] Soga S, Shiotsu Y, Akinaga S, Sharma SV (2003) Development of radicicol analogues. *Curr Cancer Drug Targets* 3: 359-369

[194] Whitesell L, Lin NU (2012) HSP90 as a platform for the assembly of more effective cancer chemotherapy. *Biochim Biophys Acta* 1823: 756-766

[195] Chiosis G (2006) Discovery and development of purine-scaffold Hsp90 inhibitors. *Curr Top Med Chem* 6: 1183-1191

[196] Chiosis G, Lucas B, Shtil A, Huezo H, Rosen N (2002) Development of a purine-scaffold novel class of Hsp90 binders that inhibit the proliferation of cancer cells and induce the degradation of Her2 tyrosine kinase. *Bioorg Med Chem* 10: 3555-3564

[197] Rodina A, Vilenchik M, Moulick K, Aguirre J, Kim J, Chiang A, Litz J, Clement CC, Kang Y, She Y, Wu N, Felts S, Wipf P, Massague J, Jiang X, Brodsky JL, Krystal GW, Chiosis G (2007) Selective compounds define Hsp90 as a major inhibitor of apoptosis in small-cell lung cancer. *Nat Chem Biol* 3: 498-507

[198] Hwang M, Moretti L, Lu B (2009) HSP90 inhibitors: multi-targeted antitumor effects and novel combinatorial therapeutic approaches in cancer therapy. *Curr Med Chem* 16: 3081-3092

[199] Marcu MG, Chadli A, Bouhouche I, Catelli M, Neckers LM (2000) The heat shock protein 90 antagonist novobiocin interacts with a previously unrecognized ATP-binding domain in the carboxyl terminus of the chaperone. *J Biol Chem* 275: 37181-37186

[200] Donnelly A, Blagg BS (2008) Novobiocin and additional inhibitors of the Hsp90 C-terminal nucleotide-binding pocket. *Curr Med Chem* 15: 2702-2717

[201] Matthews SB, Vielhauer GA, Manthe CA, Chaguturu VK, Szabla K, Matts RL, Donnelly AC, Blagg BS, Holzbeierlein JM (2010) Characterization of a novel novobiocin analogue as a putative C-terminal inhibitor of heat shock protein 90 in prostate cancer cells. *Prostate* 70: 27-36

[202] Samadi AK, Zhang X, Mukerji R, Donnelly AC, Blagg BS, Cohen MS (2011) A novel C-terminal HSP90 inhibitor KU135 induces apoptosis and cell cycle arrest in melanoma cells. *Cancer Lett* 312: 158-167

[203] Conde R, Belak ZR, Nair M, O'Carroll RF, Ovsenek N (2009) Modulation of Hsf1 activity by novobiocin and geldanamycin. *Biochem Cell Biol* 87: 845-851

[204] Cortajarena AL, Yi F, Regan L (2008) Designed TPR modules as novel anticancer agents. *ACS Chem Biol* 3: 161-166

[205] Sellers RP, Alexander LD, Johnson VA, Lin CC, Savage J, Corral R, Moss J, Slugocki TS, Singh EK, Davis MR, Ravula S, Spicer JE, Oelrich JL, Thornquist A, Pan CM, McAlpine SR (2010) Design and synthesis of Hsp90 inhibitors: exploring the SAR of Sansalvamide A derivatives. *Bioorg Med Chem* 18: 6822-6856

[206] Zhang T, Hamza A, Cao X, Wang B, Yu S, Zhan CG, Sun D (2008) A novel Hsp90 inhibitor to disrupt Hsp90/Cdc37 complex against pancreatic cancer cells. *Mol Cancer Ther* 7: 162-170

[207] Byrd CA, Bornmann W, Erdjument-Bromage H, Tempst P, Pavletich N, Rosen N, Nathan CF, Ding A (1999) Heat shock protein 90 mediates macrophage activation by Taxol and bacterial lipopolysaccharide. *Proc Natl Acad Sci U S A* 96: 5645-5650

[208] Soti C, Racz A, Csermely P (2002) A Nucleotide-dependent molecular switch controls ATP binding at the C-terminal domain of Hsp90. N-terminal nucleotide binding unmasks a C-terminal binding pocket. *J Biol Chem* 277: 7066-7075

[209] Siegelin MD (2013) Inhibition of the mitochondrial Hsp90 chaperone network: a novel, efficient treatment strategy for cancer? *Cancer Lett* 333: 133-146

[210] Plescia J, Salz W, Xia F, Pennati M, Zaffaroni N, Daidone MG, Meli M, Dohi T, Fortugno P, Nefedova Y, Gabrilovich DI, Colombo G, Altieri DC (2005) Rational design of shepherdin, a novel anticancer agent. *Cancer Cell* 7: 457-468

[211] Zhu A, Ren Y, Wang N, Jin Q, Zhang D, Yang G, Wang Q (2015) Adeno-associated virus mediated gene transfer of Shepherdin inhibits gallbladder carcinoma growth in vitro and in vivo. *Gene* 572: 87-94

[212] Kang BH, Plescia J, Song HY, Meli M, Colombo G, Beebe K, Scroggins B, Neckers L, Altieri DC (2009) Combinatorial drug design targeting multiple cancer signaling networks controlled by mitochondrial Hsp90. *J Clin Invest* 119: 454-464

[213] Klebe G (2015) Applying thermodynamic profiling in lead finding and optimization. *Nat Rev Drug Discov* 14: 95-110

[214] Holdgate GA (2007) Thermodynamics of binding interactions in the rational drug design process. *Expert Opin Drug Discov* 2: 1103-1114

[215] Chaires JB (2008) Calorimetry and thermodynamics in drug design. *Annu Rev Biophys* 37: 135-151

[216] Olsson TS, Williams MA, Pitt WR, Ladbury JE (2008) The thermodynamics of protein-ligand interaction and solvation: insights for ligand design. *J Mol Biol* 384: 1002-1017

[217] Kawasaki Y, Freire E (2011) Finding a better path to drug selectivity. *Drug Discov Today* 16: 985-990

[218] Tarcsay A, Keseru GM (2015) Is there a link between selectivity and binding thermodynamics profiles? *Drug Discov Today* 20: 86-94

[219] Perozzo R, Folkers G, Scapozza L (2004) Thermodynamics of protein-ligand interactions: history, presence, and future aspects. *J Recept Signal Transduct Res* 24: 1-52

[220] Leavitt S, Freire E (2001) Direct measurement of protein binding energetics by isothermal titration calorimetry. *Curr Opin Struct Biol* 11: 560-566

[221] Cummings MD, Farnum MA, Nelen MI (2006) Universal screening methods and applications of ThermoFluor. *J Biomol Screen* 11: 854-863

[222] Sarver RW, Peevers J, Cody WL, Ciske FL, Dyer J, Emerson SD, Hagadorn JC, Holsworth DD, Jalaie M, Kaufman M, Mastronardi M, McConnell P, Powell NA, Quin J, 3rd, Van Huis CA, Zhang E, Mochalkin I (2007) Binding thermodynamics of substituted diaminopyrimidine renin inhibitors. *Anal Biochem* 360: 30-40

[223] Freire E (2009) A thermodynamic approach to the affinity optimization of drug candidates. *Chem Biol Drug Des* 74: 468-472

[224] Nezami A, Kimura T, Hidaka K, Kiso A, Liu J, Kiso Y, Goldberg DE, Freire E (2003) High-affinity inhibition of a family of Plasmodium falciparum proteases by a designed adaptive inhibitor. *Biochemistry* 42: 8459-8464

[225] Cikotiene I, Kazlauskas E, Matuliene J, Michailoviene V, Torresan J, Jachno J, Matulis D (2009) 5-Aryl-4-(5-substituted-2,4-dihydroxyphenyl)-1,2,3-thiadiazoles as inhibitors of Hsp90 chaperone. *Bioorg Med Chem Lett* 19: 1089-1092

[226] Tellinghuisen J (2003) A study of statistical error in isothermal titration calorimetry. *Anal Biochem* 321: 79-88

[227] Wiseman T, Williston S, Brandts JF, Lin LN (1989) Rapid measurement of binding constants and heats of binding using a new titration calorimeter. *Anal Biochem* 179: 131-137

[228] Jelesarov I, Bosshard HR (1999) Isothermal titration calorimetry and differential scanning calorimetry as complementary tools to investigate the energetics of biomolecular recognition. *J Mol Recognit* 12: 3-18

[229] Broecker J, Vargas C, Keller S (2011) Revisiting the optimal c value for isothermal titration calorimetry. *Anal Biochem* 418: 307-309

[230] Slavik J (1982) Anilinonaphthalene sulfonate as a probe of membrane composition and function. *Biochim Biophys Acta* 694: 1-25

[231] Matulis D, Lovrien R (1998) 1-Anilino-8-naphthalene sulfonate anion-protein binding depends primarily on ion pair formation. *Biophys J* 74: 422-429

[232] Matulis D, Kranz JK, Salemme FR, Todd MJ (2005) Thermodynamic stability of carbonic anhydrase: measurements of binding affinity and stoichiometry using ThermoFluor. *Biochemistry* 44: 5258-5266

[233] Robertson AD, Murphy KP (1997) Protein Structure and the Energetics of Protein Stability. *Chem Rev* 97: 1251-1268

[234] Zubriene A, Gutkowska M, Matuliene J, Chaleckis R, Michailoviene V, Voroncova A, Venclovas C, Zylicz A, Zylicz M, Matulis D (2010) Thermodynamics of radicicol binding to human Hsp90 alpha and beta isoforms. *Biophys Chem* 152: 153-163

[235] ChemAxon (2012) Marvin Calculator Plugins were used for structure property prediction and calculation, MarvinSketch 5.11.3.

[236] Anandakrishnan R, Aguilar B, Onufriev AV (2012) H++ 3.0: automating pK prediction and the preparation of biomolecular structures for atomistic molecular modeling and simulations. *Nucleic Acids Res* 40: W537-541

[237] Baker BM, Murphy KP (1996) Evaluation of linked protonation effects in protein binding reactions using isothermal titration calorimetry. *Biophys J* 71: 2049-2055

[238] Sharp SY, Roe SM, Kazlauskas E, Cikotiene I, Workman P, Matulis D, Prodromou C (2012) Co-crystalization and in vitro biological characterization of 5-aryl-4-(5-substituted-2-4-dihydroxyphenyl)-1,2,3-thiadiazole Hsp90 inhibitors. *PLoS One* 7: e44642

[239] BIOVIA DS. (2015) Discovery Studio Modeling Environment, Release 4.5, San Diego: Dassault Systèmes.

[240] Schrodinger, LLC. (2015) The PyMOL Molecular Graphics System, Version 1.8.

[241] Scudiero DA, Shoemaker RH, Paull KD, Monks A, Tierney S, Nofziger TH, Currens MJ, Seniff D, Boyd MR (1988) Evaluation of a soluble tetrazolium/formazan assay for cell growth and drug sensitivity in culture using human and other tumor cell lines. *Cancer Res* 48: 4827-4833

[242] Jhaveri K, Taldone T, Modi S, Chiosis G (2012) Advances in the clinical development of heat shock protein 90 (Hsp90) inhibitors in cancers. *Biochim Biophys Acta* 1823: 742-755

[243] Dymock BW, Barril X, Brough PA, Cansfield JE, Massey A, McDonald E, Hubbard RE, Surgenor A, Roughley SD, Webb P, Workman P, Wright L, Drysdale MJ (2005) Novel, potent small-molecule inhibitors of the molecular chaperone Hsp90 discovered through structure-based design. *J Med Chem* 48: 4212-4215

[244] Sharp SY, Prodromou C, Boxall K, Powers MV, Holmes JL, Box G, Matthews TP, Cheung KM, Kalusa A, James K, Hayes A, Hardcastle A, Dymock B, Brough PA, Barril X, Cansfield JE, Wright L, Surgenor A, Foloppe N, Hubbard RE, Aherne W, Pearl L, Jones K, McDonald E, Raynaud F, Eccles S, Drysdale M, Workman P (2007) Inhibition of the heat shock protein 90 molecular chaperone in vitro and in vivo by novel, synthetic, potent resorcinylic pyrazole/isoxazole amide analogues. *Mol Cancer Ther* 6: 1198-1211

[245] Brough PA, Barril X, Borgognoni J, Chene P, Davies NG, Davis B, Drysdale MJ, Dymock B, Eccles SA, Garcia-Echeverria C, Fromont C, Hayes A, Hubbard RE, Jordan AM, Jensen MR, Massey A, Merrett A, Padfield A, Parsons R, Radimerski T, Raynaud FI, Robertson A, Roughley SD, Schoepfer J, Simmonite H, Sharp SY, Surgenor A, Valenti M, Walls S, Webb P, Wood M, Workman P, Wright L (2009) Combining hit identification strategies: fragment-based and in silico approaches to orally active 2-aminothieno[2,3-d]pyrimidine inhibitors of the Hsp90 molecular chaperone. *J Med Chem* 52: 4794-4809

[246] Freire E (2004) Isothermal titration calorimetry: controlling binding forces in lead optimization. *Drug Discov Today Technol* 1: 295-299

[247] Velazquez Campoy A, Freire E (2005) ITC in the post-genomic era...? Priceless. *Biophys Chem* 115: 115-124

[248] Ladbury JE, Klebe G, Freire E (2010) Adding calorimetric data to decision making in lead discovery: a hot tip. *Nat Rev Drug Discov* 9: 23-27

[249] Nilapwar S, Williams E, Fu C, Prodromou C, Pearl LH, Williams MA, Ladbury JE (2009) Structural-thermodynamic relationships of interactions in the N-terminal ATP-binding domain of Hsp90. *J Mol Biol* 392: 923-936

[250] Velazquez-Campoy A, Ohtaka H, Nezami A, Muzammil S, Freire E (2004) Isothermal titration calorimetry. *Curr Protoc Cell Biol* Chapter 17: Unit 17 18

[251] Cimmperman P, Baranauskiene L, Jachimoviciute S, Jachno J, Torresan J, Michailoviene V, Matuliene J, Sereikaite J, Bumelis V, Matulis D (2008) A quantitative model of thermal stabilization and destabilization of proteins by ligands. *Biophys J* 95: 3222-3231

[252] Todd M, Salemme F (2003) Direct binding assays for pharma screening-assay tutorial: Thermofluor miniaturized direct-binding assay for hts & secondary screening. *Genetic Engineering News* 23: 28-29

[253] Chiu MH, Prenner EJ (2011) Differential scanning calorimetry: An invaluable tool for a detailed thermodynamic characterization of macromolecules and their interactions. *J Pharm Bioallied Sci* 3: 39-59

[254] Clas SD, Dalton CR, Hancock BC (1999) Differential scanning calorimetry: applications in drug development. *Pharm Sci Technolo Today* 2: 311-320

[255] Senisterra GA, Finerty PJ, Jr. (2009) High throughput methods of assessing protein stability and aggregation. *Mol Biosyst* 5: 217-223

[256] Ladbury JE, Williams MA (2004) The extended interface: measuring non-local effects in biomolecular interactions. *Curr Opin Struct Biol* 14: 562-569

[257] Zubriene A, Matuliene J, Baranauskiene L, Jachno J, Torresan J, Michailoviene V, Cimmperman P, Matulis D (2009) Measurement of nanomolar dissociation constants by titration calorimetry and thermal shift assay - radicicol binding to Hsp90 and ethoxzolamide binding to CAII. *Int J Mol Sci* 10: 2662-2680

[258] Matulis D. (2008) Baltymų fizikinė chemija Lietuvos Respublikos švietimo ir mokslo ministerija, Vilniaus universitetas, Technologija.

[259] Roe SM, Prodromou C, O'Brien R, Ladbury JE, Piper PW, Pearl LH (1999) Structural basis for inhibition of the Hsp90 molecular chaperone by the antitumor antibiotics radicicol and geldanamycin. *J Med Chem* 42: 260-266

[260] Barril X, Beswick MC, Collier A, Drysdale MJ, Dymock BW, Fink A, Grant K, Howes R, Jordan AM, Massey A, Surgenor A, Wayne J, Workman P, Wright L (2006) 4-Amino derivatives of the Hsp90 inhibitor CCT018159. *Bioorg Med Chem Lett* 16: 2543-2548

[261] Gooljarsingh LT, Fernandes C, Yan K, Zhang H, Grooms M, Johanson K, Sinnamon RH, Kirkpatrick RB, Kerrigan J, Lewis T, Arnone M, King AJ, Lai Z, Copeland RA, Tummino PJ (2006) A biochemical rationale for the anticancer effects of Hsp90 inhibitors: slow, tight binding inhibition by geldanamycin and its analogues. *Proc Natl Acad Sci U S A* 103: 7625-7630

[262] Cheung KM, Matthews TP, James K, Rowlands MG, Boxall KJ, Sharp SY, Maloney A, Roe SM, Prodromou C, Pearl LH, Aherne GW, McDonald E, Workman P (2005) The identification, synthesis, protein crystal structure and in vitro biochemical evaluation of a new 3,4-diarylpyrazole class of Hsp90 inhibitors. *Bioorg Med Chem Lett* 15: 3338-3343

[263] Brough PA, Aherne W, Barril X, Borgognoni J, Boxall K, Cansfield JE, Cheung KM, Collins I, Davies NG, Drysdale MJ, Dymock B, Eccles SA, Finch H, Fink A, Hayes A, Howes R, Hubbard RE, James K, Jordan AM, Lockie A, Martins V, Massey A, Matthews TP, McDonald E, Northfield CJ, Pearl LH, Prodromou C, Ray S, Raynaud FI, Roughley SD, Sharp SY, Surgenor A, Walmsley DL, Webb P, Wood M, Workman P, Wright L (2008) 4,5-diarylisoxazole Hsp90 chaperone inhibitors: potential therapeutic agents for the treatment of cancer. *J Med Chem* 51: 196-218

[264] Bissantz C, Kuhn B, Stahl M (2010) A medicinal chemist's guide to molecular interactions. *J Med Chem* 53: 5061-5084

[265] Wilcken R, Zimmermann MO, Lange A, Joerger AC, Boeckler FM (2013) Principles and applications of halogen bonding in medicinal chemistry and chemical biology. *J Med Chem* 56: 1363-1388

[266] Taylor RK, O. (1982) Crystallographic evidence for the existence of CH...O, CH...N and CH...Cl hydrogen bonds. *J Am Chem Soc* 104: 5063-5070

[267] Aakeroy CBE, T. A.; Seddon, K. R.; Palinko, I. (1999) The C-H...Cl hydrogen bond: does it exist? *New J Chem* 23: 145-152

[268] Christensen JJH, Lee D. ; Izatt, Reed M. (1976) *Handbook of proton ionization heats: and related thermodynamic quantities*, New York: Wiley.

[269] Prodromou C, Nuttall JM, Millson SH, Roe SM, Sim TS, Tan D, Workman P, Pearl LH, Piper PW (2009) Structural basis of the radicicol resistance displayed by a fungal hsp90. *ACS Chem Biol* 4: 289-297

[270] Millson SH, Chua CS, Roe SM, Polier S, Solovieva S, Pearl LH, Sim TS, Prodromou C, Piper PW (2011) Features of the Streptomyces hygroscopicus HtpG reveal how partial geldanamycin resistance can arise with mutation to the ATP binding pocket of a eukaryotic Hsp90. *FASEB J* 25: 3828-3837